CDF-7708
September 27, 2005

Search for $H \to WW^*$ in the dilepton channel with 360 pb^{-1} of Run II Data

S. Chuang [i], M. Coca [ii], M. Kruse [ii]

[i] University of Wisconsin
[ii] Duke University

Abstract

We have searched for $p\bar{p} \to H \to WW^*$ production in the dilepton channel ($W^+W^- \to \ell^+\nu\ell^-\bar{\nu}$, where $\ell = e$ or μ) using approximately 360 pb^{-1} Tevatron Run 2 data collected by the CDF detector. We have further optimized the analysis since blessed in 4.11.1 (using 184 /pb of data, collected up to run 168890) [9], by allowing one lepton leg to be above 10 GeV, a higher $\not\!\!E_T$ threshold, removing the missing significance requirement and using a looser jet veto. This improves significantly the lower mass Higgs expected limits. We construct a likelihood function from the $\Delta\phi(\ell, \ell)$ distribution, which we use to extract cross section limits using a Bayesian procedure. For Higgs masses of 110, 120, 130, 140, 150, 160, 170, 180, 190 and 200 GeV we obtain 95% CL limits on the $p\bar{p} \to H \to WW$ cross section of 8.2, 4.5, 4.3, 4.6, 3.9, 3.9, 3.8, 4.8, 7.1 and 4.6 pb respectively.

Contents

1 Introduction **10**

2 Changes from the previous version of the note **12**
2.1 September 27th, 2005 12

3 Event Selection **13**
3.1 Objects Identification 13
3.2 Lepton identification 14
3.3 Dilepton categories 17
3.4 Event Selection 17
3.5 Selection Optimization 20

4 Monte Carlo Datasets **25**

5 Signal Acceptances **27**

6 Scale Factors **28**

7 Measuring Z$\rightarrow \ell\ell$ cross-sections **29**

8 $H \rightarrow WW$ Acceptance Systematic Uncertainties **30**
8.1 PDF Uncertainty 30
8.2 ISR-more/less 30
8.3 α_s 30
8.4 Jet Energy Scale 31
8.5 Lepton ID 31
8.6 Track Isolation 31
8.7 Trigger Efficiency 31
8.8 Combined Acceptance Systematic 34

9 Background Estimates **34**
9.1 WW background 34
9.2 $t\bar{t}$ background 34
9.3 Drell-Yan background 34
9.4 Fake background 35
9.5 $W\gamma$ background 35
9.6 WZ and ZZ background 35
9.7 Background systematic uncertainties 36

10 Data analysis **37**
10.1 Data samples and luminosity . . . 37
10.2 Energy Scale factors for Plug electrons. . . . 38
10.3 Dilepton table . . . 39

11 Grand Summary **39**

12 Cross-Section Limit Calculation **40**
12.1 $\Delta\phi$ Distributions . . . 40
12.2 The Likelihood function and Posterior Density . . . 51
12.3 Expected Limits from Pseudo-experiments . . . 52
12.4 Cross section Limits from the Data . . . 54

13 Conclusions **57**

A Comparison with the THWG's Prospects **58**

B Expected signal, backgrounds and data candidates per di-lepton channel **59**

C Detailed acceptance tables **63**

List of Tables

1 The SM Higgs production cross section and branching ratios of H→WW are presented [19]. Also we show the number of events produced in 360 pb^{-1}, where $\ell =$ e or μ. 12

2 Baseline cuts for central high-p_T isolated electrons ($E_T > 20$ GeV) (CEM) [15]. . . 15

3 Baseline cuts for plug isolated electrons (PHX) [15]. 15

4 Baseline cuts for minimum ionizing isolated tracks [12]. After passing these cuts the muon is classified as *CMUP*, *CMX* or *non-triggering* according to the definitions in the text. 16

5 Dilepton categories included in the current analysis. Shown in bold are the triggerable lepton in the data samples studied. The one exception to this is the PHX categories. Both lepton legs are required to be isolated. 18

6 Fraction of events passing various kinematics cuts, as a function of the Higgs mass. 22

8 The DY background as a function of Higgs mass with or without the cut ($\not\!\!E_T > 50$ GeV $||\Delta\phi(\not\!\!E_T$, lep/jet) > 0.35)). 25

7 Results of varying the $\not\!\!E_T$ and 1-jet E_T threshold. Defaults are $\not\!\!E_T < M_H/4$ and ${E_T}^{\text{1-jet}} < 50$ GeV. We show the default expected limits, expected limits when changing the cut for the 1-jet Et from 50 to $50 + 5, +10, +15, +20$ GeV, and also expected limits for $\not\!\!E_T < M_H/4 - 10, -5, +5, +10, +15, +20, +25, +30$ GeV. . . . 25

9 Monte Carlo datasets used for HWW analysis. 26

10 Event Selection for the HWW analysis. 28

11 Summary of trigger efficiencies. The CEM_18 trigger efficiency is run-dependent, number given above being an average over η. We use the MET_PEM trigger efficiency as estimated in 4.11.1. The contribution from dilepton categories triggered by PHX is below 15%. 28

13 PHX charge mis-identification scale factors [7]. 29

12 Summary of lepton data/MC scale factors. 29

14 Summary of Z cross-section measurements. 29

15 Sources of systematic uncertainty on the $H \to WW \to l^+l^-\nu\bar{\nu}$ acceptance. 30

16 Track isolation scale factors (data/MC) for all the lepton types used in the HWW analysis. The statistical error are all below 1%. 31

17 $W\gamma$ MC samples used to estimate the background to HWW. 35

18 Sources of systematic uncertainties on the backgrounds. To all these uncertainties we add in quadrature 6% coming from luminosity. 37

19 Luminosities of the different di-lepton categories used in the analysis. 38

20 Phoenix electron energy scale factors divided by run range, plug side ($\eta > 0$ for east; $\eta < 0$ for west) and data/MC. 39

21 The estimated backgrounds and HWW signal in 360 pb^{-1}, and the number of events observed in the data, for each of the dilepton categories. The HWW expectation uses the theoretical cross-sections and BRs discussed in Section 1. . . 40

22 The estimated backgrounds and HWW signal in $360\,\mathrm{pb}^{-1}$, and the number of events observed in the data, for each of the dilepton categories. The HWW expectation uses the theoretical cross-sections and BRs discussed in Section 1. . . 40
23 95% CL limits on $\sigma(gg \to H) \times BR(H \to WW^*)$ at $\sqrt{\hat{s}} = 1.96\,\mathrm{TeV}$ for the different Higgs obtained using our old 20-20 selection from CDF-6958, for 200 /pb. The expected limits using the new selection are also shown, as discussed above. In all cases the limits correspond to $360\,\mathrm{pb}^{-1}$. 56
24 Comparison between the current status of our analysis and the THWG's prospect for the same integrated luminosity. The THWG's prospect are taken from Table 29 of the Report of the Tevatron Higgs Working Group [19] (originally at fb^{-1} scale) and interpolated to $\mathcal{L}_{\mathrm{int}} = 360\ \mathrm{pb}^{-1}$. 58
25 Summary of the signal and background expectations for a Higgs mass of 110 GeV, for 360 pb^{-1}. Also the observed number of events is shown. 59
26 Summary of the signal and background expectations for a Higgs mass of 120 GeV, for 360 pb^{-1}. Also the observed number of events is shown. 59
27 Summary of the signal and background expectations for a Higgs mass of 130 GeV, for 360 pb^{-1}. Also the observed number of events is shown. 60
28 Summary of the signal and background expectations for a Higgs mass of 140 GeV, for 360 pb^{-1}. Also the observed number of events is shown. 60
29 Summary of the signal and background expectations for a Higgs mass of 150 GeV, for 360 pb^{-1}. Also the observed number of events is shown. 61
30 Summary of the signal and background expectations for a Higgs mass of 160 GeV, for 360 pb^{-1}. Also the observed number of events is shown. 61
31 Summary of the signal and background expectations for a Higgs mass of 170 GeV, for 360 pb^{-1}. Also the observed number of events is shown. 62
32 Summary of the signal and background expectations for a Higgs mass of 180 GeV, for 360 pb^{-1}. Also the observed number of events is shown. 62
33 Summary of the signal and background expectations for a Higgs mass of 190 GeV, for 360 pb^{-1}. Also the observed number of events is shown. 63
34 Summary of the signal and background expectations for a Higgs mass of 200 GeV, for 360 pb^{-1}. Also the observed number of events is shown. 63
35 data acceptance table, assuming $M_H^{\mathrm{SM}} = 130$ GeV 64
36 data acceptance table, assuming $M_H^{\mathrm{SM}} = 140$ GeV 65
37 data acceptance table, assuming $M_H^{\mathrm{SM}} = 150$ GeV 66
38 data acceptance table, assuming $M_H^{\mathrm{SM}} = 160$ GeV 67
39 data acceptance table, assuming $M_H^{\mathrm{SM}} = 170$ GeV 68
40 data acceptance table, assuming $M_H^{\mathrm{SM}} = 180$ GeV 69
41 HWW dilepton MC acceptance table, assuming $M_H^{\mathrm{SM}} = 160$ GeV 70
42 WW MC acceptance table, assuming $M_H^{\mathrm{SM}} = 160$ GeV 71
43 WZ MC acceptance table, assuming $M_H^{\mathrm{SM}} = 160$ GeV 72
44 $t\bar{t}$ MC acceptance table, assuming $M_H^{\mathrm{SM}} = 160$ GeV 73
45 Drell-Yan MC acceptance table, assuming $M_H^{\mathrm{SM}} = 160$ GeV 74

46 ZZ MC acceptance table, assuming $M_H^{\mathrm{SM}} = 160$ GeV 75
47 $W\gamma$ MC acceptance table, assuming $M_H^{\mathrm{SM}} = 160$ GeV 76

List of Figures

1 SM Higgs production versus the mass of the Higgs boson. 10

2 Relative branching ratios for Higgs boson decays. 11

3 Feynman diagram for the dominant production mechanism, with both final state W's decaying leptonically. 11

4 Four of the variables used in the event selection (for $M_H = 180$ GeV) are shown before cutting on that variable: (upper-left) number of jets; (upper-right) missing energy; (lower-left) dilepton invariant mass and (lower-right) $P_T(lep1) + P_T(lep2) + \not{E}_T$. 19

5 Highest lepton p_T vs the second highest lepton p_T for a 130 GeV Higgs. 21

6 Highest lepton p_T vs the second highest lepton p_T for a 180 GeV Higgs. 21

7 The fraction of events passing kinematical cuts on $p_T(max)$, $p_T(min)$, for a 130 GeV Higgs. The circled values show that the efficiency increases from 39 to 78 %, when lowering the transverse momentum requirement on the second lepton from 20 to 10 GeV. 22

8 Missing energy for the signal (M_H=160 GeV) and WW background. 23

9 Jet E_T spectrum is shown before the jet veto, for: (upper-left) any number of jets event; (upper-right) only for 1-jet events; (lower-left) the leading jet in 2-jet events; (lower-right) the second jet in 2-jet events. Also the data point are shown, for 360/pb. The plots are made after requiring 2 good leptons, with $m_{\ell\ell} > 16$ GeV. 24

10 Signal acceptance for various Higgs masses. For comparison the generation 4 values are also shown. 27

11 Track isolation distributions per trkIsol-required lepton type and the cut efficiencies from data or MC as a function of lepton p_T. 32

12 Track isolation distributions per trkIsol-required lepton type and the cut efficiencies from data or MC as a function of lepton p_T. 33

13 The mass peak of $Z \to e_{\text{TCE}} e_{\text{PHX}}$ with phoenix electron energies added plug preradiator energies and scaled up by factors as listed in Table 20. 39

14 Azimuthal angular separation between the leptons, $\Delta\phi(\ell,\ell)$, from the decay of $H \to WW^* \to \ell\nu\ell\nu$. Distributions of data, HWW^* signal ($M_H = 110$ GeV) MC, WW MC and the sum of other considered background MC samples are shown. The MCs are normalized to the expectations for the integrated luminosity for analyzed data, about 360/pb. We use the upper-left $ee + e\mu + \mu\mu$ plot to fit for a limit on the cross-section of SM HWW production at Tevatron, at the Higgs mass of $M_H = 110$ GeV. 42

15 Azimuthal angular separation between the leptons, $\Delta\phi(\ell,\ell)$, from the decay of $H \to WW^* \to \ell\nu\ell\nu$. Distributions of data, HWW^* signal ($M_H = 120$ GeV) MC, WW MC and the sum of other considered background MC samples are shown. The MCs are normalized to the expectations for the integrated luminosity for analyzed data, about 360/pb. We use the upper-left $ee + e\mu + \mu\mu$ plot to fit for a limit on the cross-section of SM HWW production at Tevatron, at the Higgs mass of $M_H = 120$ GeV. 43
16 Azimuthal angular separation between the leptons, $\Delta\phi(\ell,\ell)$, from the decay of $H \to WW^* \to \ell\nu\ell\nu$. Distributions of data, HWW^* signal ($M_H = 130$ GeV) MC, WW MC and the sum of other considered background MC samples are shown. The MCs are normalized to the expectations for the integrated luminosity for analyzed data, about 360/pb. We use the upper-left $ee + e\mu + \mu\mu$ plot to fit for a limit on the cross-section of SM HWW production at Tevatron, at the Higgs mass of $M_H = 130$ GeV. 44
17 Azimuthal angular separation between the leptons, $\Delta\phi(\ell,\ell)$, from the decay of $H \to WW^* \to \ell\nu\ell\nu$. Distributions of data, HWW^* signal ($M_H = 140$ GeV) MC, WW MC and the sum of other considered background MC samples are shown. The MCs are normalized to the expectations for the integrated luminosity for analyzed data, about 360/pb. We use the upper-left $ee + e\mu + \mu\mu$ plot to fit for a limit on the cross-section of SM HWW production at Tevatron, at the Higgs mass of $M_H = 140$ GeV. 45
18 Azimuthal angular separation between the leptons, $\Delta\phi(\ell,\ell)$, from the decay of $H \to WW^* \to \ell\nu\ell\nu$. Distributions of data, HWW^* signal ($M_H = 150$ GeV) MC, WW MC and the sum of other considered background MC samples are shown. The MCs are normalized to the expectations for the integrated luminosity for analyzed data, about 360/pb. We use the upper-left $ee + e\mu + \mu\mu$ plot to fit for a limit on the cross-section of SM HWW production at Tevatron, at the Higgs mass of $M_H = 150$ GeV. 46
19 Azimuthal angular separation between the leptons, $\Delta\phi(\ell,\ell)$, from the decay of $H \to WW^* \to \ell\nu\ell\nu$. Distributions of data, HWW^* signal ($M_H = 160$ GeV) MC, WW MC and the sum of other considered background MC samples are shown. The MCs are normalized to the expectations for the integrated luminosity for analyzed data, about 360/pb. We use the upper-left $ee + e\mu + \mu\mu$ plot to fit for a limit on the cross-section of SM HWW production at Tevatron, at the Higgs mass of $M_H = 160$ GeV. 47
20 Azimuthal angular separation between the leptons, $\Delta\phi(\ell,\ell)$, from the decay of $H \to WW^* \to \ell\nu\ell\nu$. Distributions of data, HWW^* signal ($M_H = 170$ GeV) MC, WW MC and the sum of other considered background MC samples are shown. The MCs are normalized to the expectations for the integrated luminosity for analyzed data, about 360/pb. We use the upper-left $ee + e\mu + \mu\mu$ plot to fit for a limit on the cross-section of SM HWW production at Tevatron, at the Higgs mass of $M_H = 170$ GeV. 48

21 Azimuthal angular separation between the leptons, $\Delta\phi(\ell,\ell)$, from the decay of $H \to WW^* \to \ell\nu\ell\nu$. Distributions of data, HWW^* signal ($M_H = 180$ GeV) MC, WW MC and the sum of other considered background MC samples are shown. The MCs are normalized to the expectations for the integrated luminosity for analyzed data, about 360/pb. We use the upper-left $ee + e\mu + \mu\mu$ plot to fit for a limit on the cross-section of SM HWW production at Tevatron, at the Higgs mass of $M_H = 180$ GeV. 49
22 Azimuthal angular separation between the leptons, $\Delta\phi(\ell,\ell)$, from the decay of $H \to WW^* \to \ell\nu\ell\nu$. Distributions of data, HWW^* signal ($M_H = 190$ GeV) MC, WW MC and the sum of other considered background MC samples are shown. The MCs are normalized to the expectations for the integrated luminosity for analyzed data, about 360/pb. We use the upper-left $ee + e\mu + \mu\mu$ plot to fit for a limit on the cross-section of SM HWW production at Tevatron, at the Higgs mass of $M_H = 190$ GeV. 50
23 Azimuthal angular separation between the leptons, $\Delta\phi(\ell,\ell)$, from the decay of $H \to WW^* \to \ell\nu\ell\nu$. Distributions of data, HWW^* signal ($M_H = 200$ GeV) MC, WW MC and the sum of other considered background MC samples are shown. The MCs are normalized to the expectations for the integrated luminosity for analyzed data, about 360/pb. We use the upper-left $ee + e\mu + \mu\mu$ plot to fit for a limit on the cross-section of SM HWW production at Tevatron, at the Higgs mass of $M_H = 200$ GeV. 51
24 Expected limits obtained from pseudo-experiments drawn from $\Delta\phi(\ell,\ell)$ distributions, for Higgs masses from 110-160 GeV/c^2. The red line represents the 95% CL extracted from data. 53
25 Expected limits obtained pseudo-experiments, drawn from $\Delta\phi(\ell,\ell)$ distributions, for Higgs masses from 170-200 GeV/c^2. The red line represents the 95% CL extracted from data. 54
26 The likelihood functions obtained from $\Delta\phi(\ell,\ell)$ distributions, for Higgs masses from 110-160 GeV/c^2. 55
27 The likelihood functions obtained from $\Delta\phi(\ell,\ell)$ distributions, for Higgs masses from 170-200 GeV/c^2. 56

1 Introduction

In the Standard Model, the Higgs mechanism generates the masses of the elementary particles and also stabilizes the high energy behavior of the electroweak interactions. The Standard Model does not predict the mass of the Higgs model, but there are direct and indirect constrains on the Higgs mass. The current best lower limit is $m_H > 114.4$ GeV, at 95% confidence limit (CL), established by direct searches, through the process $e^+e^- \to HZ$, by the LEP experiments [17]. The Higgs mass indirect limit, determined from the fit to the known data, is 98^{+52}_{-36} GeV and $m_H < 208$ GeV at 95% confidence level (CL) [18][1].

At the Tevatron the dominant SM Higgs boson production mechanism is gluon-gluon fusion, gg→H (Figure 1). The second Higgs production mechanism, quark-quark fusion, which produces a Higgs in association with a W boson, is about 2 orders of magnitude smaller.

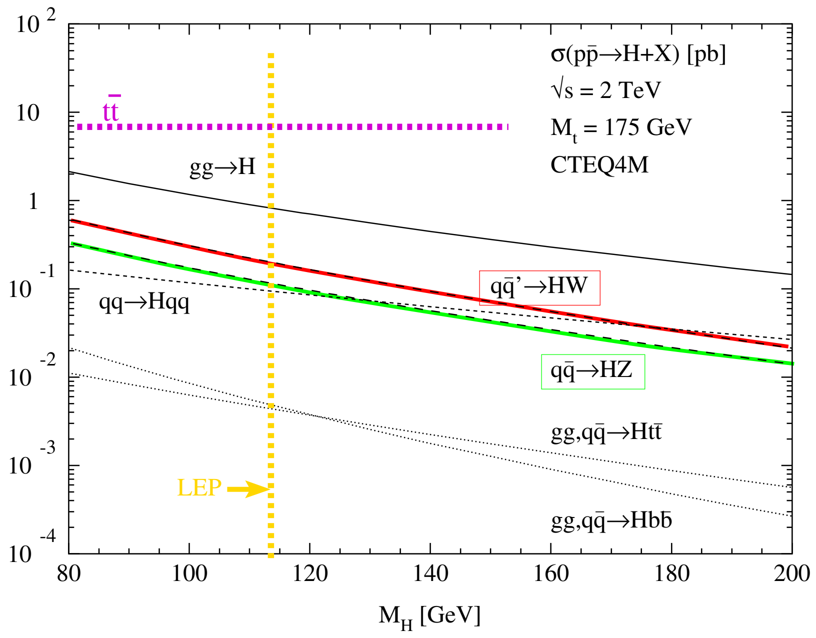

Figure 1: SM Higgs production versus the mass of the Higgs boson.

For Higgs masses greater than about 135 GeV/c^2, the decay branching ratio to W pairs becomes dominant as can be seen in Figure 2. In this analysis we search for $p\bar{p} \to H \to WW^*$ for Higgs masses ranging from 110 GeV/c^2 to 200 GeV/c^2, using the leptonic decays of both W bosons (Figure 3).

[1]This limits are obtained using the most recent top mass measurement, $m_{top} = 174.3 \pm 3.4$ GeV.

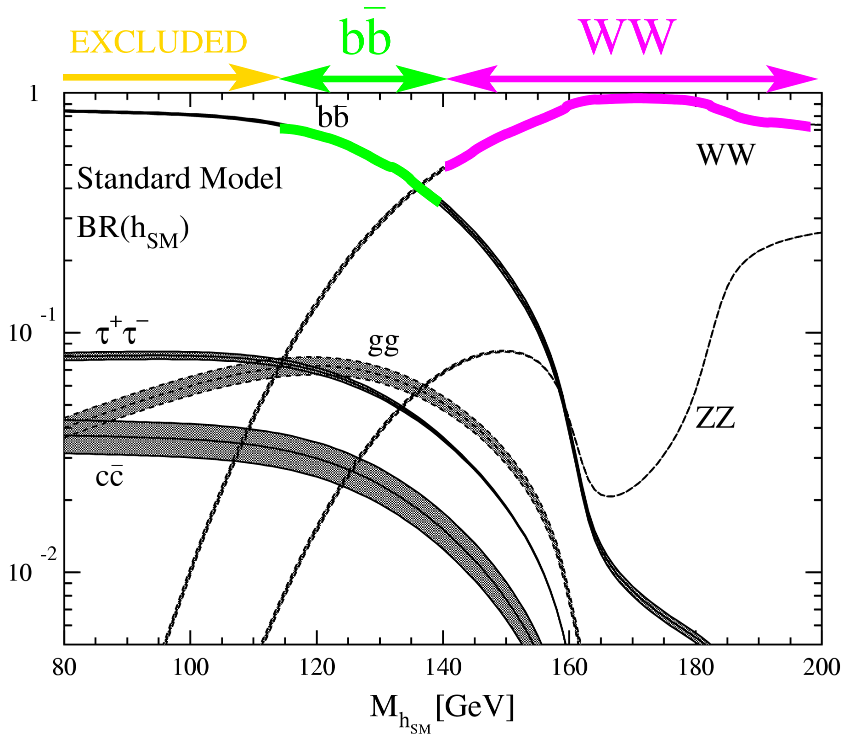

Figure 2: Relative branching ratios for Higgs boson decays.

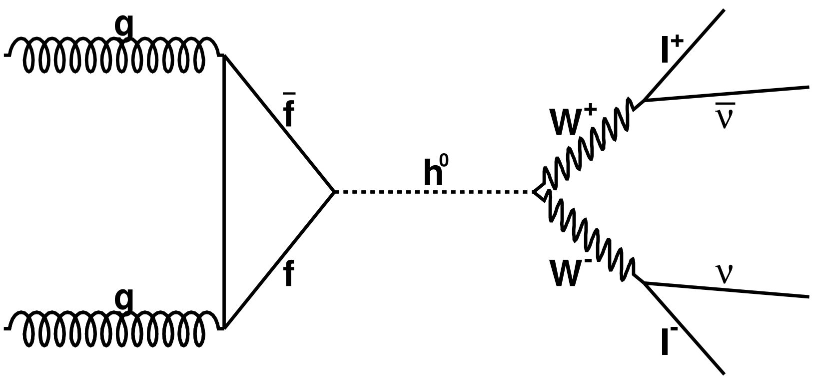

Figure 3: Feynman diagram for the dominant production mechanism, with both final state W's decaying leptonically.

At the LHC gg→H → WW → dileptons is one of the golden channels, so this analysis could be seen as a good training ground for the future, if we cannot discover the Higgs at the Tevatron [2].

[2]In fact near $M_H = 2^* M_W$ the decay mode Higgs to ZZ is suppressed, as can be seen in figure 2.

Also even if the SM cross-section for this channel is small, the new physics might enhance the signal. For example if a 4th SM generation of fermions exists, σ(gg$\rightarrow$ H) could be up to 8 times higher then the SM [2].

The standard model prediction of signal cross-sections and branching ratios, and the expected number of events in 360 pb^{-1} are shown in table 7, for different Higgs masses.

Higgs mass (GeV/c^2)	110	120	130	140	150	160	170	180	190	200
$\sigma(p\bar{p} \rightarrow H)$ (pb)	0.9	0.70	0.56	0.45	0.36	0.30	0.25	0.21	0.17	0.15
$BR(H \rightarrow WW)$	0.04	0.13	0.30	0.48	0.68	0.90	0.97	0.94	0.78	0.74
$H \rightarrow WW$ events in 360 pb^{-1}	13	33	60	78	88	97	87	71	48	34
$HWW\ell\nu\ell\nu$ events in 360 pb^{-1}	0.6	1.5	2.7	3.6	4.0	4.4	4.0	3.2	2.2	1.6

Table 1: The SM Higgs production cross section and branching ratios of H$\rightarrow$WW are presented [19]. Also we show the number of events produced in 360 pb^{-1}, where ℓ = e or μ.

Note that what we actually *observe* is the final row of numbers multiplied by the signal acceptance (which is of order 5%). Although the SM Higgs cross sections are at present too small to expect an observation, our search is also sensitive to other models as will be discussed in a later document. In addition this analysis can and will be combined with other searches using different decay channels.

2 Changes from the previous version of the note

2.1 September 27th, 2005

The following are the main changes to the analysis from the September 1st 2005 preblessing:

- We evaluated the pdf uncertainties using the JPM recommended Hessian method [3]. With the new PDF set CTEQ6M, the CTEQ group made available 40 complementary PDF sets CTEQ6M.01...CTEQ6M.40 each of which represents an up/down variation along one of the twenty eigenvectors (corresponding to 20 free parameters used in the fit). They form an orthonormal basis set spanning the full PDF parameter space [1]. Each up and down variation pair represents the range of PDF behavior that is consistent with the current global data. Each event in the Pythia HWW sample is reweighted according to the ratio of the CTEQ6M PDF values and the CTEQ6M.xx PDF values. We add the variations on acceptance in quadrature which results in (+2.76%/-3.44%). Then symmetrize and take 3% as systematic uncertainty.

  Also we compared MRST75 and MRST72, with different α_s values and find a 3.3 % difference taken as systematic error.

- We evaluated the error due to ISR on the acceptance, by generating two samples: ISR-more and ISR-less. A 3% unceratinty is assigned.

- We assign a 20% uncertainty to DY background due to the met modelling. We use the ratio between data and MC cut efficiency to quantify this.

- We updated Z→ $\ell\ell$ cross-section measurements in the electron and muons channels, after some bug fixes. The results agree well with the theoretical NNLO calculation (see section 7).

- Also the rest of the updates to the note are typos or improvements in the description of the analysis.

3 Event Selection

The signal process $p\bar{p} \to H \to W^+W^- \to \ell^+\ell^-\nu\bar{\nu}$, where $\ell = e$ or μ), results in the final state of *two leptons, missing energy (from undetected neutrinos) and no hard jets (possibly soft jets from initial state radiation(ISR)).*

3.1 Objects Identification

Leptons

We discuss lepton selection in detail in section 3.2.

Jets

The jets are the result of the fragmentation and hadronization of colored objects, such as quarks and gluons. There is assumed to be a one-to-one correspondence between a parton and its corresponding jet. The jets are clustered within a 0.4 cone and raw jet energies are applied level 5 energy corrections. We select jets with E_T(L5 corrected) > 15 GeV and $\eta_{detector} < 2.5$[3].

Missing energy

The *raw* $\not\!\!E_T$ is defined as the negative vector sum of the transverse energy in the calorimeter, both electromagnetic and hadronic:

$$\vec{\not\!\!E}_T = -\sum_i [(E_i^{em} + E_i^{had}) sin\theta_i] \times \hat{n}_i \tag{1}$$

where E_i^{em}, E_i^{had} are the electromagnetic, respectively hadronic energy of the i^{th} tower, and $\hat{n}_i$ is a transverse unit vector pointing to the center of each tower. The θ_i is the polar angle of the i^{th} tower with respect to the z=0 coordinate frame. The sum in the above equation extends to $|\eta| < 3.6$, to avoid the forward calorimeter region.

On top of the raw $\not\!\!E_T$ there are few corrections applied, before using $\not\!\!E_T$ for an event selection:

[3]From now on, unless explicitly stated, by *jet* we will refer to such an object, with E_T(L5 corrected) > 15 GeV and $\eta_{detector} < 2.5$.

- *Primary vertex correction*: The raw missing energy stored in CdfMet bank assumes that the event primary vertex is z = 0; using the full offline event information one reconstruct the event primary vertex and then recalculate ($\not{E}_{Tx}, \not{E}_{Ty}$).

- *Muon correction*: The muons are minimum ionizing particles and they deposit very little energy in the calorimeter. Therefore we add back to ($\not{E}_{Tx}$, $\not{E}_{Ty}$) the transverse energy deposited in the electromagnetic and hadronic calorimeter and subtract the COT beam constrained muon momentum components, (P_{Tx}, P_{Ty}). We correct *for all the muons*, passing the dilepton selection cuts; they could be CMUP, CMP-only, CMU-only, CMX or CMIO.

- *Jet correction*: Every jet is corrected for detector effects such as to get closer to parton level energies (as described above), before using it in the event selection. The missing energy is then corrected for the difference between the corrected and uncorrected jet transverse energies.

From this point on $\not{E}_T$ will refer to the corrected missing energy, unless explicitly stated otherwise.

3.2 Lepton identification

We select events with two leptons (electrons or muons) satisfying the criteria discussed below. To increase the signal acceptance from previous iteration of the analysis [9], we lowered the E_T requirements on the second leading lepton to 10 GeV, as will be justified in Section 3.5. For the highest p_T lepton, we follow the standard baseline cuts as recommended by the top and electroweak physics groups [15] and require that E_T to 20 GeV. For the lower E_T electron we loosen the p_T to 5 GeV for consistency with E/P cut(for electrons: E/P > 2.0).

In addition to the standard ID cuts, we require both leptons in the event to be isolated (for central electrons and all muons we require both track and calorimeter isolation, and for Phoenix electrons calorimeter isolation only). This simplifies and significantly reduces our fake background calculation and improves S/$\sqrt{B}$. We veto events with 3 leptons.

The identification of *electrons* in the *central part* of the detector is based on the cuts listed in table 2. The electrons are required not to be part of a conversion.

EM E_T	> 20 GeV
E_{HAD}/E_{EM}	$< \ 0.055 + 0.00045 \cdot$E
L_{shr}	< 0.2
Track P_T	>10 GeV/c (if EM $E_T \leq$100 GeV) >50 GeV/c (if EM E_T >100 GeV)
E/p	< 2 (if EM $E_T \leq$100 GeV)
$q \cdot \Delta x$	[-3.0, 1.5] cm
$\|\Delta z\|$	< 3 cm
χ^2	< 10
track $\|z_0\|$	< 60 cm
Track quality	3 axial and 2 stereo SL with at least 5 hits out of 12 in each SL
Fiducial	*fidele*=1 (Ces $\|X\|$ <21 cm, 9< Ces $\|Z\|$ <230 cm Tower 9 excluded, most of tower next to chimney included)

Table 2: Baseline cuts for central high-p_T isolated electrons ($E_T > 20$ GeV) (CEM) [15].

The cuts for lower E_T central electrons ($E_T > 10$ GeV) are identical with the baseline high-pt cuts, expect for $p_T > 5$ GeV.

For the identification of *electrons* in the *plug region* of the detector the silicon tracks are reconstructed with the *Phoenix* algorithm [8]. If the plug electron passes all requirements described in table 3, it is classified as Phoenix, denoted *PHX*. The cuts for lower E_T plug electrons ($E_T > 10$ GeV) are identical with the ones for PHX.

EM E_T	> 20 GeV
PhxMatch	true
E_{HAD}/E_{EM}	$< \ 0.05 + 0.026 \cdot \ln(\frac{\mathrm{E_{EM}}}{100})$ (if E_{EM} >100 GeV) $< \ 0.05$ (if $E_{EM} \leq$100 GeV)
PEM 3×3 Fit tower	$\neq$0
PEM 3×3 Fit χ^2	<10
PES 5×9 U and V	>0.65
PES based Fiducial	1.2< $\|\eta\|$ <2.0
Silicon track	2D Phoenix track
Number of Silicon Hits	$\geq$3
Track $\|z_0^{PHX}\|$	< 60 cm
$\Delta R(\mathrm{Track, PES})$	<3

Table 3: Baseline cuts for plug isolated electrons (PHX) [15].

All central electrons are required to be isolated:

- $I_{cal} < 0.1$: the ratio of calorimeter energy, excluding the electron EM energy, in a cone of 0.4 around the electron, to the electron tower energy be less than 0.1. The isolation is leakage corrected.

Track P_T	>20 GeV/c
Track $\|z_0\|$	< 60 cm
E_{EM}	< 2+Max(0,0.0115(P-100)) GeV
E_{HAD}	< 6+Max(0,0.028(P-100)) GeV
Track $\|d_0\|$	0.2 cm (if no silicon hits attached by OI) 0.02 cm (if silicon hits attached by OI)
$\|\Delta x_{CMU}\|$	< 3.0 cm (CMUP or CMU)
$\|\Delta x_{CMP}\|$	< 5.0 cm (CMUP or CMP)
$\|\Delta x_{CMX}\|$	< 6.0 cm (CMX)
Track quality	3 axial and 2 stereo SL with at least 5 out of 12 in each SL
Track $\|z_0\|$	< 60.0 cm
Fiducial Cuts ([12])	
For CMUP: For CMU-only: For CMP-only: For CMX	x-fid(CMP) < 0 cm, z-fid(CMP) < -3 cm - x-fid(CMP) < 0 cm, z-fid(CMP) < -3 cm x-fid(CMX) < 0 cm, z-fid(CMX) < -3 cm

Table 4: Baseline cuts for minimum ionizing isolated tracks [12]. After passing these cuts the muon is classified as *CMUP*, *CMX* or *non-triggering* according to the definitions in the text.

- $I_{trk} < 0.1$: the ratio of the sum of the transverse momenta for all tracks in a cone of 0.4 around the lepton in the $\eta - \phi$ plane, excluding the lepton track, to the P_T of the lepton be less than 0.1.

A muon is a minimum ionizing high-P_T track passing the baseline *muon* cuts (Table 4). All these tracks must be *calorimeter isolated* and *track isolated* following the same definitions as for electron above.

In addition we require in the data the following:

- a cosmic ray veto,
- the standard curvature correction applied for the beam position, and
- for CMX the triggering CMX leg is required to have a COT exit radius > 140 cm.

This minimum ionizing high-P_T isolated track will be classified as:

- A *CMUP* muon, if there are stubs in both the CMU and CMP detectors, with $|\Delta X|_{\rm CMU} < 3$ cm and $|\Delta X|_{\rm CMP} < 5$ cm respectively.
- A *CMX* muon, if there is one stub in the CMX detector, with $|\Delta X|_{\rm CMX} < 6$ cm.
- A *non-triggering muon*: this can be 3 different sub-categories, the information for which we will maintain for detailed studies of candidates, and internal consumption, etc., but which for presentation purposes we might lump into this one category for simplicity. A

non-triggering muon can only be the second leg in a dilepton event, and can appear in the following ways:

1. *CMU-only* (*CMP-only*) with a stub in the CMU (CMP) detector and non fiducial in the CMP (CMU) detector according to the muon fiduciality checking tool.
2. If there are no muon detector stubs, the minimum ionizing high P_t isolated track will be classified as a *CMIO*.

The cuts for lower P_T muons ($p_T > 10$ GeV) are identical to [6] and identical to those for high p_T except

- $E_{em} + E_{had} > 0.1$ GeV for CMIO;
- $E_{em} < 2$ GeV;
- $E_{had} < p_T/8 + 3.5$ GeV;
- $d_0 < 0.2$ cm;
- $\rho_{\text{COT exit}} > 140$ cm for CMIO and trigger CMX;
- trkFiducial==4 for CMIO;
- AxSeg >= 3 and StSeg >= 3 for all non-trigger muons.

3.3 Dilepton categories

We build a dilepton event with two baseline isolated leptons according to the categorizations in table 5. Compared with 4.11.1 categories, we took out PHX-PHX di-leptons, as they represent about 2% of acceptance, while bringing in large fake background.

3.4 Event Selection

After requiring events have 2 isolated leptons, of opposite charge, kinematic cuts are applied to reduce the background contributions while maintaining the bulk of the signal acceptance.

A cut on the lower bound of the $M_{\ell\ell}$ is applied to eliminate backgrounds from J/Ψ's, Upsilons and $b\bar{b}$. This does not significantly impact our Higgs signal.

The jet veto is applied to tight jets: *reclustered* jets with the JetClu 0.4 algorithm using the primary vertex and excluding towers from TCE and PHX isolated electrons, with corrected $E_T > 15$ GeV and $|\eta| < 2.5$. We correct jets using level 5 corrections. The high jet E_T threshold used increases our signal acceptance without significantly impacting our backgrounds. Only the events with 0, 1 and 2 jets, with further energy requirements, are selected. About 4% of the signal events ($M_H = 180$ GeV$/c^2$) have more than one jet, while only 0.1% have at least 3 jets.

ee		$\mu\mu$		$e\mu$	
1st leg	2nd leg	1st leg	2nd leg	1st leg	2nd leg
TCE	**TCE**	**CMUP**	**CMUP**	**TCE**	**CMUP**
	PHX		**CMX**		**CMX**
			CMU		CMU
			CMP		CMP
			CMIO		CMIO
		CMX	**CMX**	**CMUP**	PHX
			CMU	**CMX**	PHX
			CMP		
			CMIO		
				PHX	CMU
					CMP
					CMIO

Table 5: Dilepton categories included in the current analysis. Shown in bold are the triggerable lepton in the data samples studied. The one exception to this is the PHX categories. Both lepton legs are required to be isolated.

The $\not\!\!E_T$ is corrected for the primary vertex position and for the isolated muons identified in the dilepton category. The $\not\!\!E_T$ is also corrected for the jet corrections affecting tight jets (greater than 15 GeV).

The leptons are required to have opposite sign and trileptons are rejected.

An upper bound cut on $M_{\ell\ell}$ is made, which is a function of the Higgs mass.

These selection cuts depend on the mass of the Higgs and are summarized in table 10.

These cuts are very efficient for the Higgs signal (see table 41), while eliminating a significant amount of background. The exact values of the upper $M_{\ell\ell}$ bounds used were determined from maximizing $S/\sqrt{S+B}$ and then looking at the expected limits. As small variations around the maximum $S/\sqrt{S+B}$ have little impact on the expected limits, we tried to make them as simple and easy to remember as possible. So for $M_{\ell\ell}$ upper cut chosen the functional form of $M_H/2$-5.

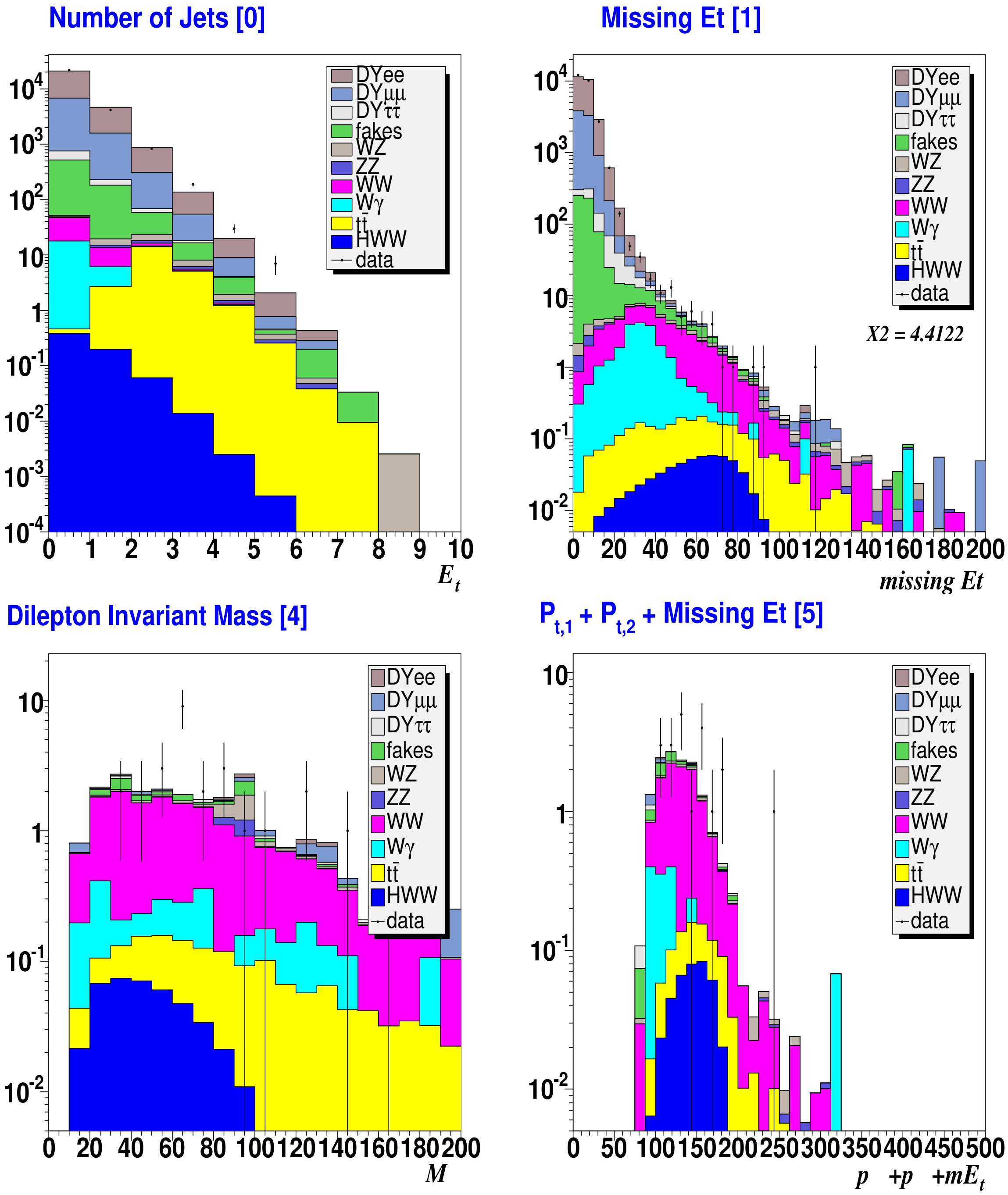

Figure 4: Four of the variables used in the event selection (for $M_H = 180$ GeV) are shown before cutting on that variable: (upper-left) number of jets; (upper-right) missing energy; (lower-left) dilepton invariant mass and (lower-right) $P_T(lep1)$ + $P_T(lep2)$+$\not{E}_T$.

Events passing these cuts are then used in the fits of the $\Delta\phi(\ell, \ell)$ distributions, discussed later.

Event selection steps are summarized in table 10.

3.5 Selection Optimization

The previous version of this analysis (which will be referred in the paper as *generation 4*) raised from the WW cross-section measurement, and therefore was not fully optimized for a Higgs search. We performed various optimizations, of which the most important ones are detailed below.

- *Lowering one of the lepton transverse momentum*

  The Higgs decays to two W boson, one on-shell, while the second is off-shell. The leptons coming from the off-shell W decay are softer than the ones from on-shell W decay, so an asymmetric cut is expected to help in this situation than the old (20, 20) cut. Figures 5, 6 show the highest vs the lowest lepton transverse momentum for two Higgs masses: 130 and 180 GeV. Figure 7 shows how the cut efficiency changes for various ($p_T(max)$, $p_T(min)$) cuts, for a M_H =130 GeV. Lowering the $p_T(min)$ from 20 to 10 GeV increases the fraction of events passing the kinematical cuts by 100%. Also the plots show that lowering the highest lepton p_T threshold is *not necessary*[4], as the acceptance gain is minimal, while the backgrounds are expected to increase. Table 6 summarizes the fraction of events passing various kinematical cuts, for three choices of
  ($p_T(max)$, $p_T(min)$): (20, 20), (20, 10) and (10, 10).
  (20, 10) is our choice as allows us to use the same triggers as in 4.11.1 and also increases the acceptance by 26-100% as compared with Gen 4.

[4]In doing the optimization we always have in mind the masses of the Higgs were we have the largest sensitivity: 160 and 170 GeV. Sure, lowering the highest lepton p_T would help for lower Higgs masses: 130 GeV or below.

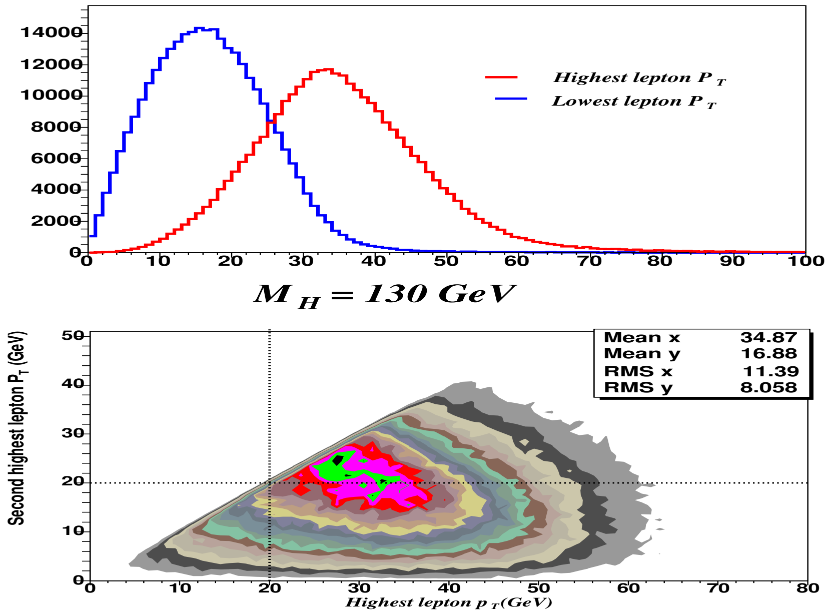

Figure 5: Highest lepton p_T vs the second highest lepton p_T for a 130 GeV Higgs.

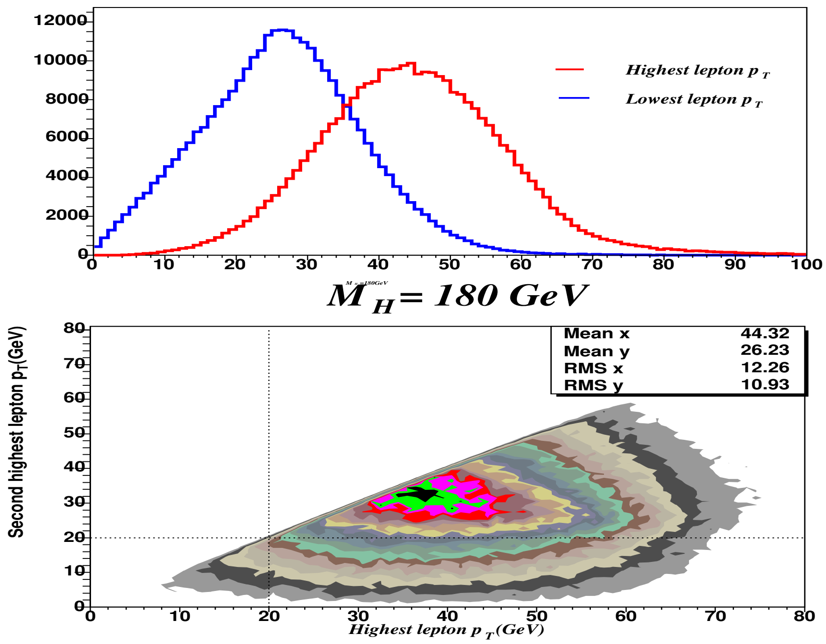

Figure 6: Highest lepton p_T vs the second highest lepton p_T for a 180 GeV Higgs.

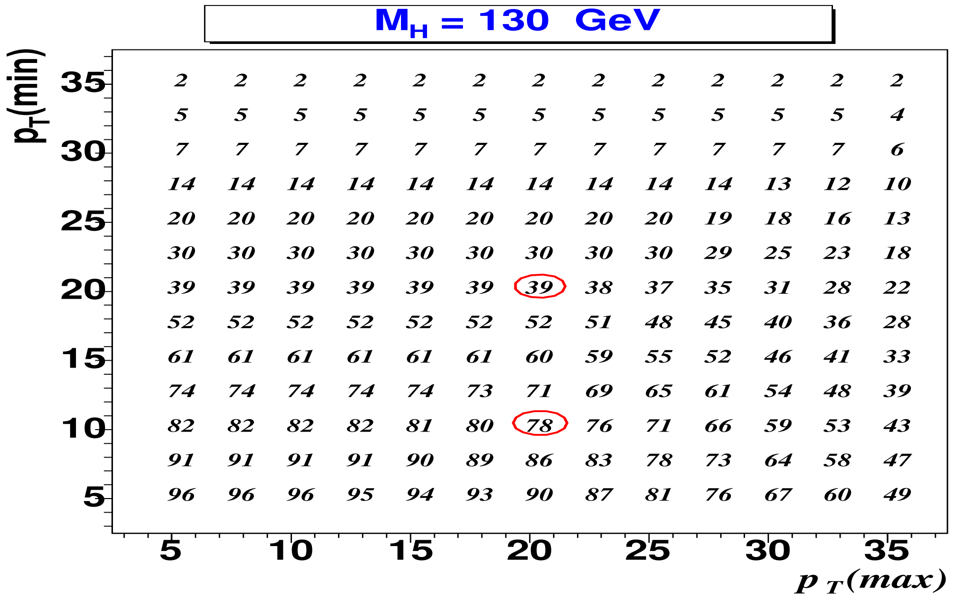

Figure 7: The fraction of events passing kinematical cuts on $p_T(max)$, $p_T(min)$, for a 130 GeV Higgs. The circled values show that the efficiency increases from 39 to 78 %, when lowering the transverse momentum requirement on the second lepton from 20 to 10 GeV.

$p_T(max)$, $p_T(min)$	ϵ(130 GeV)	ϵ(140 GeV)	ϵ(150 GeV)	ϵ(160 GeV)	ϵ(170 GeV)	ϵ(180 GeV)
(20, 20)	0.39	0.50	0.60	0.71	0.74	0.74
(20, 10)	0.78	0.84	0.88	0.83	0.92	0.93
(10, 10)	0.82	0.87	0.90	0.91	0.94	0.94

Table 6: Fraction of events passing various kinematics cuts, as a function of the Higgs mass.

- *Optimizing the missing energy*

  In the Higgs $\rightarrow$ W^+W^- $\rightarrow$ $\ell^+\nu\ell^-\bar{\nu}$, decay channel ($l = e$ or μ), the neutrinos are almost parallel (Higgs has spin 0), therefore signal missing energy tends to be higher then for WW, as also shown in figure 8. Increasing the missing energy threshold allows us to significantly reduce the total background, for a small reduction in the signal, improving S/$\sqrt{S+B}$ and the expected limits.

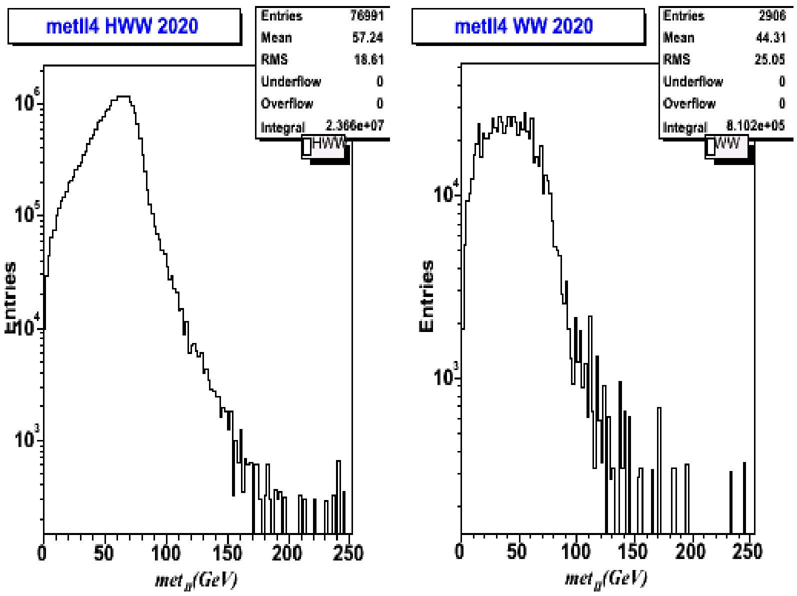

Figure 8: Missing energy for the signal (M_H=160 GeV) and WW background.

- *Changing the jet veto* The signal events tend to have very little jet activity. Only 4% of events have more than 1 jet (see section 3.1 for *jet* definition), while only 0.1% have 3 or more jets. Also the jets come from ISR, therefore are softer than the hard jets from $t\bar{t}$. Based on the above facts, we proposed to select the events with

  - 0 jets *or*
  - 1 jet $E_T < 55$ GeV *or*
  - 2 jets each $E_T < 40$ GeV.

The jet E_T spectrum for 1 jet and 2 jet events is shown in figure 9. Signal mass is 160 GeV. The new jet cut efficiency for the signal is about 90%.

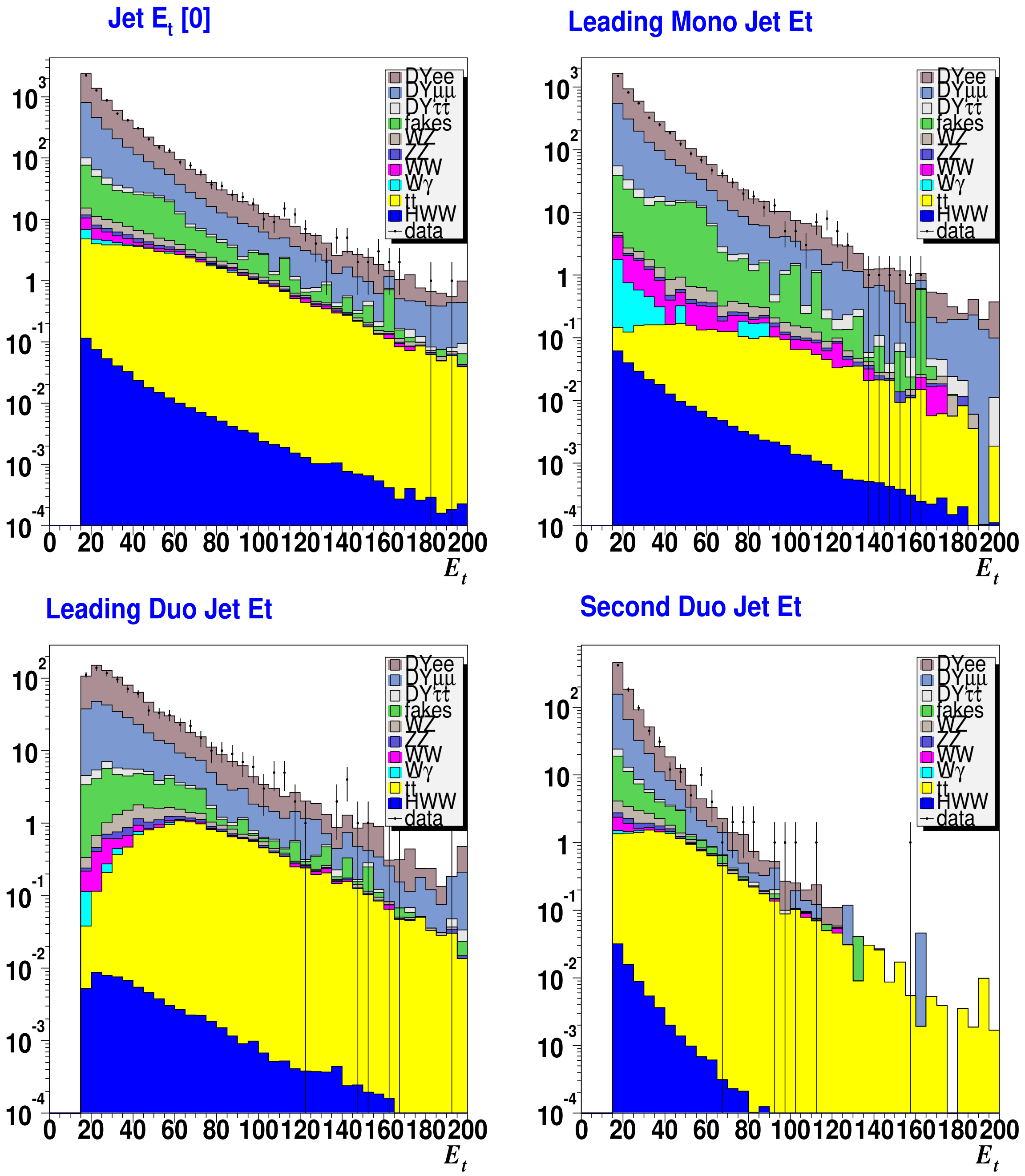

Figure 9: Jet E_T spectrum is shown before the jet veto, for: (upper-left) any number of jets event; (upper-right) only for 1-jet events; (lower-left) the leading jet in 2-jet events; (lower-right) the second jet in 2-jet events. Also the data point are shown, for 360/pb. The plots are made after requiring 2 good leptons, with $m_{\ell\ell} > 16$ GeV.

- *2D Optimization: Missing energy versus Jet E_T threshold*

Higgs mass (GeV)	110	120	130	140	150	160	170	180	190	200
DY (without $\Delta\phi$)	16.12	16.69	10.95	7.24	5.47	3.32	2.26	1.70	1.29	0.97
DY bg (with $\Delta\phi$)	2.29	1.88	1.57	1.31	1.44	0.85	0.91	0.86	0.93	0.97

Table 8: The DY background as a function of Higgs mass with or without the cut ($\not\!\!E_T > 50$ GeV $||\Delta\phi(\not\!\!E_T$, lep/jet$) > 0.35$)).

The final $\not\!\!E_T$ and jet thresholds were chosen based on the expected limits. For this we perform 1000 pseudo-experiments for each 2D point, histogram the 95% CL and use the median of the distribution as the most probable 95% CL.

M_H	$\not\!\!E_T$ def	E_Tj+5	E_Tj+10	E_Tj+15	E_Tj+20	$\not\!\!E_T$-10	$\not\!\!E_T$-5	$\not\!\!E_T$+5	$\not\!\!E_T$+10	$\not\!\!E_T$+15	$\not\!\!E_T$+20	$\not\!\!E_T$+25	$\not\!\!E_T$+30
110	10.85	10.78	10.91	11.49	11.36	12.13	11.30	10.72	11.43	13.77	23.33	39.22	46.08
120	8.4	8.2	8.305	8.341	8.53	8.586	8.716	8.02	8.283	9.746	13.55	26.68	42.58
130	6.84	6.879	6.738	6.77	7.016	7.253	6.962	6.535	7.111	7.86	10.79	16.43	31.74
140	5.7	5.669	5.742	5.856	5.596	6.357	6.107	5.77	6.111	6.636	8.219	12.38	25.35
150	5.05	4.926	5.089	4.966	5.083	5.338	5.25	4.910	5.125	5.487	6.328	8.953	14.51
160	3.95	4	3.904	3.95	3.92	4.280	4.135	3.896	3.946	4.157	4.510	5.529	7.840
170	3.72	3.678	3.677	3.694	3.618	4.196	3.847	3.672	3.670	3.826	4.142	4.95	6.529
180	3.988	3.896	3.97	3.9	3.937	4.261	4	3.9	3.844	3.91	4.287	5.3	6.952

Table 7: Results of varying the $\not\!\!E_T$ and 1-jet E_T threshold. Defaults are $\not\!\!E_T < M_H/4$ and ${E_T}^{\text{1-jet}} < 50$ GeV. We show the default expected limits, expected limits when changing the cut for the 1-jet Et from 50 to $50 + 5, +10, +15, +20$ GeV, and also expected limits for $\not\!\!E_T < M_H/4 - 10, -5, +5, +10, +15, +20, +25, +30$ GeV.

- *DY background suppression for low masses*

  We retained the cut ($\not\!\!E_T > 50$ GeV $||\Delta\phi(\not\!\!E_T$, lep/jet$) > 0.35$) from previous top, WW and HWW dilepton analyses to suppress the large DY background spared by the lower $\not\!\!E_T$ cut for lower Higgs masses. See Table 8.

4 Monte Carlo Datasets

Monte Carlo datasets were simulated using mcProduction package, runMC executable, in release 5.3.2. The samples used for signal and backgrounds, the MC generator, their dataset ids and the cross-sections are shown in table 9.

Process	Generator	Dataset ID	$\sigma(pb)$	# Events
		Signal		
H$\to$WW (M_H = 110 GeV)	PYTHIA	wexobw	0.004	1143420
H$\to$WW (M_H = 120 GeV)	PYTHIA	wexocw	0.009	1137034
H$\to$WW (M_H = 130 GeV)	PYTHIA	wexo5w	0.017	1199597
H$\to$WW (M_H = 140 GeV)	PYTHIA	wexo6w	0.022	1136447
H$\to$WW (M_H = 150 GeV)	PYTHIA	wexo7w	0.025	1162684
H$\to$WW (M_H = 160 GeV)	PYTHIA	wexo8w	0.028	1118660
H$\to$WW (M_H = 170 GeV)	PYTHIA	wexo9w	0.025	1106451.
H$\to$WW (M_H = 180 GeV)	PYTHIA	wexoaw	0.020	1153345
H$\to$WW (M_H = 190 GeV)	PYTHIA	wexodw	0.014	-
H$\to$WW(M_H = 200 GeV)	PYTHIA	wexoew	0.011	-
		Backgrounds		
Z/γ $\to$ ee	PYTHIA	zewk6d	355.2 $\times$ 1.4	3108482.
Z/γ $\to$ $\mu\mu$	PYTHIA	zewk6m	355.2 $\times$ 1.4	3216951
Z/γ $\to$ $\tau\tau$	PYTHIA	zewk8t	355.2 $\times$ 1.4	3338836
Z/γ $\to$ $\ell\ell$	PYTHIA	sexo8t	17354.0 $\times$ 1.4	3164279
WW	PYTHIA	wtop1w	12.4	419728
WZ	PYTHIA	wtop1z	3.65	407438
ZZ	PYTHIA	ztopcz	1.39	397086
W γ $\to e^+\nu$ γ	PYTHIA	ktop2e	22.35	68273
W γ $\to e^+\nu$ γ	PYTHIA	ktop3e	22.35	102473
W γ $\to\mu^+\nu\gamma$	PYTHIA	ktop2m	22.35	93073
W γ $\to\mu^+\nu$ γ	PYTHIA	ktop3m	22.35	103608
t$\bar{t}$	PYTHIA	ttopel	6.7	1142339

Table 9: Monte Carlo datasets used for HWW analysis.

5 Signal Acceptances

The signal acceptance was evaluated using PYTHIA MC samples for each Higgs mass (110-200 GeV). The samples used are wexo5w-wexoew, and consist of about 1.2M events each, with both W bosons forced to decay leptonically: $W \to l\nu$, where $l = e, \mu, \tau$. The HWW acceptances with respect to the numbers of events decaying leptonically, are shown in Fig 10. Also on the same plot the values from 4.11.1 analysis are shown. After the optimization we increased the acceptance up to a factor of 3, for lower Higgs masses.

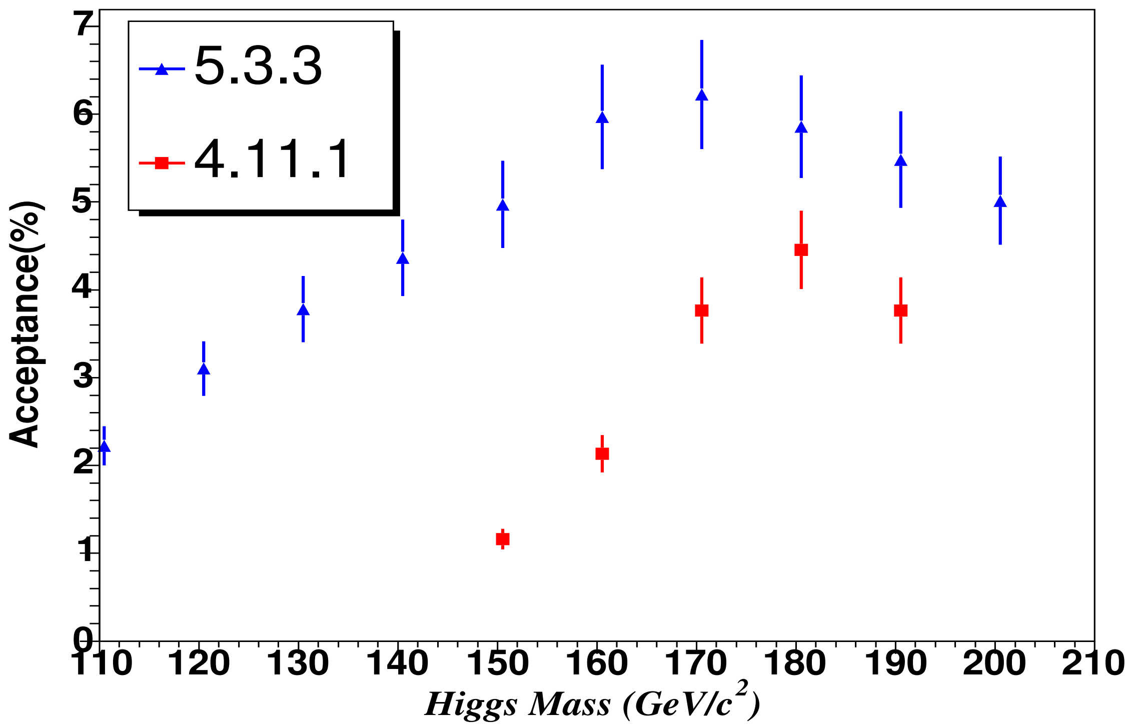

Figure 10: Signal acceptance for various Higgs masses. For comparison the generation 4 values are also shown.

Table 41 shows the detailed signal efficiencies after every single cut, for a Higgs of 160 GeV.

Index	Event Selection
1	two leptons with ${p_T}^{\ell_{\text{trigger, non-trigger}}} > 20, 10$ GeV
2	$M_{\ell\ell} > 16$ GeV
3	nJets($E_T > 15$ GeV) = 0 || nJets($E_T < 55$) = 1 || nJets($E_T < 40$) = 2
4	$\not\!\!E_T > M_H/4$
5	$M_H > 150$ GeV || ($\not\!\!E_T > 50$ GeV || $\Delta\phi(\not\!\!E_T$, lep/jet) > 0.35)
6	opposite lepton charge signs
7	$M_{ll} < M_H/2 - 5$ GeV
8	${E_T}^{\ell_1} + {E_T}^{\ell_2} + \not\!\!E_T < M_H$

Table 10: Event Selection for the HWW analysis.

6 Scale Factors

We correct for trigger inefficiencies (see Table 11) using the official blessed values.We correct for the difference in lepton identification efficiencies between data and MC by applying the scale factors shown in Table 12. We also correct PHX for charge mis-identification as shown in Table 13 after requiring the event selection cut [6] as in Table 10.

Lepton Type	Trigger Efficiency
TCE	0.962 ± 0.066 [10]
PHX	0.955 ± 0.019 [11]
CMUP	0.908 ± 0.005 [12]
CMX	0.965 ± 0.004 [12]

Table 11: Summary of trigger efficiencies. The CEM_18 trigger efficiency is run-dependent, number given above being an average over η. We use the MET_PEM trigger efficiency as estimated in 4.11.1. The contribution from dilepton categories triggered by PHX is below 15%.

$\lvert\eta_{\mathrm{PHX\ PES}}\rvert$ Range	Data/MC Scale Factor
$1.2 < \lvert\eta\rvert < 1.4$	$(1 - 0.061)/(1 - 0.061)$
$1.4 < \lvert\eta\rvert < 1.6$	$(1 - 0.099)/(1 - 0.097)$
$1.6 < \lvert\eta\rvert < 1.8$	$(1 - 0.150)/(1 - 0.143)$
$1.8 < \lvert\eta\rvert < 2.0$	$(1 - 0.168)/(1 - 0.138)$

Table 13: PHX charge mis-identification scale factors [7].

Lepton Type	ID×Reconstruction Scale Factor	
	$p_T < 20$ GeV	$p_T > 20$ GeV
TCE	1.03 ± 0.02 [5]	0.996 ± 0.005 [7]
PHX	-	0.948 ± 0.016 [7]
CMUP	0.85 ± 0.05 [6]	0.892 ± 0.009 [12]
CMX	0.90 ± 0.05 [6]	0.999 ± 0.006 [12]
CMU	-	0.889 ± 0.010 [12]
CMP	-	0.907 ± 0.009 [12]
CMIO	1.00 ± 1.00 [6]	0.995 ± 0.003 [12]

Table 12: Summary of lepton data/MC scale factors.

7 Measuring Z→ $\ell\ell$ cross-sections

To validate the scale factors discussed in section 6, we measured four Z cross-sections, two in the electron and two in the muon channels. The results are shown in table 14.

For the muon cross-sections, the first muon in the trigger one, while the second can be any muon, used in current analysis: CMUP/CMX/CMU/CMP/CMIO, all defined in section 3. The results agree very well with an independent measurement, performed using the same amount of data, $\sigma(\mathrm{Z}\rightarrow_{\mu\mu})$= 261.2 ± 2.7$\pm^{5.8}_{6.9}$ ± 15.1pb([4]).

Also the measurements agree with the NNLO calculation: $\sigma(\mathrm{Z}\rightarrow_{\ell\ell})$= 250.5 ± 3.8 pb.

Dilepton Type	σ_Z (pb)
TCE-TCE	$259.3 \pm 3.3(stat) \pm 5.4(syst) \pm 15.4(lumi)$
TCE-PHX	$262.6 \pm 3.2(stat) \pm 23.0(syst) \pm 15.5(lumi)$
CMUP-CM(UP/X/U/P/IO)	$260.9 \pm 3.5(stat) \pm 5.8(syst) \pm 15.4(lumi)$
CMX-CM(UP/X/U/P/IO	$259.7 \pm 4.6(stat) \pm 5.4(syst) \pm 15.3(lumi)$

Table 14: Summary of Z cross-section measurements.

8 $H \rightarrow WW$ Acceptance Systematic Uncertainties

Potential sources of systematic uncertainty on the $H \rightarrow WW \rightarrow l^+l^-\nu\bar{\nu}$ acceptance are summarized in table 15 and described below.

	Systematic Error (%)
ISR	3
α_s	3.3
PDF Acceptance	3
Jet Energy Scale	1
Lepton ID	2
Track Isolation	2
Trigger Efficiency	1
Combined	6

Table 15: Sources of systematic uncertainty on the $H \rightarrow WW \rightarrow l^+l^-\nu\bar{\nu}$ acceptance.

8.1 PDF Uncertainty

We evaluated the pdf uncertainties using the JPM recommended Hessian method [3]. With the new PDF set CTEQ6M, the CTEQ group made available 40 complementary PDF sets CTEQ6M.01...CTEQ6M.40, each of which represents an up/down variation along one of the twenty eigenvectors (corresponding to 20 free parameters used in the fit). They form an orthonormal basis set spanning the full PDF parameter space [1]. Each up and down variation pair represents the range of PDF behavior that is consistent with the current global data used in the fit. Each event in the Pythia HWW sample is reweighted according to the ratio of the CTEQ6M PDF values and the CTEQ6M.xx PDF values. We add the variations on acceptance in quadrature, which results in (+2.76%/-3.44%). Then symmetrize and take 3% as systematic uncertainty.

8.2 ISR-more/less

We generated two samples, for 160 GeV Higgs mass, with more/less initial state radiation settings, kindly provided by Un-ki Yang. We estimate the change in the acceptance and find to be 3%, which is assigned as a systematic uncertainty.

8.3 α_s

We compare the acceptance for two sets of PDFs: MRST72 ($\alpha_s = 0.1175$) and MRST75 ($\alpha_s = 0.1125$), with different α_s. There is a 3.3 % difference, which is assigned as a uncertainty.

8.4 Jet Energy Scale

To estimate the systematic uncertainty associated with the jet energy scale, we follow the prescription described in [16]: Vary each jet correction factor by +1 σ, respectively -1 σ, and sum the variations on acceptance in quadrature to get up/down errors. This prescription is used for all the Higgs masses signal samples. The uncertainties are within 1%, and this is due to the fact that we raised the jet threshold compared with generation 4.11.1 analysis to 50 GeV and all jets in the signal events come from ISR.

8.5 Lepton ID

Using the identification and reconstruction efficiencies scale factors (data/MC) shown in table 12, we estimate an uncertainty of 2%.

8.6 Track Isolation

We determine the track isolation efficiency ϵ_{triso} using Z→ ee and Z→ mm data samples.

$$\epsilon_{triso} = \frac{N_{\ell \mathrm{id+caliso+trkiso}}}{N_{\ell \mathrm{id+caliso}}} \tag{2}$$

where the denominator represent the number of leptons passing all the id cuts, including calorimeter isolation; the numerator consist of all the denominator leptons passing also the track isolation. The scale factors shown in table 16 are well within 1% of unity. See also figures 11 and 12, where "prediction" refers to Monte Carlo-based efficiency, while "observation" is the data track isolation efficiency. We take the uncertainty on single lepton 1%, and total uncertainty 2%.

Lep.Type	Data/MC SF
TCE	1.00
CMUP	1.00
CMX	0.99
CMP	1.00
CMU	0.99
CMIO	0.99

Table 16: Track isolation scale factors (data/MC) for all the lepton types used in the HWW analysis. The statistical error are all below 1%.

8.7 Trigger Efficiency

Central trigger efficiencies are all below 1%, the largest one is on MET_PEM trigger [13]. This affects only categories triggered by the PHX electrons, representing about 15% of the total. The overall uncertainty becomes 1%.

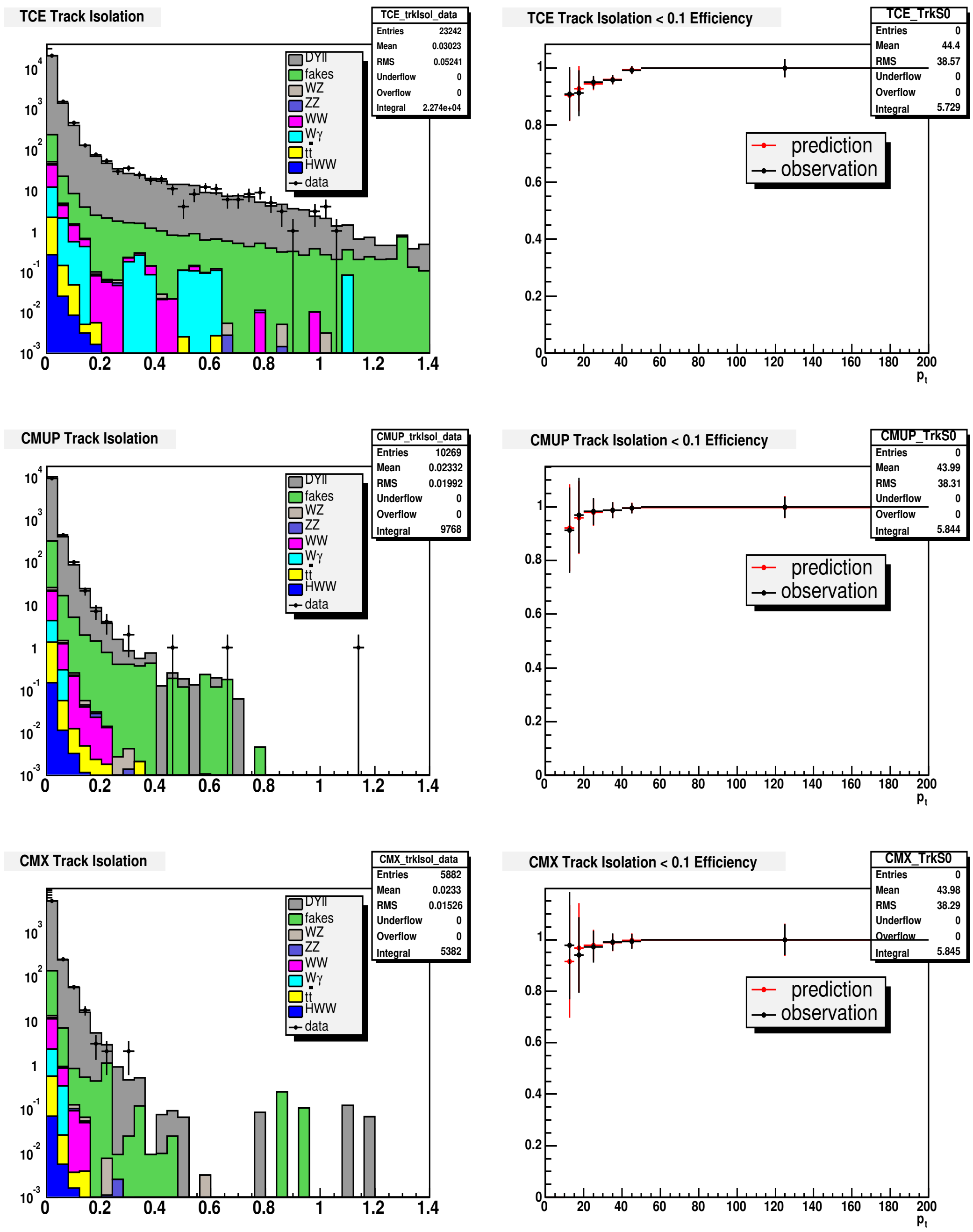

Figure 11: Track isolation distributions per trkIsol-required lepton type and the cut efficiencies from data or MC as a function of lepton p_T.

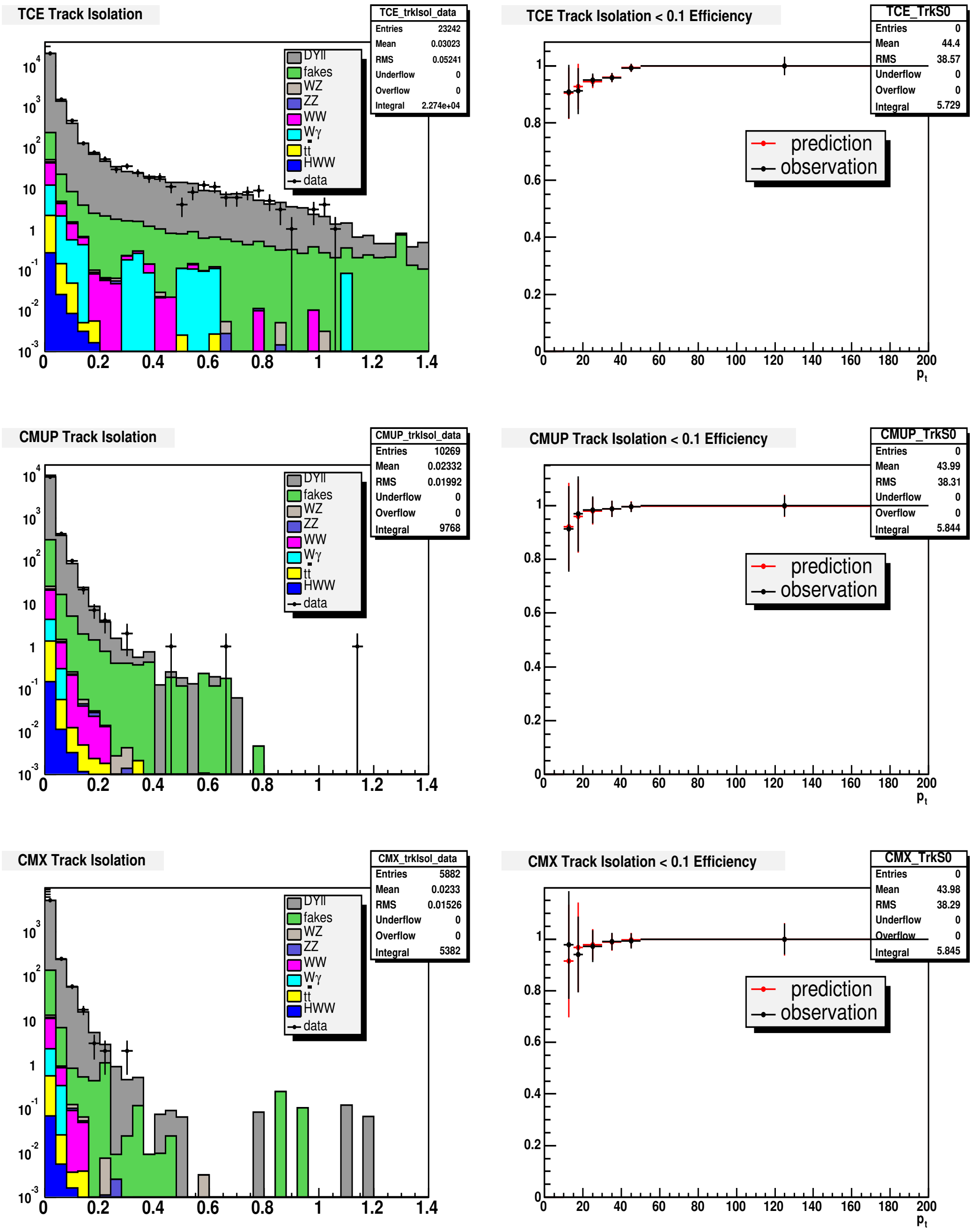

Figure 12: Track isolation distributions per trkIsol-required lepton type and the cut efficiencies from data or MC as a function of lepton p_T.

8.8 Combined Acceptance Systematic

The sources of systematic uncertainties from table 15, added in quadrature, result in an uncertainty of 6% of the HWW signal.

9 Background Estimates

The main background (50 to 60% of the total) is from SM WW production. Smaller contributions arise from $t\bar{t}$, WZ, ZZ, $W\gamma$, Drell-Yan e^+e^-, $\mu^+\mu^-$ and $\tau^+\tau^-$, and $W + jets$ events, where a jet fakes a lepton. All the backgrounds are estimated using Monte Carlo samples, except for the fake contribution, determined entirely from data.

9.1 WW background

To estimate the WW background, we used a PYTHIA MC sample (dataset ID: wtop1w) of 0.4M inclusive WW events. A cross-section $\sigma(p\bar{p} \to WW) = 12.4 \pm 0.8$ pb is assumed to estimate the sample luminosity. The efficiencies of the WW background after each of the cuts for HWW search are shown in Table 42, for $M_H = 160$ GeV criteria. The cuts $M_{\ell\ell} < M_H/2$ and requiring large missing energy are relatively effective on reducing the inclusive WW dilepton background.

9.2 $t\bar{t}$ background

$t\bar{t}$ background is estimated using a PYTHIA MC sample (dataset ID: ttopel) consisting of 1.2M $t\bar{t}$ events. The sample assumed the mass of top quark $m_{\rm top} = 178$ GeV and the (theoretical best) cross-section $\sigma(p\bar{p} \to t\bar{t}) = 6.7$ pb. Acceptance of the $t\bar{t}$ background through each of the cuts for HWW search is in Table 44, for $M_H = 160$ GeV criteria. We see that the 0-jet cut is very effective in reducing the $t\bar{t}$ background. We will switch to a 175 GeV sample soon.(closer to top mass world average.)

9.3 Drell-Yan background

To estimate the Drell-Yan ll background, we used a PYTHIA MC sample (dataset id: sexo8t), of 3M $Z/\gamma^* \to ll$ events. ee, $\mu\mu$, and $\tau\tau$ were generated together. The sample was HEPG-filtered, with the efficiency around 2.9%, requiring two leptons, e or μ; the electrons with p_T >3.6 GeV and $|\eta|$ <1.4, the muons with pt>4.8 GeV and $|\eta|$ <1.4. The process was leading order only, so a factor $k_{\rm NNLO/LO} \simeq 1.38$ was applied. The process cross-section was determined to be 17354 pb. Acceptance of the DY ll background through each of the cuts for HWW search is in Table 45, for $M_H = 160$ GeV criteria . Also we cross-checked the estimate using electroweak samples with extra min bias, *zewk6d, zewd6m* and *zewk8t.* The estimates are consistent. We see that the cut on the upper $M_{\ell\ell}$ mass bound is the most effective on reducing the Drell-Yan background.

9.4 Fake background

The main source of fakes is W + multi-jet processes, with one jet/track misidentified as a lepton. To estimate the background due to fakes we use the following procedure:

- Step 1: calculate the jet-like-objects faking a lepton probability, i.e.fake ratio, for each lepton type using Jet 20, Jet 50, Jet 70 and Jet 100 samples. Use the average fake ratio over all four jet samples in step 2.

- Step 2: search the high-p_t electron/muon inclusive data samples for jet-like objects (defined in step 1) that might fake a lepton and passing the event selection criteria (described in section 3) – let's call such events "fakeable events".

- Step 3: apply the fake ratios to the fakeable objects to estimate how many events in data might be fakes.

The fake background, with few associated cross-checks, has been evaluated using data, and written up in a separate note [11]. In this document we just give the results for brevity.

9.5 $W\gamma$ background

The samples used to estimate this background were generated using Baur and Berger's WGAMMA program [21], using the following cuts: $|\eta^{lepton}| < 10$, $E_T^{\gamma} > 5.0$ GeV, $|\eta^{gamma}| < 10$ and $\Delta R(l, \gamma) > 0.2$ [20]. The details about four samples used are shown in table 47. The systematic uncertainties on $W\gamma$ are shown in table 18. The first three uncertainties are taken from the W+γ PRL. [22].

Sample	Events	Cross-section (pb)	DFC ID
W$\gamma \to e^+\nu$	70k	22.35	ktop2e
W$\gamma \to e^-\nu$	100k	22.35	ktop3e
W$\gamma \to \mu^+\nu$	90k	22.35	ktop2m
W$\gamma \to \mu^-\nu$	100k	22.35	ktop3m

Table 17: $W\gamma$ MC samples used to estimate the background to HWW.

9.6 WZ and ZZ background

To estimate the WZ background we used a PYTHIA MC sample (dataset ID: wtop1z) of 0.4M inclusive WZ events. The cross-section is $\sigma(p\bar{p} \to WZ) = 3.96$ pb. Acceptance of the WZ background through each of the cuts for HWW search is in Table 43, for $M_H = 160$ GeV criteria. A ZZ PYTHIA sample containing 0.4M events (dataset id: ztopcz) was used to estimate the background from ZZ. The ZZ cross-section is $\sigma(p\bar{p} \to WZ) = 1.39$ pb (NLO).

9.7 Background systematic uncertainties

We summarize the systematic uncertainties on the backgrounds in table 18.

For WW/WZ we determined the jet energy scale uncertainty to be 1%.

The fake uncertainty and details of the fake calculation are described in [11].

We are in the process of checking the systematic uncertainty due to MC generators for $t\bar{t}$. The current value (6%) was determined in the context of top dilepton analysis [23]. Similarly for ISR/FSR uncertainties. Also we are redoing the jet energy scale systematic uncertainty.

For Wγ we use an uncertainty due to the events unweighting and K-factor error, described in [20], page 14. This is appropriate as we used the same 4.11.1 samples used in [20], stripped for HEPG and reprocessed with 5.3.2 Simulation.

For Drell-Yan we were worried about the missing energy or jet multiplicity modeling of the MC. We selected events with 2 leptons passing the analysis cuts. We checked the ratio of missing energy cut efficiency for data and MC for various thresholds. The numbers agree well within the errors, however the statistics is very limited beyond 30 GeV. We use the statistical errors as an estimate of the potential difference in the met cut efficiency between data and MC; we quote a 20 % uncertainty on DY due to missing energy cut.

- $\frac{\epsilon_{data}}{\epsilon_{MC}} = 0.92 \pm 0.06$, for $\not{E}_T > 20$ GeV

- $\frac{\epsilon_{data}}{\epsilon_{MC}} = 1.02 \pm 0.15$, for $\not{E}_T > 30$ GeV

- $\frac{\epsilon_{data}}{\epsilon_{MC}} = 1.13 \pm 0.13$, for $\not{E}_T > 40$ GeV

Also we compared the cut efficiency for data and MC for jet veto cut and they agree well. We restrict to the events with 0, 1 or two jets.

Background	Source	Uncertainty (%)
WW	Jet Veto ("jet modeling")	6
	PDF/Q^2 Effect on $\sigma(WW)$	5
	Generator/Parton Shower Model	4
	Lepton ID SF	2
	Jet Energy Scale	1
	PDFs on Acceptance	1
	Track Isolation	2
	Trigger Efficiency	1
WW	Total	9
WZ/ZZ	Total (same as WW)	9
Fakes	Different Jet Samples	100
$t\bar{t}$	Lepton ID SF	2
	Jet Energy Scale	5
	MC Generators (Pythia vs Herwig)	6
	PDF's	1
	ISR/FSR	1.7
$t\bar{t}$	Total	8
Drell-Yan	Jet Energy Scale	1
	Lepton ID SF	2
	Track Isolation	2
	PDF on Acceptance	2
	Trigger Efficiency	1
	Missing Energy Data/MC	20
Drell-Yan	Total	20
W γ	Factorization scale	2
	Renormalization scale	3
	PDF	5
	Jet Energy Scale	1
	Unweighting and k-factor error	2
W γ	Total	7

Table 18: Sources of systematic uncertainties on the backgrounds. To all these uncertainties we add in quadrature 6% coming from luminosity.

10 Data analysis

10.1 Data samples and luminosity

We use the inclusive high-P_T lepton triggered samples, processed with version 5.3.1 Production. The central electrons (CEM) came in on $ELECTRON\_CENTRAL\_18$ trigger and correspond to the datasets bhel0d. The muons were collected on the two triggers: $MUON\_CMUP18$ and $MUON\_CMX18$ and are in the bhmu0d dataset. The plug electron samples we use were also processed with 5.3.1 Production; they were collected with MET_PEM trigger, which additionally requires large missing energy ($\not\!\!E_T > 15$ GeV), to keep the rates low. The associated dataset is ptop00, stripped from bpel0d.

Version 7 of the DQM good run list of the Top, EWK and Exotics groups is applied [5]. This covers all the runs numbers up to 186598 and does not include the "COT-compromised" period, where the lower gains affected the COT tracking efficiency (run range 179096-182842). However we note the following:

- In the ee channel we apply the good run list without muon requirements.
- We have applied the good run list without silicon checks to the events that do not contain a PHX in the dilepton category.
- For dilepton events with a PHX (TCE-PHX, PHX-PHX, CMUP-PHX, CMX-PHX, PHX-CMU, PHX-CMP, PHX-CMIO) the good run list with good silicon has been applied. Only about 15% of the acceptance comes from events with a plug electron.

Dilepton Combination Type	Good Run List	Offline $\mathcal{L}_{int}$ (pb^{-1}) +1.9% correction and $\pm$5.9% errors
TCE-TCE	1001	374 ± 22
PHX-{TCE, PHX}	1101	343 ± 21
TCE-{CMUP, CMU, CMP, CMIO}	1031	366 ± 22
TCE-CMX	1021	333 ± 20
PHX-{CMUP, CMU, CMP, CMIO}	1131	337 ± 20
PHX-CMX	1121	310 ± 19
CMUP-{CMUP, CMU, CMP, CMIO}	0031	378 ± 23
CMX-{CMUP, CMX, CMU, CMP, CMIO}	0011	339 ± 20

Table 19: Luminosities of the different di-lepton categories used in the analysis.

.

The luminosities relevant for our dilepton categories are summarized in table 19. These luminosities, together with the relative acceptances in the HWW dilepton categories, gives us an average luminosity of:

$$\mathcal{L}_{HWW} = (360 \pm 22)\,\mathrm{pb}^{-1}$$

10.2 Energy Scale factors for Plug electrons.

We correct phoenix electron energy with scale factors as listed in Table 20, bringing the $Z \to e_{\mathrm{TCE}} e_{\mathrm{PHX}}$ mass peak to 91 GeV as shown in Figure 13. The run range division was inherited from 4.11.1 diboson analyses [13, 14].

[5] http://www-cdf.fnal.gov/internal/dqm/goodrun/v7/goodv7.html

run range	Data		MC	
	east	west	east	west
141544-159600	1.041	1.048	1.38	1.039
159601-163600	1.035	1.030	1.41	1.037
163601-168889	1.047	1.033	1.40	1.039
168890-186598	1.080	1.077	1.37	1.039

Table 20: Phoenix electron energy scale factors divided by run range, plug side ($\eta > 0$ for east; $\eta < 0$ for west) and data/MC.

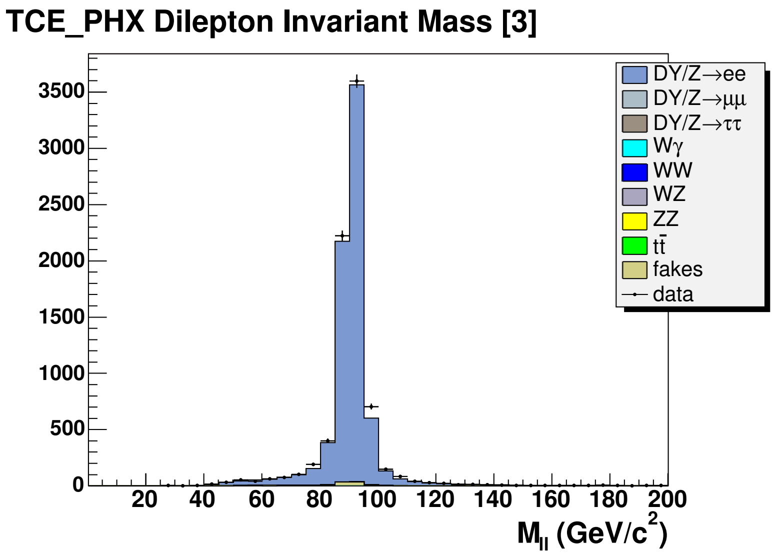

Figure 13: The mass peak of $Z \to e_{\mathrm{TCE}} e_{\mathrm{PHX}}$ with phoenix electron energies added plug pre-radiator energies and scaled up by factors as listed in Table 20.

10.3 Dilepton table

The result of the event selection described in Section 2, applied to the datasets described above, are shown in tables 21, 22, 25-34. The number of candidates depend on the particular mass of the Higgs boson we search for.

11 Grand Summary

The summary of all the backgrounds, signal acceptances, and data analysis for 360 pb^{-1} are shown in table 21 and 22. The tables 27-32 show the distributions of the signal and backgrounds per ee, $e\mu$ and $\mu\mu$ channels.

M_H	110	120	130	140	150
WW	3.839 ± 0.403	5.469 ± 0.574	6.756 ± 0.709	7.919 ± 0.831	9.104 ± 0.956
WZ	0.143 ± 0.019	0.232 ± 0.030	0.283 ± 0.037	0.333 ± 0.043	0.367 ± 0.048
ZZ	0.023 ± 0.004	0.024 ± 0.005	0.027 ± 0.005	0.032 ± 0.006	0.035 ± 0.007
$t\bar{t}$	0.076 ± 0.008	0.114 ± 0.012	0.152 ± 0.017	0.208 ± 0.023	0.282 ± 0.031
W γ	2.732 ± 0.201	2.553 ± 0.188	2.211 ± 0.162	1.679 ± 0.123	1.307 ± 0.096
DY$\ell\ell$	2.294 ± 0.574	1.882 ± 0.470	1.566 ± 0.391	1.312 ± 0.328	1.442 ± 0.361
Fakes	1.643 ± 1.643	1.730 ± 1.730	1.844 ± 1.844	1.600 ± 1.600	1.564 ± 1.564
Total back	10.752 ± 1.798	12.004 ± 1.892	12.838 ± 2.021	13.083 ± 1.837	14.101 ± 1.871
HWW	0.028 ± 0.002	0.094 ± 0.006	0.206 ± 0.012	0.326 ± 0.020	0.435 ± 0.026
Data	8	7	9	14	15

Table 21: The estimated backgrounds and HWW signal in $360\,\mathrm{pb}^{-1}$, and the number of events observed in the data, for each of the dilepton categories. The HWW expectation uses the theoretical cross-sections and BRs discussed in Section 1.

M_H	160	170	180	190	200
WW	9.752 ± 1.024	9.857 ± 1.035	9.761 ± 1.025	9.512 ± 0.999	9.075 ± 0.953
WZ	0.361 ± 0.047	0.372 ± 0.048	0.429 ± 0.056	0.566 ± 0.074	0.840 ± 0.109
ZZ	0.035 ± 0.007	0.043 ± 0.008	0.060 ± 0.011	0.138 ± 0.026	0.294 ± 0.055
$t\bar{t}$	0.346 ± 0.038	0.392 ± 0.043	0.454 ± 0.050	0.512 ± 0.056	0.567 ± 0.062
W γ	1.073 ± 0.079	0.836 ± 0.061	0.769 ± 0.057	0.619 ± 0.045	0.533 ± 0.039
DY$\ell\ell$	0.851 ± 0.213	0.915 ± 0.229	0.858 ± 0.215	0.931 ± 0.233	0.967 ± 0.242
Fakes	1.398 ± 1.398	1.240 ± 1.240	1.053 ± 1.053	1.299 ± 1.299	1.213 ± 1.213
Total back	13.815 ± 1.749	13.655 ± 1.634	13.384 ± 1.488	13.578 ± 1.658	13.489 ± 1.568
HWW	0.576 ± 0.035	0.540 ± 0.032	0.408 ± 0.025	0.237 ± 0.014	0.214 ± 0.013
Data	18	19	20	20	17

Table 22: The estimated backgrounds and HWW signal in $360\,\mathrm{pb}^{-1}$, and the number of events observed in the data, for each of the dilepton categories. The HWW expectation uses the theoretical cross-sections and BRs discussed in Section 1.

12 Cross-Section Limit Calculation

Now we proceed to extract 95% credibility limits (C.L.) on the Standard Model $\sigma \times BR(p\bar{p} \to H \to WW^*)$.

12.1 $\Delta\phi$ Distributions

The distributions of $\Delta\phi$ between the 2 leptons in events passing the selection criteria described in Section 2, are used to set limits on the $p\bar{p} \to H \to WW^*$ cross section. These distributions are given in Figures 14-21. The scalar nature of the Higgs boson gives a tendency of the leptons to be closer in ϕ than that from WW production, making this variable a good discriminator. Rather than simply cut on the variable (and hence loose some signal acceptance), we form a binned likelihood of the observed spectrum to a combination of signal and background, and use this to extract cross section limits. This procedure is discussed in detail below.

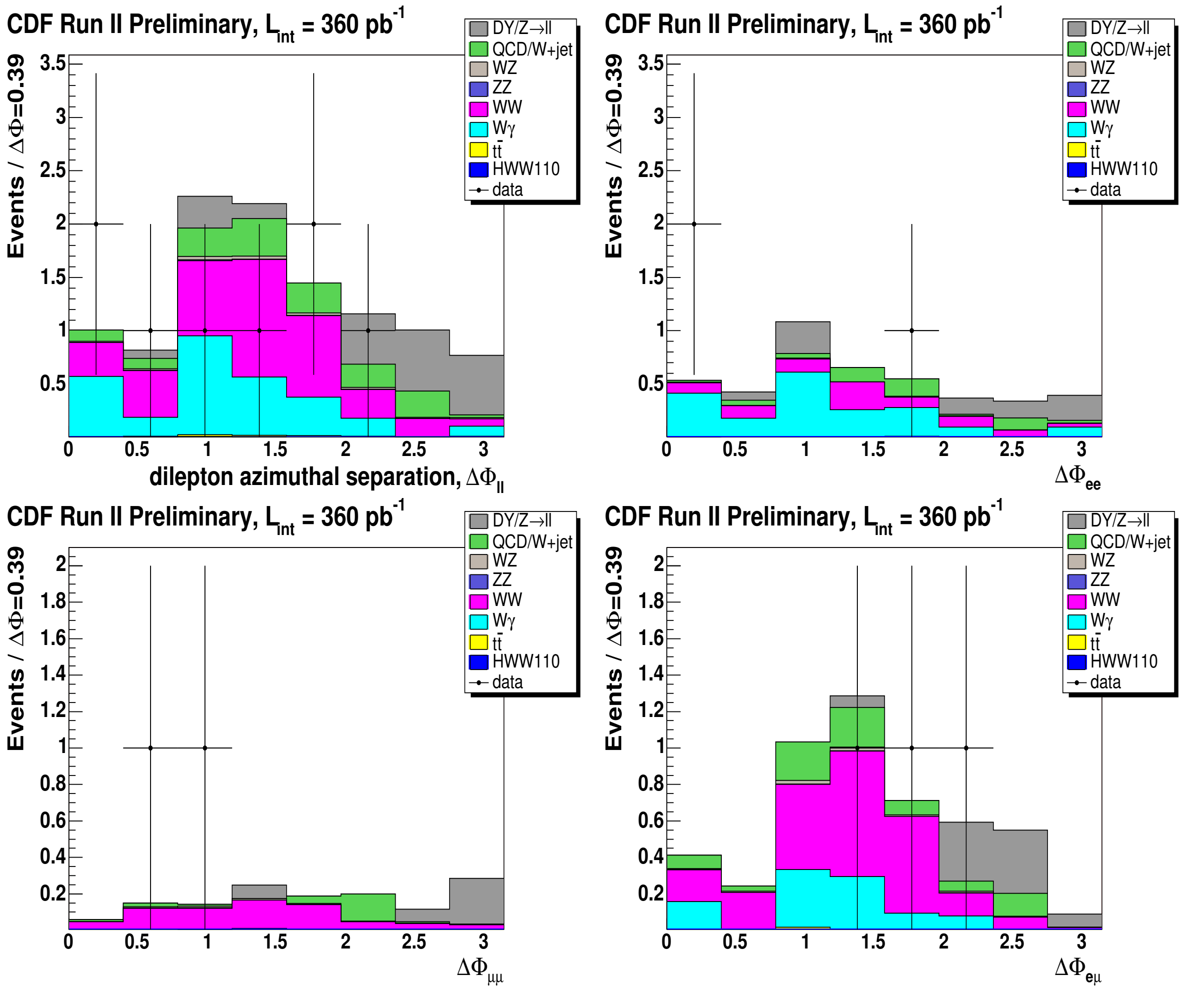

Figure 14: Azimuthal angular separation between the leptons, $\Delta\phi(\ell, \ell)$, from the decay of $H \to WW^* \to \ell\nu\ell\nu$. Distributions of data, HWW^* signal ($M_H = 110$ GeV) MC, WW MC and the sum of other considered background MC samples are shown. The MCs are normalized to the expectations for the integrated luminosity for analyzed data, about 360/pb. We use the upper-left $ee + e\mu + \mu\mu$ plot to fit for a limit on the cross-section of SM HWW production at Tevatron, at the Higgs mass of $M_H = 110$ GeV.

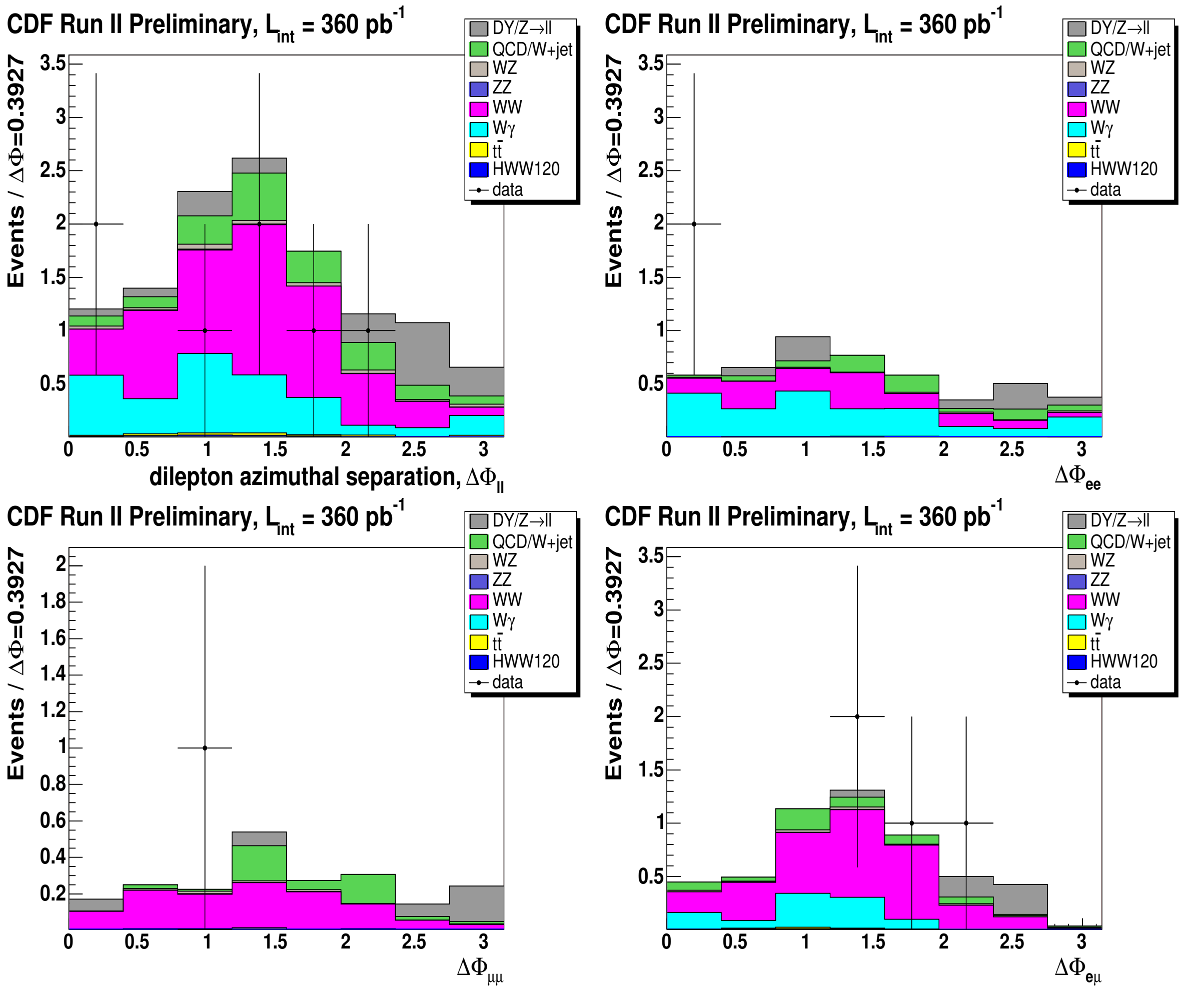

Figure 15: Azimuthal angular separation between the leptons, $\Delta\phi(\ell, \ell)$, from the decay of $H \to WW^* \to \ell\nu\ell\nu$. Distributions of data, HWW^* signal ($M_H = 120$ GeV) MC, WW MC and the sum of other considered background MC samples are shown. The MCs are normalized to the expectations for the integrated luminosity for analyzed data, about 360/pb. We use the upper-left $ee + e\mu + \mu\mu$ plot to fit for a limit on the cross-section of SM HWW production at Tevatron, at the Higgs mass of $M_H = 120$ GeV.

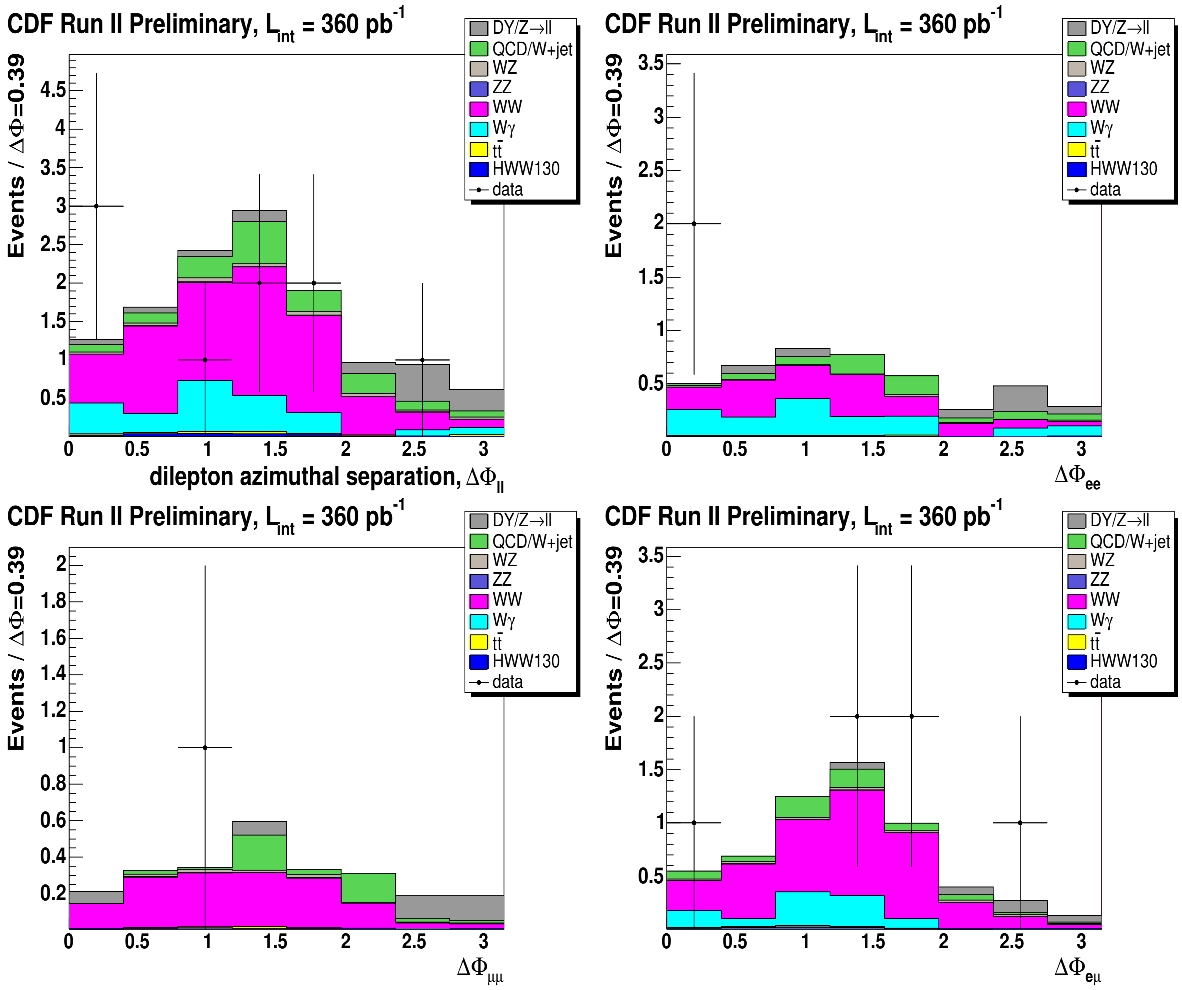

Figure 16: Azimuthal angular separation between the leptons, $\Delta\phi(\ell, \ell)$, from the decay of $H \to WW^* \to \ell\nu\ell\nu$. Distributions of data, HWW^* signal ($M_H = 130$ GeV) MC, WW MC and the sum of other considered background MC samples are shown. The MCs are normalized to the expectations for the integrated luminosity for analyzed data, about 360/pb. We use the upper-left $ee + e\mu + \mu\mu$ plot to fit for a limit on the cross-section of SM HWW production at Tevatron, at the Higgs mass of $M_H = 130$ GeV.

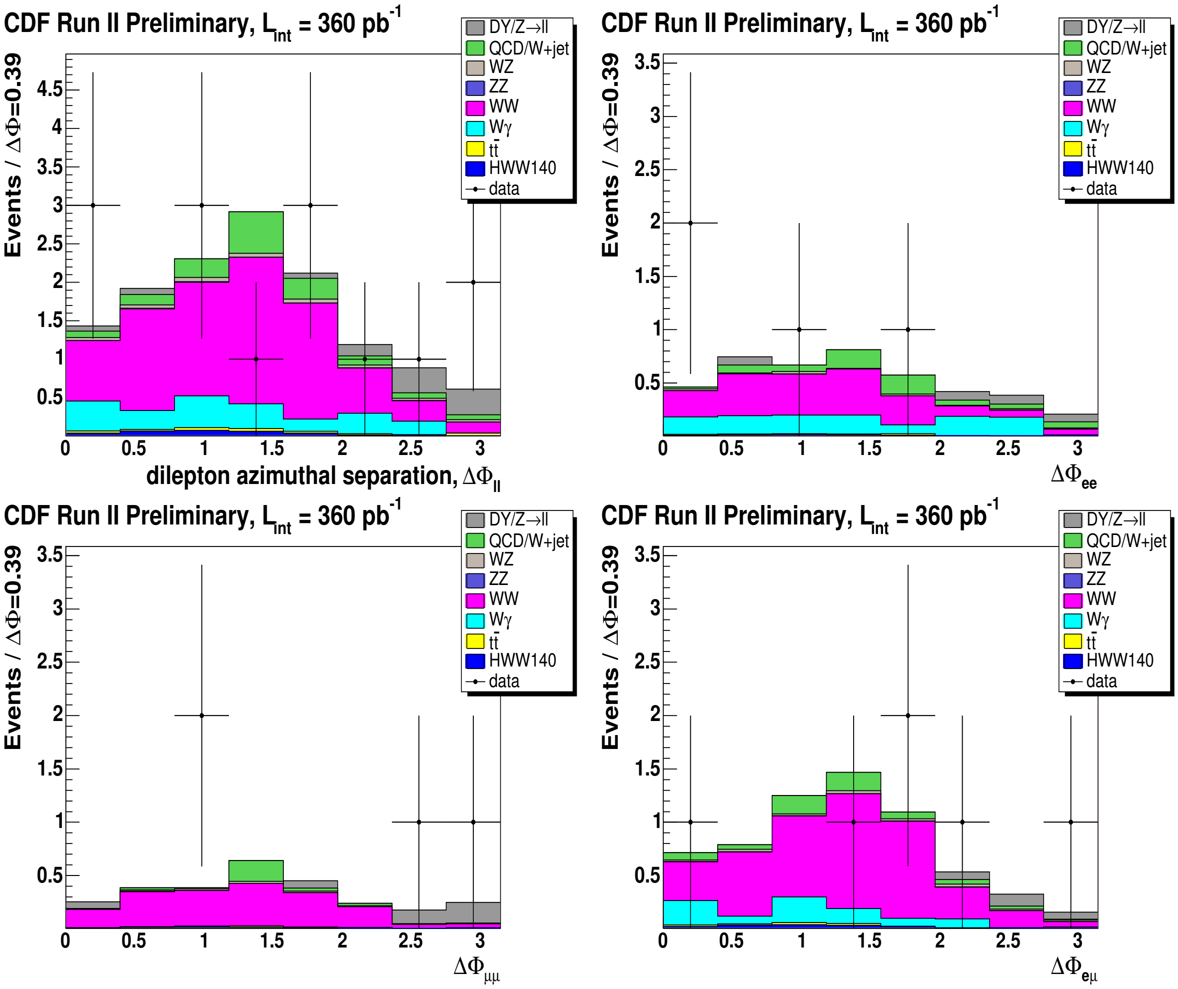

Figure 17: Azimuthal angular separation between the leptons, $\Delta\phi(\ell, \ell)$, from the decay of $H \to WW^* \to \ell\nu\ell\nu$. Distributions of data, HWW^* signal ($M_H = 140$ GeV) MC, WW MC and the sum of other considered background MC samples are shown. The MCs are normalized to the expectations for the integrated luminosity for analyzed data, about 360/pb. We use the upper-left $ee + e\mu + \mu\mu$ plot to fit for a limit on the cross-section of SM HWW production at Tevatron, at the Higgs mass of $M_H = 140$ GeV.

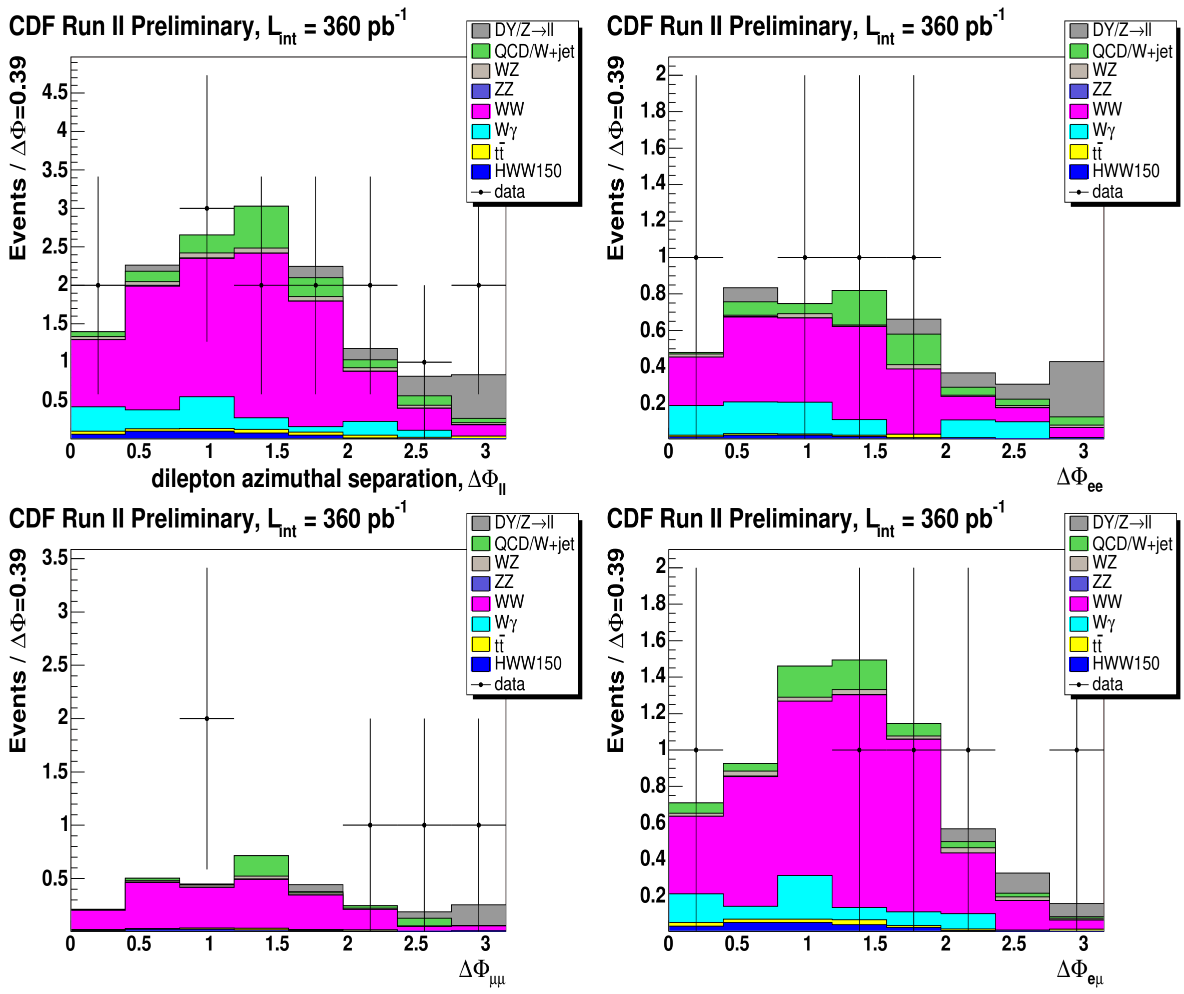

Figure 18: Azimuthal angular separation between the leptons, $\Delta\phi(\ell,\ell)$, from the decay of $H \to WW^* \to \ell\nu\ell\nu$. Distributions of data, HWW^* signal ($M_H = 150$ GeV) MC, WW MC and the sum of other considered background MC samples are shown. The MCs are normalized to the expectations for the integrated luminosity for analyzed data, about 360/pb. We use the upper-left $ee + e\mu + \mu\mu$ plot to fit for a limit on the cross-section of SM HWW production at Tevatron, at the Higgs mass of $M_H = 150$ GeV.

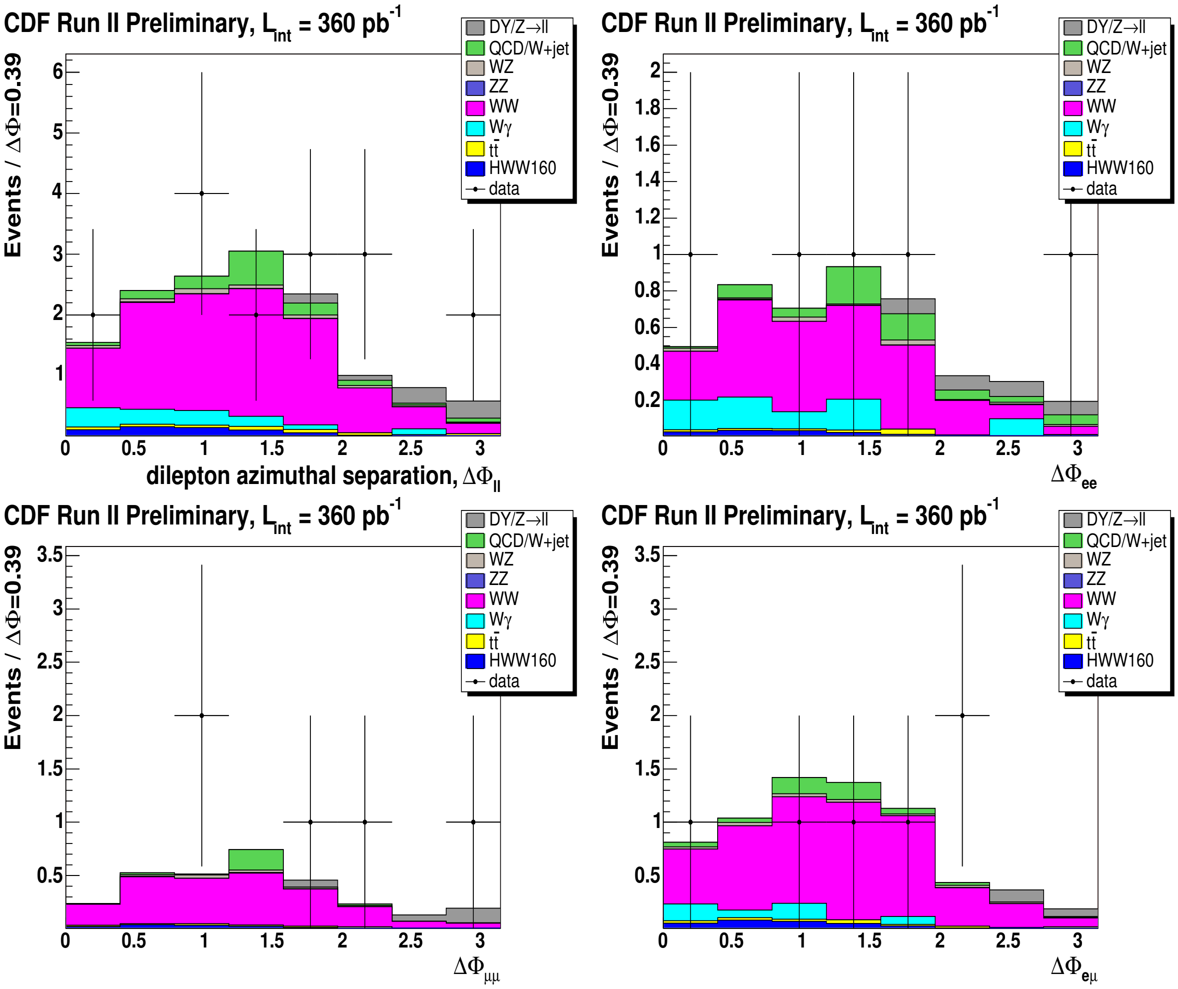

Figure 19: Azimuthal angular separation between the leptons, $\Delta\phi(\ell,\ell)$, from the decay of $H \to WW^* \to \ell\nu\ell\nu$. Distributions of data, HWW^* signal ($M_H = 160$ GeV) MC, WW MC and the sum of other considered background MC samples are shown. The MCs are normalized to the expectations for the integrated luminosity for analyzed data, about 360/pb. We use the upper-left $ee + e\mu + \mu\mu$ plot to fit for a limit on the cross-section of SM HWW production at Tevatron, at the Higgs mass of $M_H = 160$ GeV.

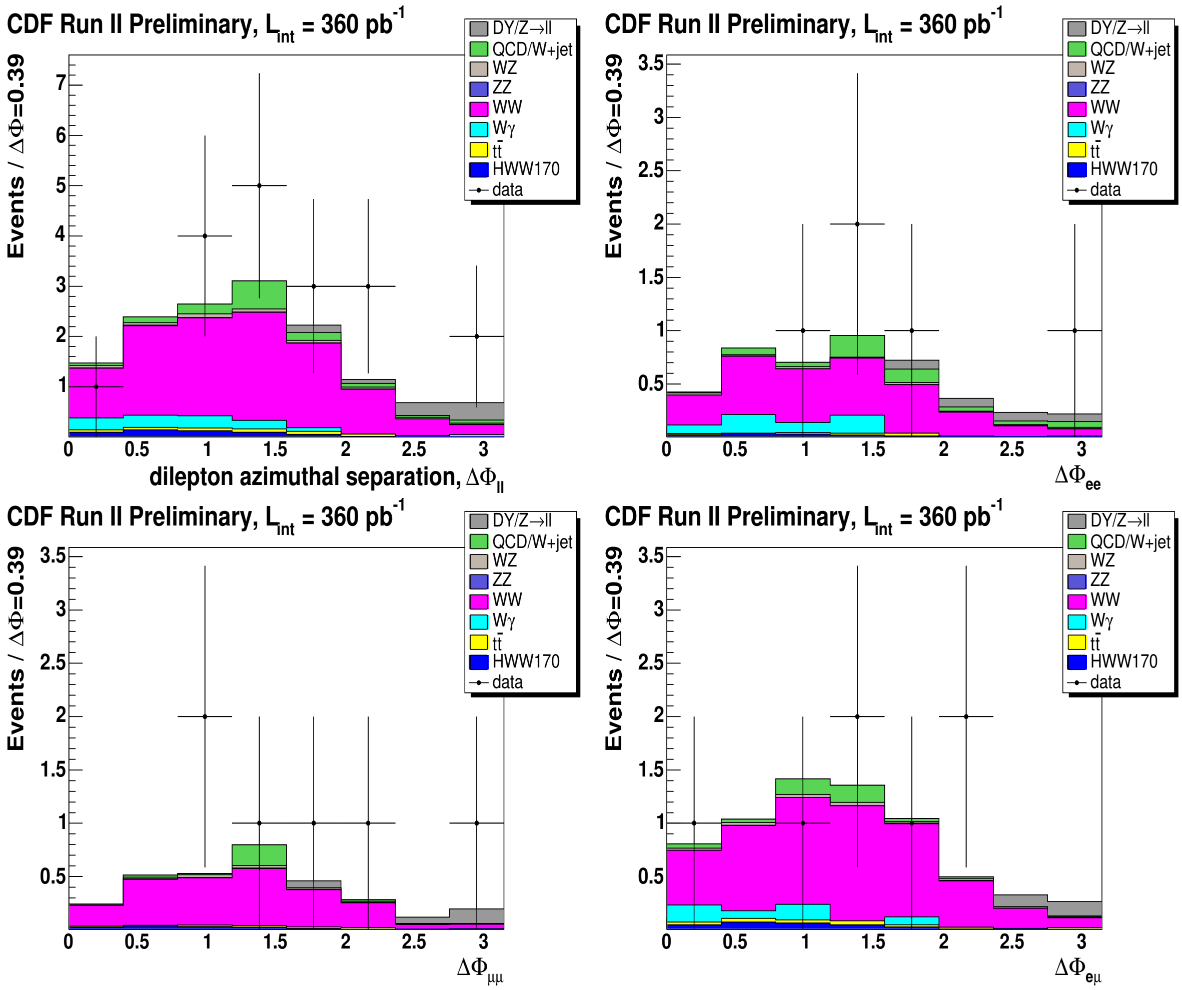

Figure 20: Azimuthal angular separation between the leptons, $\Delta\phi(\ell,\ell)$, from the decay of $H \to WW^* \to \ell\nu\ell\nu$. Distributions of data, HWW^* signal ($M_H = 170$ GeV) MC, WW MC and the sum of other considered background MC samples are shown. The MCs are normalized to the expectations for the integrated luminosity for analyzed data, about 360/pb. We use the upper-left $ee + e\mu + \mu\mu$ plot to fit for a limit on the cross-section of SM HWW production at Tevatron, at the Higgs mass of $M_H = 170$ GeV.

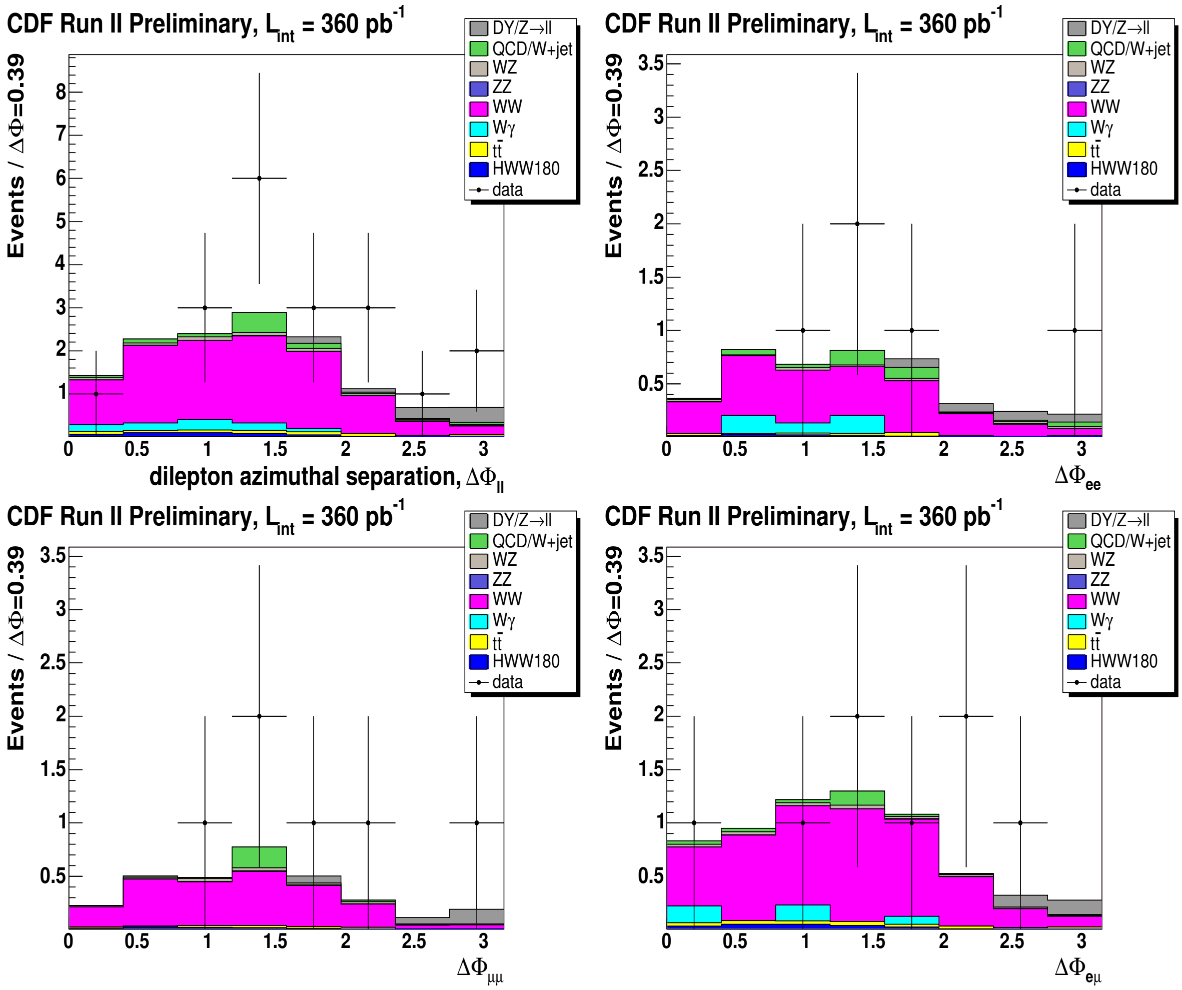

Figure 21: Azimuthal angular separation between the leptons, $\Delta\phi(\ell, \ell)$, from the decay of $H \to WW^* \to \ell\nu\ell\nu$. Distributions of data, HWW^* signal ($M_H = 180$ GeV) MC, WW MC and the sum of other considered background MC samples are shown. The MCs are normalized to the expectations for the integrated luminosity for analyzed data, about 360/pb. We use the upper-left $ee + e\mu + \mu\mu$ plot to fit for a limit on the cross-section of SM HWW production at Tevatron, at the Higgs mass of $M_H = 180$ GeV.

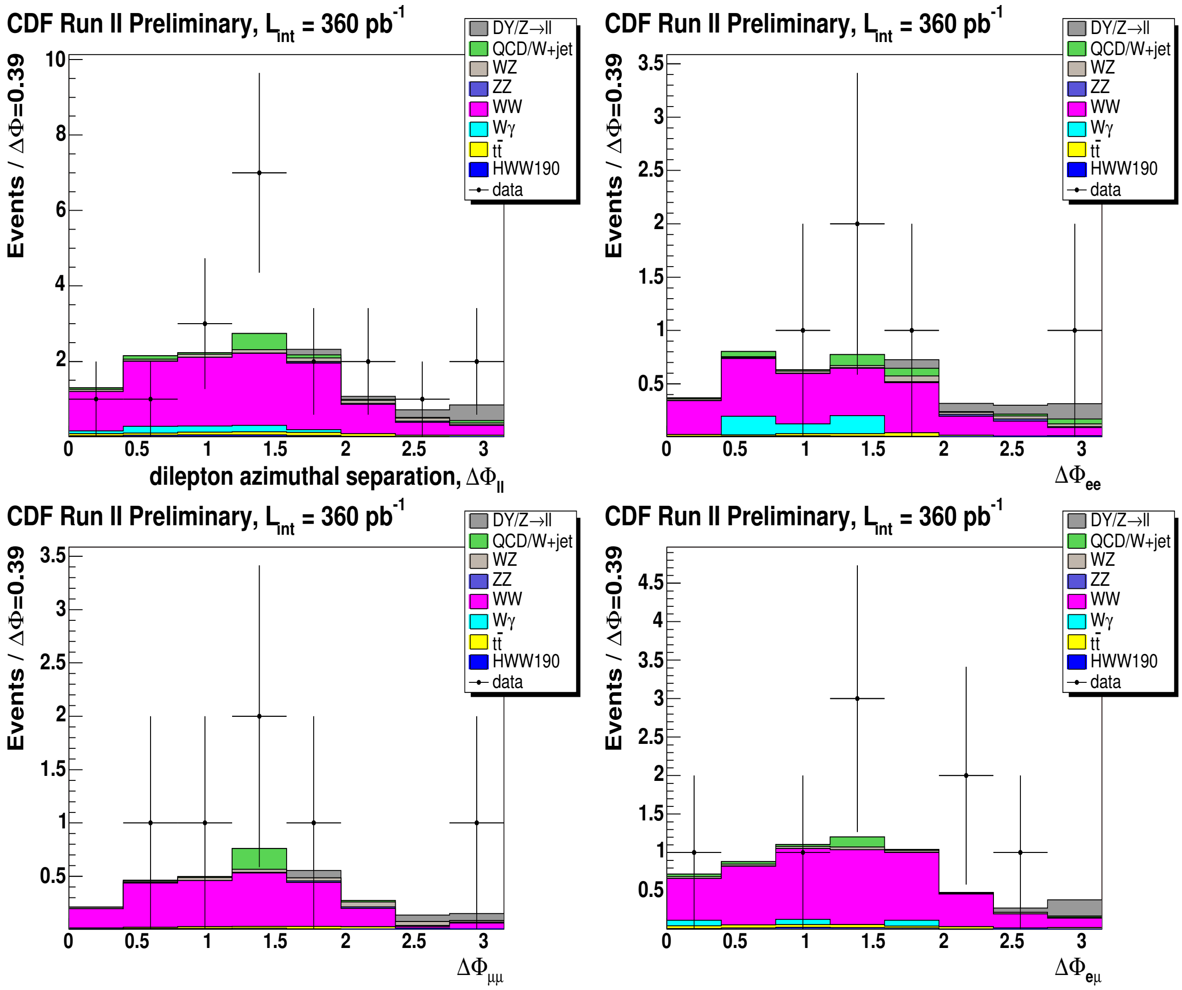

Figure 22: Azimuthal angular separation between the leptons, $\Delta\phi(\ell,\ell)$, from the decay of $H \to WW^* \to \ell\nu\ell\nu$. Distributions of data, HWW^* signal ($M_H = 190$ GeV) MC, WW MC and the sum of other considered background MC samples are shown. The MCs are normalized to the expectations for the integrated luminosity for analyzed data, about 360/pb. We use the upper-left $ee + e\mu + \mu\mu$ plot to fit for a limit on the cross-section of SM HWW production at Tevatron, at the Higgs mass of $M_H = 190$ GeV.

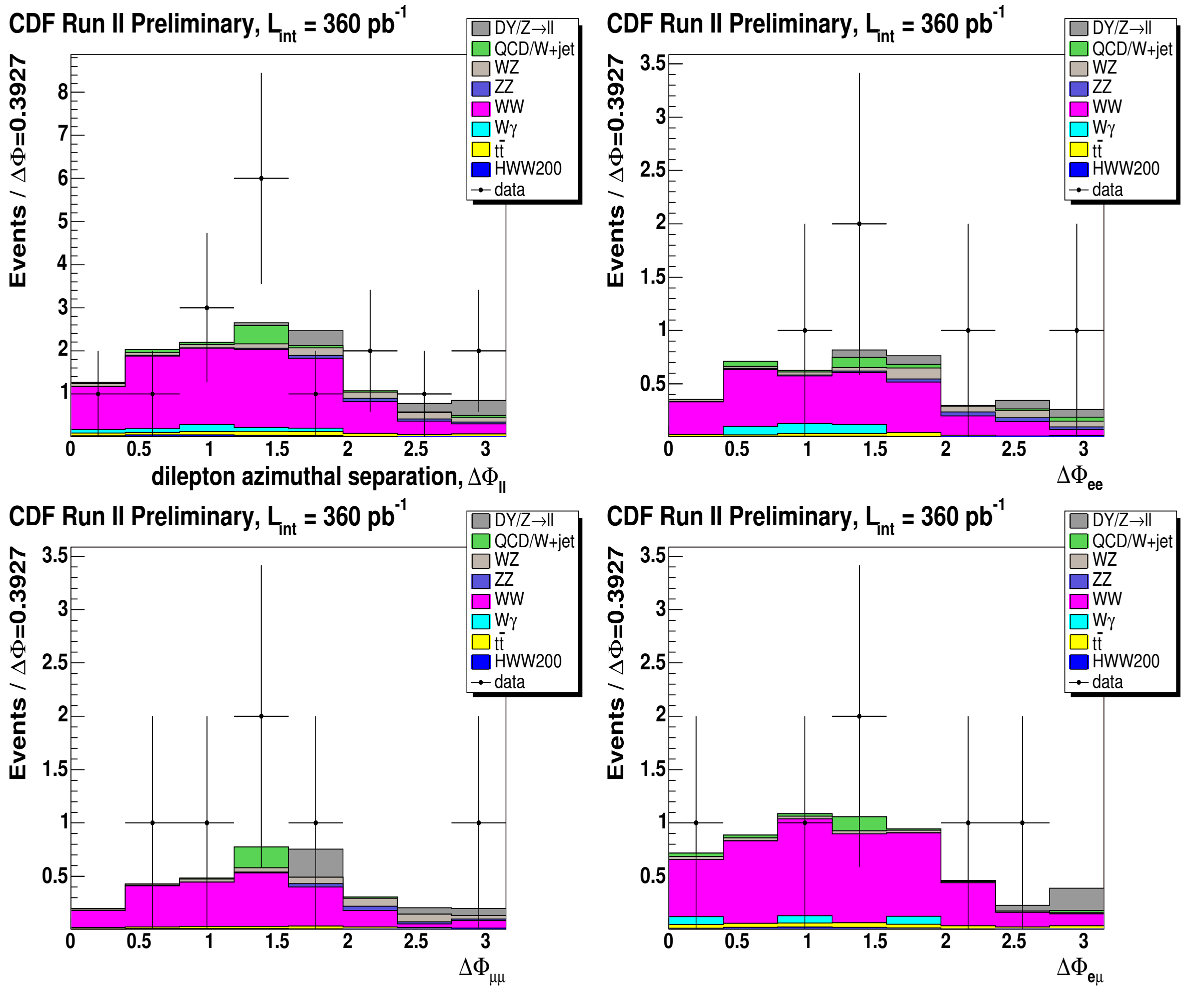

Figure 23: Azimuthal angular separation between the leptons, $\Delta\phi(\ell,\ell)$, from the decay of $H \to WW^* \to \ell\nu\ell\nu$. Distributions of data, HWW^* signal ($M_H = 200$ GeV) MC, WW MC and the sum of other considered background MC samples are shown. The MCs are normalized to the expectations for the integrated luminosity for analyzed data, about 360/pb. We use the upper-left $ee + e\mu + \mu\mu$ plot to fit for a limit on the cross-section of SM HWW production at Tevatron, at the Higgs mass of $M_H = 200$ GeV.

12.2 The Likelihood function and Posterior Density

A binned likelihood is used to compare the $\Delta\phi(\ell,\ell)$ spectrum in the data to a combination of expected distributions from the background processes and the $H \to WW^*$ signal, as a function of Higgs mass. The likelihood function is the usual product of Poisson probabilities over each bin, comparing the observed bin content to that expected.

A Bayesian procedure is used to extract cross section limits. For each Higgs mass, a posterior density is obtained by multiplying the likelihood function with prior densities for all the parameters in the likelihood: integrated luminosity, background normalizations, signal efficiency, and the product $\sigma'_H \equiv \sigma_H \times BR(H \to WW^*)$ of the signal production cross section σ_{H^0} by the branching ratio for $H \to WW^*$. With one exception, these priors are truncated Gaussian densities constraining a given parameter to its expected value within its uncertainty. The exception is σ'_H: since nothing is presumed known *a priori* about this, it is assigned a uniform prior. The posterior density is then integrated over all parameters except σ'_H, and a 95% credibility level (C.L.) upper limit on σ'_H is obtained by calculating the 95$^{\text{th}}$ percentile of the resulting distribution. For now, we have assumed no correlations in the posterior density, between the systematic uncertainties of the signal and backgrounds. This assumption is not strictly correct, as there are correlations, but the effect is expected to be small, and we will revisit this assumption later.

12.3 Expected Limits from Pseudo-experiments

We obtain expected cross section limits from the average obtained from 1000 pseudo-experiments. The pseudo-experiments are generated for each Higgs mass as follows:

0) Assume zero signal

1) Use the mean and sigmas for WW, and "all other backgrounds". Gaussian fluctuate these means about their uncertainties to generate 2 new numbers.

2) Poisson fluctuate these numbers, and take the integer of them. This gives us a number of WW and "other" for a given pseudo-experiment.

3) Using these integers, randomly sample from the $\Delta\phi$ distributions for WW and "other" to generate the $\Delta\phi$ distribution for the pseudo-experiment.

4) Find the limit from the pseudo-experiment exactly as done for the data.

5) Repeat 1000 times.

6) The most likely 95% CL limit from the distribution of 1000 pseudo-experiments is our *expected limit*.

The distributions of limits from pseudo-experiments are given in figures 24 and 25. The resultant expected limits are given in Table 23 together with the limits obtained from the data.

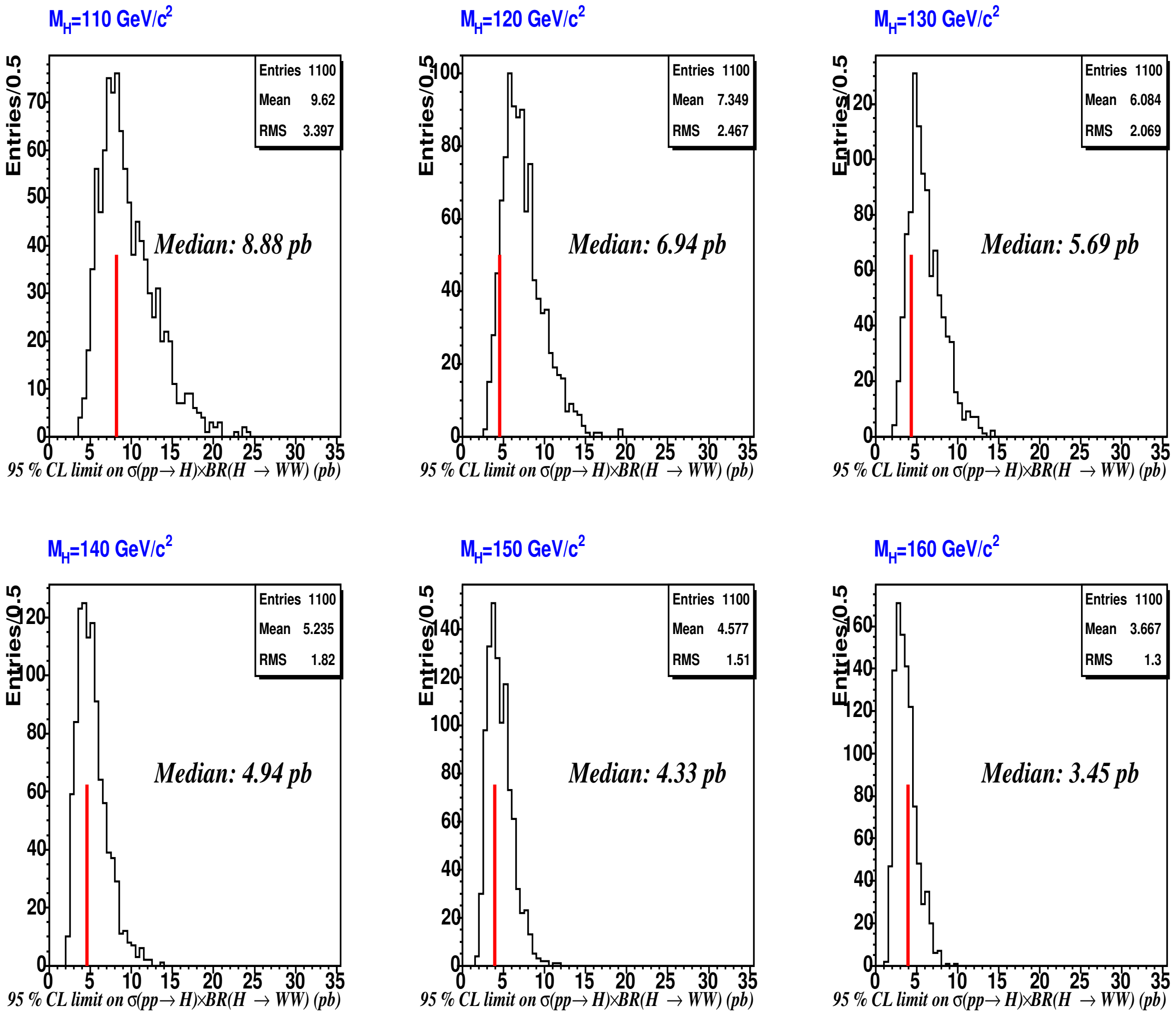

Figure 24: Expected limits obtained from pseudo-experiments drawn from $\Delta\phi(\ell,\ell)$ distributions, for Higgs masses from 110-160 GeV$/c^2$. The red line represents the 95% CL extracted from data.

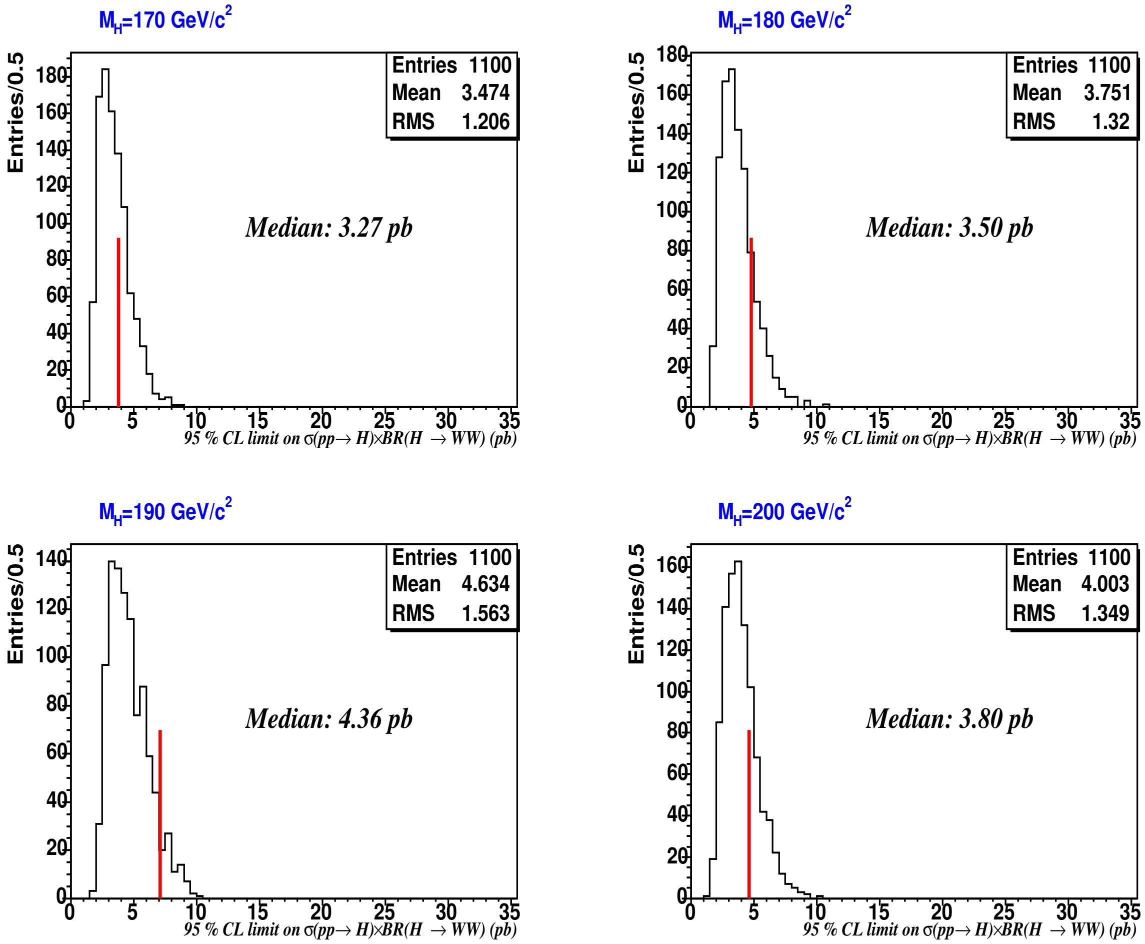

Figure 25: Expected limits obtained pseudo-experiments, drawn from $\Delta\phi(\ell,\ell)$ distributions, for Higgs masses from 170-200 GeV$/c^2$. The red line represents the 95% CL extracted from data.

12.4 Cross section Limits from the Data

The 95% CL cross section limits on $\sigma_H \times BR(H \rightarrow WW^*)$ are summarized in Table 23, and plotted in figures 26 and 27.

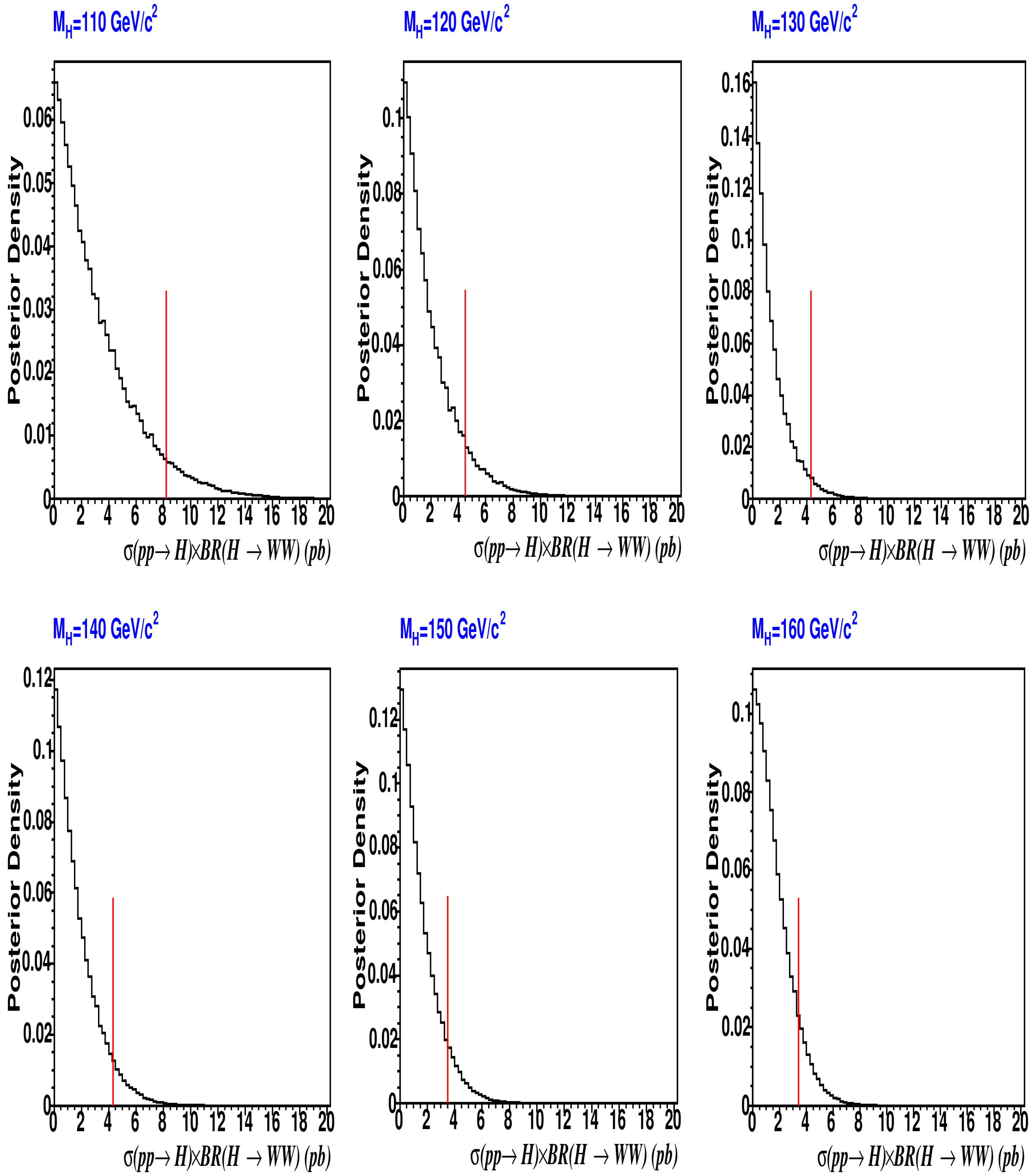

Figure 26: The likelihood functions obtained from $\Delta\phi(\ell,\ell)$ distributions, for Higgs masses from 110-160 GeV/c^2.

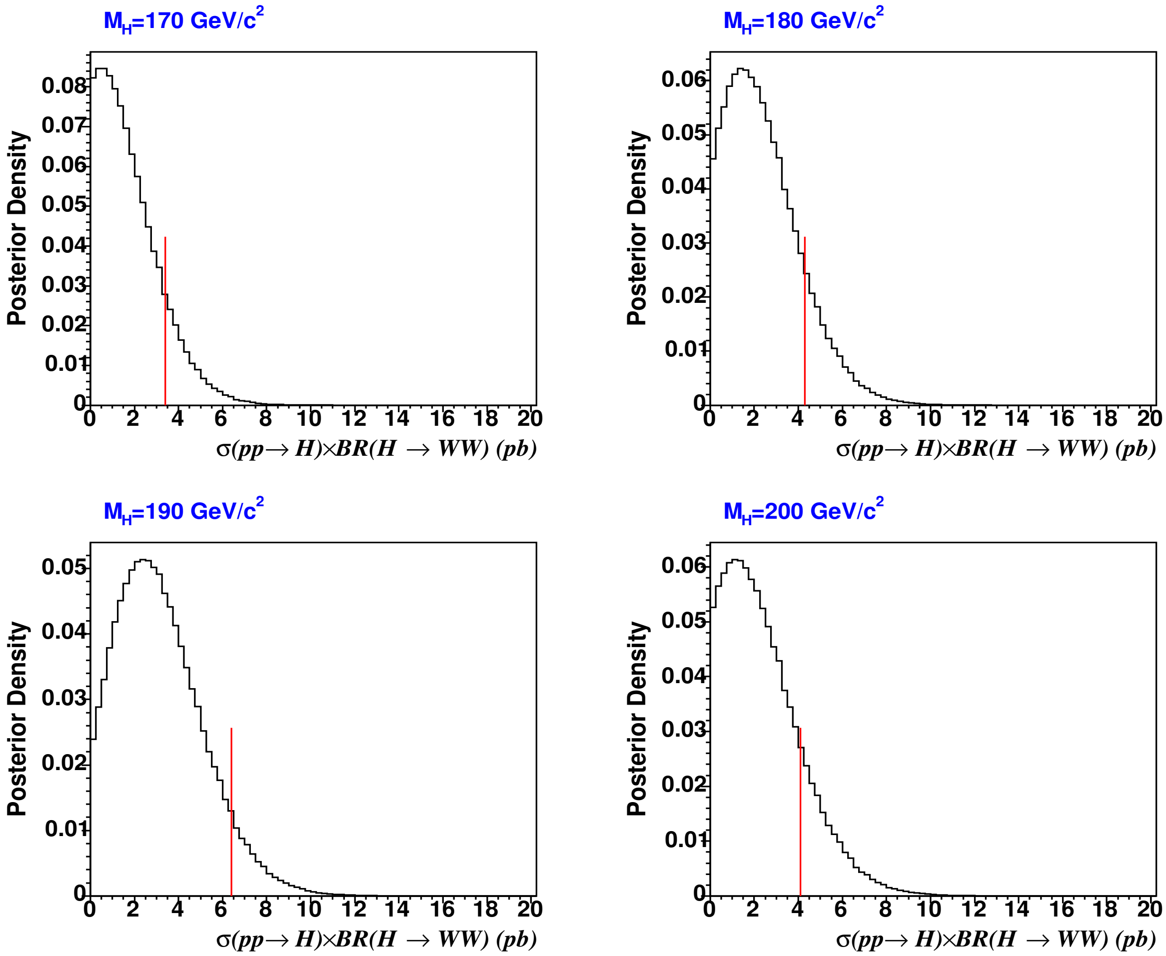

Figure 27: The likelihood functions obtained from $\Delta\phi(\ell,\ell)$ distributions, for Higgs masses from 170-200 GeV/c^2.

	M_H (GeV/c^2)									
95% CL Limit	110	120	130	140	150	160	170	180	190	200
$\Delta\phi$ (old) 4.11.1	-	-	-	17.8	9.4	5.6	5.6	6.4	-	-
$\Delta\phi$ (expected, new)	8.9	6.9	5.7	4.9	4.3	3.5	3.2	3.5	4.3	3.8
$\Delta\phi$ (new)	**8.2**	**4.5**	**4.3**	**4.6**	**3.9**	**3.9**	**3.8**	**4.8**	**7.1**	**4.6**

Table 23: 95% CL limits on $\sigma(gg \to H) \times BR(H \to WW^*)$ at $\sqrt{\hat{s}} = 1.96\,\text{TeV}$ for the different Higgs obtained using our old 20-20 selection from CDF-6958, for 200 /pb. The expected limits using the new selection are also shown, as discussed above. In all cases the limits correspond to $360\,\text{pb}^{-1}$.

13 Conclusions

We have studied the production of SM HWW to dilepton channels ($ee + e\mu + \mu\mu$) at Tevatron in 360/pb CDF Run II data. We do not see an excess over the SM expected background, so we proceed to set a 95% C.L. limit on the Standard-Model cross-section $\times$ branching ratio $\sigma \cdot \mathrm{BR}_{\mathrm{SM}}(p\bar{p} \to H \to WW^*)$ at center-of-mass energy $\sqrt{\hat{s}} = 1.96$ TeV, for Higgs masses between 110 - 200 GeV.

References

[1] J. Pumplin*et al.*-“New Generation of Parton Distributions with Uncertainties from Global QCD Analysis”,hep-ph/0201195

[2] S. Sultansoy,“The ”Golden Mode” at the Upgraded Tevatron?”,hep-ex/0010037.

[3] S. Miller, “Pdf Acceptance Uncertainties for $t\bar{t}$ Cross Section”, JPM March 19, 2004.

[4] David Dagenhart, “Measurement of the Z Production Cross Section”, CDF-7865.

[5] Martin Griffiths, Beate Heinemann, Giulia Manca, “Central Electron ID Efficiencies at Medium Energy”, CDF-7309.

[6] D.Bortoletto, A.Canepa, O.Gonzalez, E.Lytken, “Search for the associated production of chargino and neutralino in dimuon+lepton events”, CDF-7714.

[7] C.Hill, J.Incandela, and C.Mills, “Electron Identification in Offline Release 5.3”, CDF-7309.

[8] Tim Nelson, Rick Snider, David Stuart, “Forward Electron Tracking with the PhoenixMods Package”, CDF-6278.

[9] Sunny S.Chuang, D.Carlsmith, Susana Cabrera, Mark Kruse, Dustin McGivern, David Waters, “Search for a SM Higgs Boson in the gg→H→WW* Dilepton Channel with 200/pb Run II Data at CDF”, CDF-6958.

[10] Yoshio Ishizawa and Jason Nielsen, “Trigger Efficiencies for High Et Electrons”, CDF-7401.

[11] Shan-Huei Chuang, Mark Kruse, Mircea Coca “Lepton Fake Estimate Using 314.2/pb CDF Run II Data”, CDF-7497

[12] V.Martin, “High-Pt Muon ID Cuts and Efficiencies for use with 5.3.1 Data and 5.3.3 MC”, CDF-7367.

[13] S.Cabrera, S.Carron, S.Chuang, J.Deng, A.Goshaw, Y.Huang, M.Kruse, D.McGivern, D.Waters, “WW Production in the Dilepton channel with 200/pb”, CDF-6909

[14] S.Cabrera, J.Deng, A.Goshaw, C.Hays, Y.Huang, M.Kruse- Measurement of ZZ+ZW cross section using Run II data, CDF-6920

[15] Joint Physics Meeting High-Pt Lepton ID http://www-cdf.fnal.gov/internal/physics/joint_physics/index.html.

[16] Jet Energy and Resolution Group "Jet Energy Corrections Systematic Uncertainties" http://www-cdf.fnal.gov/internal/physics/top/jets/systematics.html.

[17] R.Barate *et al.*, ALEPH Collaboration", hep-ex/0306033 (Phys.Lett.B 565), 2003

[18] Tomura, Tomonobu, Top Mass at the Tevatron, HCP 2005, 4-9 July 2005

[19] M.Carena *et al.*, Report of the Tevatron Higgs Working Group, hep-ph/0010338

[20] D.Benjamin *et al.*, Measurement of the Wgamma and Zgamma Production Cross Sections using 200/pb of Run 2 Data, CDF-6601

[21] U.Baur, Berger El., Probing the WW gamma vertex at the Fermilab Tevatron Collider, Phys Rev D .41, 1476 (1990).

[22] B.Heinemann, A.Goshaw, M.Kirby, N.Tanimoto, H.Hayward - Measurement of Wgamma and Zgamma Production in $p\bar{p}$ collisions at sqrt(s)=1.96 TeV, CDF 7165

[23] M.Tecchio - Acceptance and background systematics for the Top Dilepton cross-section measurement, CDF 6590

A Comparison with the THWG's Prospects

Higgs Mass (GeV)	140	150	160	170	180	190
Total Background : Ours	20.45	18.7	16.69	14.92	13.75	-
THWG	15.84	10.80	1.58	0.86	1.37	2.70
S/$\sqrt{\text{B}}$ for 360/pb: Ours	0.07	0.094	0.13	0.13	0.10	-
THWG	0.23	0.31	0.43	0.42	0.30	0.19

Table 24: Comparison between the current status of our analysis and the THWG's prospect for the same integrated luminosity. The THWG's prospect are taken from Table 29 of the Report of the Tevatron Higgs Working Group [19] (originally at fb^{-1} scale) and interpolated to $\mathcal{L}_{\text{int}} = 360$ pb^{-1}.

B Expected signal, backgrounds and data candidates per di-lepton channel

110 GeV	ee	$e\mu$	$\mu\mu$	ll
WW	0.896 ± 0.094	2.261 ± 0.237	0.682 ± 0.072	3.839 ± 0.403
WZ	0.031 ± 0.004	0.076 ± 0.010	0.036 ± 0.005	0.143 ± 0.019
ZZ	0.007 ± 0.001	0.007 ± 0.001	0.009 ± 0.002	0.023 ± 0.004
$t\bar{t}$	0.027 ± 0.003	0.025 ± 0.003	0.025 ± 0.003	0.076 ± 0.008
W γ	1.869 ± 0.137	0.863 ± 0.063	0.000 ± 0.000	2.732 ± 0.201
Drell-Yan $\ell\ell$	1.015 ± 0.254	0.756 ± 0.189	0.523 ± 0.131	2.294 ± 0.574
Fakes	0.583 ± 0.583	0.809 ± 0.809	0.251 ± 0.251	1.643 ± 1.643
Total Back	4.429 ± 0.657	4.795 ± 0.866	1.527 ± 0.292	10.752 ± 1.798
HWW	0.007 ± 0.000	0.014 ± 0.001	0.006 ± 0.000	0.028 ± 0.002
Data	3	3	2	8

Table 25: Summary of the signal and background expectations for a Higgs mass of 110 GeV, for 360 pb^{-1}. Also the observed number of events is shown.

120 GeV	ee	$e\mu$	$\mu\mu$	ll
WW	1.318 ± 0.138	2.957 ± 0.310	1.194 ± 0.125	5.469 ± 0.574
WZ	0.064 ± 0.008	0.111 ± 0.014	0.057 ± 0.007	0.232 ± 0.030
ZZ	0.007 ± 0.001	0.006 ± 0.001	0.010 ± 0.002	0.024 ± 0.005
$t\bar{t}$	0.035 ± 0.004	0.045 ± 0.005	0.033 ± 0.004	0.114 ± 0.012
W γ	1.696 ± 0.125	0.857 ± 0.063	0.000 ± 0.000	2.553 ± 0.188
Drell-Yan $\ell\ell$	0.864 ± 0.216	0.486 ± 0.122	0.531 ± 0.133	1.882 ± 0.470
Fakes	0.654 ± 0.654	0.602 ± 0.602	0.475 ± 0.475	1.730 ± 1.730
Total Back	4.639 ± 0.714	5.065 ± 0.691	2.301 ± 0.509	12.004 ± 1.892
HWW	0.025 ± 0.001	0.048 ± 0.003	0.022 ± 0.001	0.094 ± 0.006
Data	2	4	1	7

Table 26: Summary of the signal and background expectations for a Higgs mass of 120 GeV, for 360 pb^{-1}. Also the observed number of events is shown.

130 GeV	ee	$e\mu$	$\mu\mu$	ll
WW	1.655 ± 0.174	3.625 ± 0.381	1.476 ± 0.155	6.756 ± 0.709
WZ	0.069 ± 0.009	0.138 ± 0.018	0.076 ± 0.010	0.283 ± 0.037
ZZ	0.007 ± 0.001	0.008 ± 0.002	0.012 ± 0.002	0.027 ± 0.005
$t\bar{t}$	0.048 ± 0.005	0.060 ± 0.007	0.044 ± 0.005	0.152 ± 0.017
W γ	1.284 ± 0.094	0.927 ± 0.068	0.000 ± 0.000	2.211 ± 0.162
Drell-Yan $\ell\ell$	0.715 ± 0.179	0.315 ± 0.079	0.536 ± 0.134	1.566 ± 0.391
Fakes	0.701 ± 0.701	0.688 ± 0.688	0.455 ± 0.455	1.844 ± 1.844
Total Back	4.480 ± 0.750	5.761 ± 0.793	2.597 ± 0.499	12.838 ± 2.021
HWW	0.053 ± 0.003	0.106 ± 0.006	0.047 ± 0.003	0.206 ± 0.012
Data	2	6	1	9

Table 27: Summary of the signal and background expectations for a Higgs mass of 130 GeV, for 360 pb^{-1}. Also the observed number of events is shown.

140 GeV	ee	$e\mu$	$\mu\mu$	ll
WW	1.901 ± 0.200	4.195 ± 0.440	1.823 ± 0.191	7.919 ± 0.831
WZ	0.085 ± 0.011	0.161 ± 0.021	0.087 ± 0.011	0.333 ± 0.043
ZZ	0.011 ± 0.002	0.009 ± 0.002	0.012 ± 0.002	0.032 ± 0.006
$t\bar{t}$	0.063 ± 0.007	0.090 ± 0.010	0.056 ± 0.006	0.208 ± 0.023
W γ	0.965 ± 0.071	0.715 ± 0.053	0.000 ± 0.000	1.679 ± 0.123
Drell-Yan $\ell\ell$	0.477 ± 0.119	0.250 ± 0.062	0.585 ± 0.146	1.312 ± 0.328
Fakes	0.674 ± 0.674	0.640 ± 0.640	0.286 ± 0.286	1.600 ± 1.600
Total Back	4.175 ± 0.716	6.060 ± 0.781	2.849 ± 0.374	13.083 ± 1.837
HWW	0.081 ± 0.005	0.168 ± 0.010	0.077 ± 0.005	0.326 ± 0.020
Data	4	6	4	14

Table 28: Summary of the signal and background expectations for a Higgs mass of 140 GeV, for 360 pb^{-1}. Also the observed number of events is shown.

150 GeV	ee	$e\mu$	$\mu\mu$	ll
WW	2.333 ± 0.245	4.704 ± 0.494	2.068 ± 0.217	9.104 ± 0.956
WZ	0.099 ± 0.013	0.165 ± 0.021	0.103 ± 0.013	0.367 ± 0.048
ZZ	0.010 ± 0.002	0.009 ± 0.002	0.016 ± 0.003	0.035 ± 0.007
$t\bar{t}$	0.075 ± 0.008	0.126 ± 0.014	0.081 ± 0.009	0.282 ± 0.031
W γ	0.725 ± 0.053	0.582 ± 0.043	0.000 ± 0.000	1.307 ± 0.096
Drell-Yan $\ell\ell$	0.793 ± 0.198	0.255 ± 0.064	0.393 ± 0.098	1.442 ± 0.361
Fakes	0.629 ± 0.629	0.598 ± 0.598	0.337 ± 0.337	1.564 ± 1.564
Total Back	4.664 ± 0.706	6.439 ± 0.780	2.998 ± 0.413	14.101 ± 1.871
HWW	0.105 ± 0.006	0.225 ± 0.014	0.105 ± 0.006	0.435 ± 0.026
Data	5	5	5	15

Table 29: Summary of the signal and background expectations for a Higgs mass of 150 GeV, for 360 pb^{-1}. Also the observed number of events is shown.

160 GeV	ee	$e\mu$	$\mu\mu$	ll
WW	2.583 ± 0.271	4.986 ± 0.523	2.184 ± 0.229	9.752 ± 1.024
WZ	0.099 ± 0.013	0.162 ± 0.021	0.101 ± 0.013	0.361 ± 0.047
ZZ	0.012 ± 0.002	0.006 ± 0.001	0.017 ± 0.003	0.035 ± 0.007
$t\bar{t}$	0.098 ± 0.011	0.161 ± 0.018	0.086 ± 0.009	0.346 ± 0.038
W γ	0.653 ± 0.048	0.419 ± 0.031	0.000 ± 0.000	1.073 ± 0.079
Drell-Yan $\ell\ell$	0.399 ± 0.100	0.184 ± 0.046	0.268 ± 0.067	0.851 ± 0.213
Fakes	0.635 ± 0.635	0.517 ± 0.517	0.247 ± 0.247	1.398 ± 1.398
Total Back	4.478 ± 0.699	6.435 ± 0.738	2.902 ± 0.344	13.815 ± 1.749
HWW	0.137 ± 0.008	0.299 ± 0.018	0.140 ± 0.008	0.576 ± 0.035
Data	7	6	5	18

Table 30: Summary of the signal and background expectations for a Higgs mass of 160 GeV, for 360 pb^{-1}. Also the observed number of events is shown.

170 GeV	ee	$e\mu$	$\mu\mu$	ll
WW	2.669 ± 0.280	4.953 ± 0.520	2.235 ± 0.235	9.857 ± 1.035
WZ	0.098 ± 0.013	0.165 ± 0.021	0.109 ± 0.014	0.372 ± 0.048
ZZ	0.017 ± 0.003	0.007 ± 0.001	0.019 ± 0.004	0.043 ± 0.008
$t\bar{t}$	0.108 ± 0.012	0.188 ± 0.021	0.096 ± 0.011	0.392 ± 0.043
W γ	0.417 ± 0.031	0.419 ± 0.031	0.000 ± 0.000	0.836 ± 0.061
Drell-Yan $\ell\ell$	0.399 ± 0.100	0.248 ± 0.062	0.268 ± 0.067	0.915 ± 0.229
Fakes	0.623 ± 0.623	0.362 ± 0.362	0.255 ± 0.255	1.240 ± 1.240
Total Back	4.329 ± 0.691	6.343 ± 0.638	2.983 ± 0.354	13.655 ± 1.634
HWW	0.130 ± 0.008	0.278 ± 0.017	0.132 ± 0.008	0.540 ± 0.032
Data	6	7	6	19

Table 31: Summary of the signal and background expectations for a Higgs mass of 170 GeV, for 360 pb^{-1}. Also the observed number of events is shown.

180 GeV	ee	$e\mu$	$\mu\mu$	ll
WW	2.640 ± 0.277	4.948 ± 0.519	2.173 ± 0.228	9.761 ± 1.025
WZ	0.112 ± 0.014	0.185 ± 0.024	0.132 ± 0.017	0.429 ± 0.056
ZZ	0.027 ± 0.005	0.007 ± 0.001	0.026 ± 0.005	0.060 ± 0.011
$t\bar{t}$	0.123 ± 0.013	0.221 ± 0.024	0.110 ± 0.012	0.454 ± 0.050
W γ	0.417 ± 0.031	0.353 ± 0.026	0.000 ± 0.000	0.769 ± 0.057
Drell-Yan $\ell\ell$	0.399 ± 0.100	0.192 ± 0.048	0.268 ± 0.067	0.858 ± 0.215
Fakes	0.483 ± 0.483	0.324 ± 0.324	0.245 ± 0.245	1.053 ± 1.053
Total Back	4.199 ± 0.567	6.230 ± 0.616	2.955 ± 0.342	13.384 ± 1.488
HWW	0.100 ± 0.006	0.211 ± 0.013	0.098 ± 0.006	0.408 ± 0.025
Data	6	8	6	20

Table 32: Summary of the signal and background expectations for a Higgs mass of 180 GeV, for 360 pb^{-1}. Also the observed number of events is shown.

190 GeV	ee	$e\mu$	$\mu\mu$	ll
WW	2.636 ± 0.277	4.759 ± 0.500	2.118 ± 0.222	9.512 ± 0.999
WZ	0.189 ± 0.025	0.176 ± 0.023	0.200 ± 0.026	0.566 ± 0.074
ZZ	0.074 ± 0.014	0.008 ± 0.001	0.057 ± 0.011	0.138 ± 0.026
$t\bar{t}$	0.142 ± 0.016	0.241 ± 0.026	0.129 ± 0.014	0.512 ± 0.056
W γ	0.417 ± 0.031	0.202 ± 0.015	0.000 ± 0.000	0.619 ± 0.045
Drell-Yan $\ell\ell$	0.470 ± 0.118	0.266 ± 0.066	0.195 ± 0.049	0.931 ± 0.233
Fakes	0.391 ± 0.391	0.662 ± 0.662	0.245 ± 0.245	1.299 ± 1.299
Total Back	4.318 ± 0.495	6.314 ± 0.833	2.946 ± 0.336	13.578 ± 1.658
HWW	0.059 ± 0.004	0.123 ± 0.007	0.055 ± 0.003	0.237 ± 0.014
Data	6	8	6	20

Table 33: Summary of the signal and background expectations for a Higgs mass of 190 GeV, for 360 pb^{-1}. Also the observed number of events is shown.

200 GeV	ee	$e\mu$	$\mu\mu$	ll
WW	2.618 ± 0.275	4.424 ± 0.465	2.032 ± 0.213	9.075 ± 0.953
WZ	0.366 ± 0.048	0.159 ± 0.021	0.315 ± 0.041	0.840 ± 0.109
ZZ	0.163 ± 0.031	0.008 ± 0.001	0.123 ± 0.023	0.294 ± 0.055
$t\bar{t}$	0.148 ± 0.016	0.269 ± 0.029	0.150 ± 0.016	0.567 ± 0.062
W γ	0.331 ± 0.024	0.202 ± 0.015	0.000 ± 0.000	0.533 ± 0.039
Drell-Yan $\ell\ell$	0.308 ± 0.077	0.266 ± 0.066	0.393 ± 0.098	0.967 ± 0.242
Fakes	0.338 ± 0.338	0.639 ± 0.639	0.235 ± 0.235	1.213 ± 1.213
Total Back	4.273 ± 0.447	5.967 ± 0.794	3.249 ± 0.336	13.489 ± 1.568
HWW	0.053 ± 0.003	0.111 ± 0.007	0.050 ± 0.003	0.214 ± 0.013
Data	5	6	6	17

Table 34: Summary of the signal and background expectations for a Higgs mass of 200 GeV, for 360 pb^{-1}. Also the observed number of events is shown.

C Detailed acceptance tables

We present next the full tables of the number of data events after every selection cut, for all Higgs masses. Also we show the full tables for all backgrounds, for $M_H = 160$ GeV/c^2. For simplicity we introduce the notations: $M_u \equiv M_H/2 - 5$ GeV (the upper cut on $M_{\ell\ell}$.) and $H_T \equiv {p_T}^{\ell_1} + {p_T}^{\ell_2} + \not{E}_T$.

Categ	Lep ID	Lep1 Isol	Lep2 Isol	$M_{\ell\ell} > 16$	jet veto	$\not\!\!E_t$	opp sign	$M_{\ell\ell} < M_u$	$H_T < M_H$
TCE-TCE	9584 0.10 ± 0.00	8306 86.67 ± 0.35	7313 88.04 ± 0.36	7216 98.67 ± 0.13	6961 96.47 ± 0.22	15 0.22 ± 0.06	15 100.00 ± 0.00	3 20.00 ± 10.33	3 100.00 ± 0.00
TCE-PHX	9539 0.10 ± 0.00	8707 91.28 ± 0.29	8485 97.45 ± 0.17	8480 99.94 ± 0.03	8227 97.02 ± 0.18	18 0.22 ± 0.05	12 66.67 ± 11.11	5 41.67 ± 14.23	4 80.00 ± 17.89
ee	21607 0.23 ± 0.00	19463 90.08 ± 0.20	18172 93.37 ± 0.18	18066 99.42 ± 0.06	17494 96.83 ± 0.13	39 0.22 ± 0.04	28 71.79 ± 7.21	8 28.57 ± 8.54	7 87.50 ± 11.69
TCE-CMUP	372 0.00 ± 0.00	109 29.30 ± 2.36	84 77.06 ± 4.03	81 96.43 ± 2.02	70 86.42 ± 3.81	5 7.14 ± 3.08	4 80.00 ± 17.89	1 25.00 ± 21.65	1 100.00 ± 0.00
TCE-CMX	219 0.00 ± 0.00	52 23.74 ± 2.88	41 78.85 ± 5.66	41 100.00 ± 0.00	37 90.24 ± 4.63	6 16.22 ± 6.06	6 100.00 ± 0.00	1 16.67 ± 15.21	1 100.00 ± 0.00
TCE-CMU	52 0.00 ± 0.00	14 26.92 ± 6.15	9 64.29 ± 12.81	9 100.00 ± 0.00	8 88.89 ± 10.48	0 0.00 ± 0.00	0 0.00 ± 0.00	0 0.00 ± 0.00	0 0.00 ± 0.00
TCE-CMP	105 0.00 ± 0.00	25 23.81 ± 4.16	14 56.00 ± 9.93	14 100.00 ± 0.00	12 85.71 ± 9.35	1 8.33 ± 7.98	1 100.00 ± 0.00	0 0.00 ± 0.00	0 0.00 ± 0.00
TCE-CMIO	146 0.00 ± 0.00	37 25.34 ± 3.60	6 16.22 ± 6.06	6 100.00 ± 0.00	6 100.00 ± 0.00	2 33.33 ± 19.25	2 100.00 ± 0.00	1 50.00 ± 35.36	1 100.00 ± 0.00
PHX-CMUP	120 0.00 ± 0.00	80 66.67 ± 4.30	36 45.00 ± 5.56	36 100.00 ± 0.00	33 91.67 ± 4.61	4 12.12 ± 5.68	1 25.00 ± 21.65	0 0.00 ± 0.00	0 0.00 ± 0.00
PHX-CMX	64 0.00 ± 0.00	50 78.12 ± 5.17	24 48.00 ± 7.07	24 100.00 ± 0.00	24 100.00 ± 0.00	1 4.17 ± 4.08	1 100.00 ± 0.00	1 100.00 ± 0.00	1 100.00 ± 0.00
PHX-CMU	22 0.00 ± 0.00	16 72.73 ± 9.50	5 31.25 ± 11.59	5 100.00 ± 0.00	5 100.00 ± 0.00	0 0.00 ± 0.00	0 0.00 ± 0.00	0 0.00 ± 0.00	0 0.00 ± 0.00
PHX-CMP	46 0.00 ± 0.00	38 82.61 ± 5.59	9 23.68 ± 6.90	9 100.00 ± 0.00	7 77.78 ± 13.86	2 28.57 ± 17.07	2 100.00 ± 0.00	1 50.00 ± 35.36	1 100.00 ± 0.00
PHX-CMIO	77 0.00 ± 0.00	55 71.43 ± 5.15	4 7.27 ± 3.50	4 100.00 ± 0.00	4 100.00 ± 0.00	1 25.00 ± 21.65	0 0.00 ± 0.00	0 0.00 ± 0.00	0 0.00 ± 0.00
$e\mu$	1223 0.01 ± 0.00	476 38.92 ± 1.39	232 48.74 ± 2.29	229 98.71 ± 0.74	206 89.96 ± 1.99	22 10.68 ± 2.15	17 77.27 ± 8.93	5 29.41 ± 11.05	5 100.00 ± 0.00
CMUP-CMUP	2668 0.03 ± 0.00	2258 84.63 ± 0.70	2106 93.27 ± 0.53	2086 99.05 ± 0.21	2010 96.36 ± 0.41	4 0.20 ± 0.10	3 75.00 ± 21.65	1 33.33 ± 27.22	0 0.00 ± 0.00
CMUP-CMX	2531 0.03 ± 0.00	2438 96.33 ± 0.37	2273 93.23 ± 0.51	2260 99.43 ± 0.16	2175 96.24 ± 0.40	4 0.18 ± 0.09	3 75.00 ± 21.65	1 33.33 ± 27.22	0 0.00 ± 0.00
CMUP-CMU	931 0.01 ± 0.00	884 94.95 ± 0.72	845 95.59 ± 0.69	841 99.53 ± 0.24	811 96.43 ± 0.64	0 0.00 ± 0.00	0 0.00 ± 0.00	0 0.00 ± 0.00	0 0.00 ± 0.00
CMUP-CMP	1285 0.01 ± 0.00	1152 89.65 ± 0.85	1069 92.80 ± 0.76	1059 99.06 ± 0.29	1017 96.03 ± 0.60	5 0.49 ± 0.22	5 100.00 ± 0.00	2 40.00 ± 21.91	1 50.00 ± 35.36
CMUP-CMIO	515 0.01 ± 0.00	404 78.45 ± 1.81	374 92.57 ± 1.30	371 99.20 ± 0.46	357 96.23 ± 0.99	0 0.00 ± 0.00	0 0.00 ± 0.00	0 0.00 ± 0.00	0 0.00 ± 0.00
CMX-CMX	1116 0.01 ± 0.00	858 76.88 ± 1.26	796 92.77 ± 0.88	794 99.75 ± 0.18	773 97.36 ± 0.57	1 0.13 ± 0.13	0 0.00 ± 0.00	0 0.00 ± 0.00	0 0.00 ± 0.00
CMX-CMU	506 0.01 ± 0.00	486 96.05 ± 0.87	454 93.42 ± 1.12	451 99.34 ± 0.38	440 97.56 ± 0.73	0 0.00 ± 0.00	0 0.00 ± 0.00	0 0.00 ± 0.00	0 0.00 ± 0.00
CMX-CMP	555 0.01 ± 0.00	539 97.12 ± 0.71	499 92.58 ± 1.13	496 99.40 ± 0.35	477 96.17 ± 0.86	1 0.21 ± 0.21	0 0.00 ± 0.00	0 0.00 ± 0.00	0 0.00 ± 0.00
CMX-CMIO	176 0.00 ± 0.00	161 91.48 ± 2.10	144 89.44 ± 2.42	144 100.00 ± 0.00	137 95.14 ± 1.79	0 0.00 ± 0.00	0 0.00 ± 0.00	0 0.00 ± 0.00	0 0.00 ± 0.00
$\mu\mu$	10283 0.11 ± 0.00	9180 89.27 ± 0.31	8560 93.25 ± 0.26	8502 99.32 ± 0.09	8197 96.41 ± 0.20	15 0.18 ± 0.05	11 73.33 ± 11.42	4 36.36 ± 14.50	1 25.00 ± 21.65
total	33113 0.35 ± 0.00	29119 87.94 ± 0.18	26964 92.60 ± 0.15	26797 99.38 ± 0.05	25897 96.64 ± 0.11	76 0.29 ± 0.03	56 73.68 ± 5.05	17 30.36 ± 6.14	13 76.47 ± 10.29

Table 35: data acceptance table, assuming $M_H^{\rm SM} = 130$ GeV

Categ	Lep ID	Lep1 Isol	Lep2 Isol	$M_{\ell\ell} > 16$	jet veto	$\not\!\!E_t$	opp sign	$M_{\ell\ell} < M_u$	$H_T < M_H$
TCE-TCE	9584 0.10 ± 0.00	8306 86.67 ± 0.35	7313 88.04 ± 0.36	7216 98.67 ± 0.13	6961 96.47 ± 0.22	12 0.17 ± 0.05	12 100.00 ± 0.00	3 25.00 ± 12.50	2 66.67 ± 27.22
TCE-PHX	9539 0.10 ± 0.00	8707 91.28 ± 0.29	8485 97.45 ± 0.17	8480 99.94 ± 0.03	8227 97.02 ± 0.18	15 0.18 ± 0.05	9 60.00 ± 12.65	6 66.67 ± 15.71	5 83.33 ± 15.21
ee	21607 0.23 ± 0.00	19463 90.08 ± 0.20	18172 93.37 ± 0.18	18066 99.42 ± 0.06	17494 96.83 ± 0.13	32 0.18 ± 0.03	22 68.75 ± 8.19	9 40.91 ± 10.48	7 77.78 ± 13.86
TCE-CMUP	372 0.00 ± 0.00	109 29.30 ± 2.36	84 77.06 ± 4.03	81 96.43 ± 2.02	70 86.42 ± 3.81	5 7.14 ± 3.08	4 80.00 ± 17.89	2 50.00 ± 25.00	1 50.00 ± 35.36
TCE-CMX	219 0.00 ± 0.00	52 23.74 ± 2.88	41 78.85 ± 5.66	41 100.00 ± 0.00	37 90.24 ± 4.63	5 13.51 ± 5.62	5 100.00 ± 0.00	2 40.00 ± 21.91	2 100.00 ± 0.00
TCE-CMU	52 0.00 ± 0.00	14 26.92 ± 6.15	9 64.29 ± 12.81	9 100.00 ± 0.00	8 88.89 ± 10.48	0 0.00 ± 0.00	0 0.00 ± 0.00	0 0.00 ± 0.00	0 0.00 ± 0.00
TCE-CMP	105 0.00 ± 0.00	25 23.81 ± 4.16	14 56.00 ± 9.93	14 100.00 ± 0.00	12 85.71 ± 9.35	1 8.33 ± 7.98	1 100.00 ± 0.00	0 0.00 ± 0.00	0 0.00 ± 0.00
TCE-CMIO	146 0.00 ± 0.00	37 25.34 ± 3.60	6 16.22 ± 6.06	6 100.00 ± 0.00	6 100.00 ± 0.00	1 16.67 ± 15.21	1 100.00 ± 0.00	0 0.00 ± 0.00	0 0.00 ± 0.00
PHX-CMUP	120 0.00 ± 0.00	80 66.67 ± 4.30	36 45.00 ± 5.56	36 100.00 ± 0.00	33 91.67 ± 4.61	4 12.12 ± 5.68	1 25.00 ± 21.65	0 0.00 ± 0.00	0 0.00 ± 0.00
PHX-CMX	64 0.00 ± 0.00	50 78.12 ± 5.17	24 48.00 ± 7.07	24 100.00 ± 0.00	24 100.00 ± 0.00	1 4.17 ± 4.08	1 100.00 ± 0.00	1 100.00 ± 0.00	1 100.00 ± 0.00
PHX-CMU	22 0.00 ± 0.00	16 72.73 ± 9.50	5 31.25 ± 11.59	5 100.00 ± 0.00	5 100.00 ± 0.00	0 0.00 ± 0.00	0 0.00 ± 0.00	0 0.00 ± 0.00	0 0.00 ± 0.00
PHX-CMP	46 0.00 ± 0.00	38 82.61 ± 5.59	9 23.68 ± 6.90	9 100.00 ± 0.00	7 77.78 ± 13.86	2 28.57 ± 17.07	2 100.00 ± 0.00	1 50.00 ± 35.36	1 100.00 ± 0.00
PHX-CMIO	77 0.00 ± 0.00	55 71.43 ± 5.15	4 7.27 ± 3.50	4 100.00 ± 0.00	4 100.00 ± 0.00	1 25.00 ± 21.65	0 0.00 ± 0.00	0 0.00 ± 0.00	0 0.00 ± 0.00
$e\mu$	1223 0.01 ± 0.00	476 38.92 ± 1.39	232 48.74 ± 2.29	229 98.71 ± 0.74	206 89.96 ± 1.99	20 9.71 ± 2.06	15 75.00 ± 9.68	6 40.00 ± 12.65	5 83.33 ± 15.21
CMUP-CMUP	2668 0.03 ± 0.00	2258 84.63 ± 0.70	2106 93.27 ± 0.53	2086 99.05 ± 0.21	2010 96.36 ± 0.41	4 0.20 ± 0.10	3 75.00 ± 21.65	2 66.67 ± 27.22	2 100.00 ± 0.00
CMUP-CMX	2531 0.03 ± 0.00	2438 96.33 ± 0.37	2273 93.23 ± 0.51	2260 99.43 ± 0.16	2175 96.24 ± 0.40	4 0.18 ± 0.09	3 75.00 ± 21.65	2 66.67 ± 27.22	1 50.00 ± 35.36
CMUP-CMU	931 0.01 ± 0.00	884 94.95 ± 0.72	845 95.59 ± 0.69	841 99.53 ± 0.24	811 96.43 ± 0.64	0 0.00 ± 0.00	0 0.00 ± 0.00	0 0.00 ± 0.00	0 0.00 ± 0.00
CMUP-CMP	1285 0.01 ± 0.00	1152 89.65 ± 0.85	1069 92.80 ± 0.76	1059 99.06 ± 0.29	1017 96.03 ± 0.60	4 0.39 ± 0.20	4 100.00 ± 0.00	2 50.00 ± 25.00	1 50.00 ± 35.36
CMUP-CMIO	515 0.01 ± 0.00	404 78.45 ± 1.81	374 92.57 ± 1.30	371 99.20 ± 0.46	357 96.23 ± 0.99	0 0.00 ± 0.00	0 0.00 ± 0.00	0 0.00 ± 0.00	0 0.00 ± 0.00
CMX-CMX	1116 0.01 ± 0.00	858 76.88 ± 1.26	796 92.77 ± 0.88	794 99.75 ± 0.18	773 97.36 ± 0.57	1 0.13 ± 0.13	0 0.00 ± 0.00	0 0.00 ± 0.00	0 0.00 ± 0.00
CMX-CMU	506 0.01 ± 0.00	486 96.05 ± 0.87	454 93.42 ± 1.12	451 99.34 ± 0.38	440 97.56 ± 0.73	0 0.00 ± 0.00	0 0.00 ± 0.00	0 0.00 ± 0.00	0 0.00 ± 0.00
CMX-CMP	555 0.01 ± 0.00	539 97.12 ± 0.71	499 92.58 ± 1.13	496 99.40 ± 0.35	477 96.17 ± 0.86	0 0.00 ± 0.00	0 0.00 ± 0.00	0 0.00 ± 0.00	0 0.00 ± 0.00
CMX-CMIO	176 0.00 ± 0.00	161 91.48 ± 2.10	144 89.44 ± 2.42	144 100.00 ± 0.00	137 95.14 ± 1.79	0 0.00 ± 0.00	0 0.00 ± 0.00	0 0.00 ± 0.00	0 0.00 ± 0.00
$\mu\mu$	10283 0.11 ± 0.00	9180 89.27 ± 0.31	8560 93.25 ± 0.26	8502 99.32 ± 0.09	8197 96.41 ± 0.20	13 0.16 ± 0.04	10 76.92 ± 11.69	6 60.00 ± 15.49	4 66.67 ± 19.25
total	33113 0.35 ± 0.00	29119 87.94 ± 0.18	26964 92.60 ± 0.15	26797 99.38 ± 0.05	25897 96.64 ± 0.11	65 0.25 ± 0.03	47 72.31 ± 5.55	21 44.68 ± 7.25	16 76.19 ± 9.29

Table 36: data acceptance table, assuming $M_H^{\rm SM} = 140$ GeV

Categ	Lep ID	Lep1 Isol	Lep2 Isol	$M_{\ell\ell} > 16$	jet veto	$\not\!\!E_t$	opp sign	$M_{\ell\ell} < M_u$	$H_T < M_H$
TCE-TCE	9584 0.10 ± 0.00	8306 86.67 ± 0.35	7313 88.04 ± 0.36	7216 98.67 ± 0.13	6961 96.47 ± 0.22	9 0.13 ± 0.04	9 100.00 ± 0.00	3 33.33 ± 15.71	2 66.67 ± 27.22
TCE-PHX	9539 0.10 ± 0.00	8707 91.28 ± 0.29	8485 97.45 ± 0.17	8480 99.94 ± 0.03	8227 97.02 ± 0.18	13 0.16 ± 0.04	7 53.85 ± 13.83	5 71.43 ± 17.07	4 80.00 ± 17.89
ee	21607 0.23 ± 0.00	19463 90.08 ± 0.20	18172 93.37 ± 0.18	18066 99.42 ± 0.06	17494 96.83 ± 0.13	27 0.15 ± 0.03	17 62.96 ± 9.29	8 47.06 ± 12.11	6 75.00 ± 15.31
TCE-CMUP	372 0.00 ± 0.00	109 29.30 ± 2.36	84 77.06 ± 4.03	81 96.43 ± 2.02	70 86.42 ± 3.81	4 5.71 ± 2.77	3 75.00 ± 21.65	1 33.33 ± 27.22	0 0.00 ± 0.00
TCE-CMX	219 0.00 ± 0.00	52 23.74 ± 2.88	41 78.85 ± 5.66	41 100.00 ± 0.00	37 90.24 ± 4.63	4 10.81 ± 5.10	4 100.00 ± 0.00	2 50.00 ± 25.00	2 100.00 ± 0.00
TCE-CMU	52 0.00 ± 0.00	14 26.92 ± 6.15	9 64.29 ± 12.81	9 100.00 ± 0.00	8 88.89 ± 10.48	0 0.00 ± 0.00	0 0.00 ± 0.00	0 0.00 ± 0.00	0 0.00 ± 0.00
TCE-CMP	105 0.00 ± 0.00	25 23.81 ± 4.16	14 56.00 ± 9.93	14 100.00 ± 0.00	12 85.71 ± 9.35	1 8.33 ± 7.98	1 100.00 ± 0.00	0 0.00 ± 0.00	0 0.00 ± 0.00
TCE-CMIO	146 0.00 ± 0.00	37 25.34 ± 3.60	6 16.22 ± 6.06	6 100.00 ± 0.00	6 100.00 ± 0.00	1 16.67 ± 15.21	1 100.00 ± 0.00	1 100.00 ± 0.00	0 0.00 ± 0.00
PHX-CMUP	120 0.00 ± 0.00	80 66.67 ± 4.30	36 45.00 ± 5.56	36 100.00 ± 0.00	33 91.67 ± 4.61	4 12.12 ± 5.68	1 25.00 ± 21.65	0 0.00 ± 0.00	0 0.00 ± 0.00
PHX-CMX	64 0.00 ± 0.00	50 78.12 ± 5.17	24 48.00 ± 7.07	24 100.00 ± 0.00	24 100.00 ± 0.00	1 4.17 ± 4.08	1 100.00 ± 0.00	1 100.00 ± 0.00	1 100.00 ± 0.00
PHX-CMU	22 0.00 ± 0.00	16 72.73 ± 9.50	5 31.25 ± 11.59	5 100.00 ± 0.00	5 100.00 ± 0.00	0 0.00 ± 0.00	0 0.00 ± 0.00	0 0.00 ± 0.00	0 0.00 ± 0.00
PHX-CMP	46 0.00 ± 0.00	38 82.61 ± 5.59	9 23.68 ± 6.90	9 100.00 ± 0.00	7 77.78 ± 13.86	2 28.57 ± 17.07	2 100.00 ± 0.00	1 50.00 ± 35.36	1 100.00 ± 0.00
PHX-CMIO	77 0.00 ± 0.00	55 71.43 ± 5.15	4 7.27 ± 3.50	4 100.00 ± 0.00	4 100.00 ± 0.00	1 25.00 ± 21.65	0 0.00 ± 0.00	0 0.00 ± 0.00	0 0.00 ± 0.00
$e\mu$	1223 0.01 ± 0.00	476 38.92 ± 1.39	232 48.74 ± 2.29	229 98.71 ± 0.74	206 89.96 ± 1.99	18 8.74 ± 1.97	13 72.22 ± 10.56	6 46.15 ± 13.83	4 66.67 ± 19.25
CMUP-CMUP	2668 0.03 ± 0.00	2258 84.63 ± 0.70	2106 93.27 ± 0.53	2086 99.05 ± 0.21	2010 96.36 ± 0.41	3 0.15 ± 0.09	3 100.00 ± 0.00	2 66.67 ± 27.22	2 100.00 ± 0.00
CMUP-CMX	2531 0.03 ± 0.00	2438 96.33 ± 0.37	2273 93.23 ± 0.51	2260 99.43 ± 0.16	2175 96.24 ± 0.40	3 0.14 ± 0.08	3 100.00 ± 0.00	3 100.00 ± 0.00	2 66.67 ± 27.22
CMUP-CMU	931 0.01 ± 0.00	884 94.95 ± 0.72	845 95.59 ± 0.69	841 99.53 ± 0.24	811 96.43 ± 0.64	0 0.00 ± 0.00	0 0.00 ± 0.00	0 0.00 ± 0.00	0 0.00 ± 0.00
CMUP-CMP	1285 0.01 ± 0.00	1152 89.65 ± 0.85	1069 92.80 ± 0.76	1059 99.06 ± 0.29	1017 96.03 ± 0.60	4 0.39 ± 0.20	4 100.00 ± 0.00	2 50.00 ± 25.00	1 50.00 ± 35.36
CMUP-CMIO	515 0.01 ± 0.00	404 78.45 ± 1.81	374 92.57 ± 1.30	371 99.20 ± 0.46	357 96.23 ± 0.99	0 0.00 ± 0.00	0 0.00 ± 0.00	0 0.00 ± 0.00	0 0.00 ± 0.00
CMX-CMX	1116 0.01 ± 0.00	858 76.88 ± 1.26	796 92.77 ± 0.88	794 99.75 ± 0.18	773 97.36 ± 0.57	1 0.13 ± 0.13	0 0.00 ± 0.00	0 0.00 ± 0.00	0 0.00 ± 0.00
CMX-CMU	506 0.01 ± 0.00	486 96.05 ± 0.87	454 93.42 ± 1.12	451 99.34 ± 0.38	440 97.56 ± 0.73	0 0.00 ± 0.00	0 0.00 ± 0.00	0 0.00 ± 0.00	0 0.00 ± 0.00
CMX-CMP	555 0.01 ± 0.00	539 97.12 ± 0.71	499 92.58 ± 1.13	496 99.40 ± 0.35	477 96.17 ± 0.86	0 0.00 ± 0.00	0 0.00 ± 0.00	0 0.00 ± 0.00	0 0.00 ± 0.00
CMX-CMIO	176 0.00 ± 0.00	161 91.48 ± 2.10	144 89.44 ± 2.42	144 100.00 ± 0.00	137 95.14 ± 1.79	0 0.00 ± 0.00	0 0.00 ± 0.00	0 0.00 ± 0.00	0 0.00 ± 0.00
$\mu\mu$	10283 0.11 ± 0.00	9180 89.27 ± 0.31	8560 93.25 ± 0.26	8502 99.32 ± 0.09	8197 96.41 ± 0.20	11 0.13 ± 0.04	10 90.91 ± 8.67	7 70.00 ± 14.49	5 71.43 ± 17.07
total	33113 0.35 ± 0.00	29119 87.94 ± 0.18	26964 92.60 ± 0.15	26797 99.38 ± 0.05	25897 96.64 ± 0.11	56 0.22 ± 0.03	40 71.43 ± 6.04	21 52.50 ± 7.90	15 71.43 ± 9.86

Table 37: data acceptance table, assuming $M_H^{\rm SM} = 150$ GeV

Categ	Lep ID	Lep1 Isol	Lep2 Isol	$M_{\ell\ell} > 16$	jet veto	$\not{E}_t$	opp sign	$M_{\ell\ell} < M_u$	$H_T < M_H$
TCE-TCE	9584 0.10 ± 0.00	8306 86.67 ± 0.35	7313 88.04 ± 0.36	7216 98.67 ± 0.13	6961 96.47 ± 0.22	7 0.10 ± 0.04	7 100.00 ± 0.00	3 42.86 ± 18.70	3 100.00 ± 0.00
TCE-PHX	9539 0.10 ± 0.00	8707 91.28 ± 0.29	8485 97.45 ± 0.17	8480 99.94 ± 0.03	8227 97.02 ± 0.18	13 0.16 ± 0.04	7 53.85 ± 13.83	5 71.43 ± 17.07	5 100.00 ± 0.00
ee	21607 0.23 ± 0.00	19463 90.08 ± 0.20	18172 93.37 ± 0.18	18066 99.42 ± 0.06	17494 96.83 ± 0.13	25 0.14 ± 0.03	15 60.00 ± 9.80	8 53.33 ± 12.88	8 100.00 ± 0.00
TCE-CMUP	372 0.00 ± 0.00	109 29.30 ± 2.36	84 77.06 ± 4.03	81 96.43 ± 2.02	70 86.42 ± 3.81	3 4.29 ± 2.42	3 100.00 ± 0.00	2 66.67 ± 27.22	1 50.00 ± 35.36
TCE-CMX	219 0.00 ± 0.00	52 23.74 ± 2.88	41 78.85 ± 5.66	41 100.00 ± 0.00	37 90.24 ± 4.63	4 10.81 ± 5.10	4 100.00 ± 0.00	2 50.00 ± 25.00	2 100.00 ± 0.00
TCE-CMU	52 0.00 ± 0.00	14 26.92 ± 6.15	9 64.29 ± 12.81	9 100.00 ± 0.00	8 88.89 ± 10.48	0 0.00 ± 0.00	0 0.00 ± 0.00	0 0.00 ± 0.00	0 0.00 ± 0.00
TCE-CMP	105 0.00 ± 0.00	25 23.81 ± 4.16	14 56.00 ± 9.93	14 100.00 ± 0.00	12 85.71 ± 9.35	1 8.33 ± 7.98	1 100.00 ± 0.00	0 0.00 ± 0.00	0 0.00 ± 0.00
TCE-CMIO	146 0.00 ± 0.00	37 25.34 ± 3.60	6 16.22 ± 6.06	6 100.00 ± 0.00	6 100.00 ± 0.00	1 16.67 ± 15.21	1 100.00 ± 0.00	1 100.00 ± 0.00	0 0.00 ± 0.00
PHX-CMUP	120 0.00 ± 0.00	80 66.67 ± 4.30	36 45.00 ± 5.56	36 100.00 ± 0.00	33 91.67 ± 4.61	4 12.12 ± 5.68	1 25.00 ± 21.65	0 0.00 ± 0.00	0 0.00 ± 0.00
PHX-CMX	64 0.00 ± 0.00	50 78.12 ± 5.17	24 48.00 ± 7.07	24 100.00 ± 0.00	24 100.00 ± 0.00	0 0.00 ± 0.00	0 0.00 ± 0.00	0 0.00 ± 0.00	0 0.00 ± 0.00
PHX-CMU	22 0.00 ± 0.00	16 72.73 ± 9.50	5 31.25 ± 11.59	5 100.00 ± 0.00	5 100.00 ± 0.00	0 0.00 ± 0.00	0 0.00 ± 0.00	0 0.00 ± 0.00	0 0.00 ± 0.00
PHX-CMP	46 0.00 ± 0.00	38 82.61 ± 5.59	9 23.68 ± 6.90	9 100.00 ± 0.00	7 77.78 ± 13.86	2 28.57 ± 17.07	2 100.00 ± 0.00	1 50.00 ± 35.36	1 100.00 ± 0.00
PHX-CMIO	77 0.00 ± 0.00	55 71.43 ± 5.15	4 7.27 ± 3.50	4 100.00 ± 0.00	4 100.00 ± 0.00	1 25.00 ± 21.65	0 0.00 ± 0.00	0 0.00 ± 0.00	0 0.00 ± 0.00
$e\mu$	1223 0.01 ± 0.00	476 38.92 ± 1.39	232 48.74 ± 2.29	229 98.71 ± 0.74	206 89.96 ± 1.99	16 7.77 ± 1.86	12 75.00 ± 10.83	6 50.00 ± 14.43	4 66.67 ± 19.25
CMUP-CMUP	2668 0.03 ± 0.00	2258 84.63 ± 0.70	2106 93.27 ± 0.53	2086 99.05 ± 0.21	2010 96.36 ± 0.41	3 0.15 ± 0.09	3 100.00 ± 0.00	3 100.00 ± 0.00	3 100.00 ± 0.00
CMUP-CMX	2531 0.03 ± 0.00	2438 96.33 ± 0.37	2273 93.23 ± 0.51	2260 99.43 ± 0.16	2175 96.24 ± 0.40	2 0.09 ± 0.06	2 100.00 ± 0.00	2 100.00 ± 0.00	1 50.00 ± 35.36
CMUP-CMU	931 0.01 ± 0.00	884 94.95 ± 0.72	845 95.59 ± 0.69	841 99.53 ± 0.24	811 96.43 ± 0.64	0 0.00 ± 0.00	0 0.00 ± 0.00	0 0.00 ± 0.00	0 0.00 ± 0.00
CMUP-CMP	1285 0.01 ± 0.00	1152 89.65 ± 0.85	1069 92.80 ± 0.76	1059 99.06 ± 0.29	1017 96.03 ± 0.60	2 0.20 ± 0.14	2 100.00 ± 0.00	1 50.00 ± 35.36	0 0.00 ± 0.00
CMUP-CMIO	515 0.01 ± 0.00	404 78.45 ± 1.81	374 92.57 ± 1.30	371 99.20 ± 0.46	357 96.23 ± 0.99	0 0.00 ± 0.00	0 0.00 ± 0.00	0 0.00 ± 0.00	0 0.00 ± 0.00
CMX-CMX	1116 0.01 ± 0.00	858 76.88 ± 1.26	796 92.77 ± 0.88	794 99.75 ± 0.18	773 97.36 ± 0.57	0 0.00 ± 0.00	0 0.00 ± 0.00	0 0.00 ± 0.00	0 0.00 ± 0.00
CMX-CMU	506 0.01 ± 0.00	486 96.05 ± 0.87	454 93.42 ± 1.12	451 99.34 ± 0.38	440 97.56 ± 0.73	0 0.00 ± 0.00	0 0.00 ± 0.00	0 0.00 ± 0.00	0 0.00 ± 0.00
CMX-CMP	555 0.01 ± 0.00	539 97.12 ± 0.71	499 92.58 ± 1.13	496 99.40 ± 0.35	477 96.17 ± 0.86	0 0.00 ± 0.00	0 0.00 ± 0.00	0 0.00 ± 0.00	0 0.00 ± 0.00
CMX-CMIO	176 0.00 ± 0.00	161 91.48 ± 2.10	144 89.44 ± 2.42	144 100.00 ± 0.00	137 95.14 ± 1.79	0 0.00 ± 0.00	0 0.00 ± 0.00	0 0.00 ± 0.00	0 0.00 ± 0.00
$\mu\mu$	10283 0.11 ± 0.00	9180 89.27 ± 0.31	8560 93.25 ± 0.26	8502 99.32 ± 0.09	8197 96.41 ± 0.20	7 0.09 ± 0.03	7 100.00 ± 0.00	6 85.71 ± 13.23	4 66.67 ± 19.25
total	33113 0.35 ± 0.00	29119 87.94 ± 0.18	26964 92.60 ± 0.15	26797 99.38 ± 0.05	25897 96.64 ± 0.11	48 0.19 ± 0.03	34 70.83 ± 6.56	20 58.82 ± 8.44	16 80.00 ± 8.94

Table 38: data acceptance table, assuming $M_H^{\rm SM} = 160$ GeV

Categ	Lep ID	Lep1 Isol	Lep2 Isol	$M_{\ell\ell} > 16$	jet veto	$\not\!\!E_t$	opp sign	$M_{\ell\ell} < M_u$	$H_T < M_H$
TCE-TCE	9584	8306	7313	7216	6961	6	6	2	2
	0.10 ± 0.00	86.67 ± 0.35	88.04 ± 0.36	98.67 ± 0.13	96.47 ± 0.22	0.09 ± 0.04	100.00 ± 0.00	33.33 ± 19.25	100.00 ± 0.00
TCE-PHX	9539	8707	8485	8480	8227	10	6	4	4
	0.10 ± 0.00	91.28 ± 0.29	97.45 ± 0.17	99.94 ± 0.03	97.02 ± 0.18	0.12 ± 0.04	60.00 ± 15.49	66.67 ± 19.25	100.00 ± 0.00
ee	21607	19463	18172	18066	17494	19	13	6	6
	0.23 ± 0.00	90.08 ± 0.20	93.37 ± 0.18	99.42 ± 0.06	96.83 ± 0.13	0.11 ± 0.02	68.42 ± 10.66	46.15 ± 13.83	100.00 ± 0.00
TCE-CMUP	372	109	84	81	70	3	3	2	2
	0.00 ± 0.00	29.30 ± 2.36	77.06 ± 4.03	96.43 ± 2.02	86.42 ± 3.81	4.29 ± 2.42	100.00 ± 0.00	66.67 ± 27.22	100.00 ± 0.00
TCE-CMX	219	52	41	41	37	4	4	2	2
	0.00 ± 0.00	23.74 ± 2.88	78.85 ± 5.66	100.00 ± 0.00	90.24 ± 4.63	10.81 ± 5.10	100.00 ± 0.00	50.00 ± 25.00	100.00 ± 0.00
TCE-CMU	52	14	9	9	8	0	0	0	0
	0.00 ± 0.00	26.92 ± 6.15	64.29 ± 12.81	100.00 ± 0.00	88.89 ± 10.48	0.00 ± 0.00	0.00 ± 0.00	0.00 ± 0.00	0.00 ± 0.00
TCE-CMP	105	25	14	14	12	1	1	0	0
	0.00 ± 0.00	23.81 ± 4.16	56.00 ± 9.93	100.00 ± 0.00	85.71 ± 9.35	8.33 ± 7.98	100.00 ± 0.00	0.00 ± 0.00	0.00 ± 0.00
TCE-CMIO	146	37	6	6	6	1	1	1	0
	0.00 ± 0.00	25.34 ± 3.60	16.22 ± 6.06	100.00 ± 0.00	100.00 ± 0.00	16.67 ± 15.21	100.00 ± 0.00	100.00 ± 0.00	0.00 ± 0.00
PHX-CMUP	120	80	36	36	33	4	1	0	0
	0.00 ± 0.00	66.67 ± 4.30	45.00 ± 5.56	100.00 ± 0.00	91.67 ± 4.61	12.12 ± 5.68	25.00 ± 21.65	0.00 ± 0.00	0.00 ± 0.00
PHX-CMX	64	50	24	24	24	0	0	0	0
	0.00 ± 0.00	78.12 ± 5.17	48.00 ± 7.07	100.00 ± 0.00	100.00 ± 0.00	0.00 ± 0.00	0.00 ± 0.00	0.00 ± 0.00	0.00 ± 0.00
PHX-CMU	22	16	5	5	5	0	0	0	0
	0.00 ± 0.00	72.73 ± 9.50	31.25 ± 11.59	100.00 ± 0.00	100.00 ± 0.00	0.00 ± 0.00	0.00 ± 0.00	0.00 ± 0.00	0.00 ± 0.00
PHX-CMP	46	38	9	9	7	2	2	1	1
	0.00 ± 0.00	82.61 ± 5.59	23.68 ± 6.90	100.00 ± 0.00	77.78 ± 13.86	28.57 ± 17.07	100.00 ± 0.00	50.00 ± 35.36	100.00 ± 0.00
PHX-CMIO	77	55	4	4	4	1	0	0	0
	0.00 ± 0.00	71.43 ± 5.15	7.27 ± 3.50	100.00 ± 0.00	100.00 ± 0.00	25.00 ± 21.65	0.00 ± 0.00	0.00 ± 0.00	0.00 ± 0.00
$e\mu$	1223	476	232	229	206	16	12	6	5
	0.01 ± 0.00	38.92 ± 1.39	48.74 ± 2.29	98.71 ± 0.74	89.96 ± 1.99	7.77 ± 1.86	75.00 ± 10.83	50.00 ± 14.43	83.33 ± 15.21
CMUP-CMUP	2668	2258	2106	2086	2010	3	3	3	3
	0.03 ± 0.00	84.63 ± 0.70	93.27 ± 0.53	99.05 ± 0.21	96.36 ± 0.41	0.15 ± 0.09	100.00 ± 0.00	100.00 ± 0.00	100.00 ± 0.00
CMUP-CMX	2531	2438	2273	2260	2175	2	2	2	1
	0.03 ± 0.00	96.33 ± 0.37	93.23 ± 0.51	99.43 ± 0.16	96.24 ± 0.40	0.09 ± 0.06	100.00 ± 0.00	100.00 ± 0.00	50.00 ± 35.36
CMUP-CMU	931	884	845	841	811	0	0	0	0
	0.01 ± 0.00	94.95 ± 0.72	95.59 ± 0.69	99.53 ± 0.24	96.43 ± 0.64	0.00 ± 0.00	0.00 ± 0.00	0.00 ± 0.00	0.00 ± 0.00
CMUP-CMP	1285	1152	1069	1059	1017	2	2	1	1
	0.01 ± 0.00	89.65 ± 0.85	92.80 ± 0.76	99.06 ± 0.29	96.03 ± 0.60	0.20 ± 0.14	100.00 ± 0.00	50.00 ± 35.36	100.00 ± 0.00
CMUP-CMIO	515	404	374	371	357	0	0	0	0
	0.01 ± 0.00	78.45 ± 1.81	92.57 ± 1.30	99.20 ± 0.46	96.23 ± 0.99	0.00 ± 0.00	0.00 ± 0.00	0.00 ± 0.00	0.00 ± 0.00
CMX-CMX	1116	858	796	794	773	0	0	0	0
	0.01 ± 0.00	76.88 ± 1.26	92.77 ± 0.88	99.75 ± 0.18	97.36 ± 0.57	0.00 ± 0.00	0.00 ± 0.00	0.00 ± 0.00	0.00 ± 0.00
CMX-CMU	506	486	454	451	440	0	0	0	0
	0.01 ± 0.00	96.05 ± 0.87	93.42 ± 1.12	99.34 ± 0.38	97.56 ± 0.73	0.00 ± 0.00	0.00 ± 0.00	0.00 ± 0.00	0.00 ± 0.00
CMX-CMP	555	539	499	496	477	0	0	0	0
	0.01 ± 0.00	97.12 ± 0.71	92.58 ± 1.13	99.40 ± 0.35	96.17 ± 0.86	0.00 ± 0.00	0.00 ± 0.00	0.00 ± 0.00	0.00 ± 0.00
CMX-CMIO	176	161	144	144	137	0	0	0	0
	0.00 ± 0.00	91.48 ± 2.10	89.44 ± 2.42	100.00 ± 0.00	95.14 ± 1.79	0.00 ± 0.00	0.00 ± 0.00	0.00 ± 0.00	0.00 ± 0.00
$\mu\mu$	10283	9180	8560	8502	8197	7	7	6	5
	0.11 ± 0.00	89.27 ± 0.31	93.25 ± 0.26	99.32 ± 0.09	96.41 ± 0.20	0.09 ± 0.03	100.00 ± 0.00	85.71 ± 13.23	83.33 ± 15.21
total	33113	29119	26964	26797	25897	42	32	18	16
	0.35 ± 0.00	87.94 ± 0.18	92.60 ± 0.15	99.38 ± 0.05	96.64 ± 0.11	0.16 ± 0.03	76.19 ± 6.57	56.25 ± 8.77	88.89 ± 7.41

Table 39: data acceptance table, assuming $M_H^{\mathrm{SM}} = 170$ GeV

Categ	Lep ID	Lep1 Isol	Lep2 Isol	$M_{\ell\ell} > 16$	jet veto	$\not\!\!E_t$	opp sign	$M_{\ell\ell} < M_u$	$H_T < M_H$
TCE-TCE	9584 0.10 ± 0.00	8306 86.67 ± 0.35	7313 88.04 ± 0.36	7216 98.67 ± 0.13	6961 96.47 ± 0.22	5 0.07 ± 0.03	5 100.00 ± 0.00	2 40.00 ± 21.91	2 100.00 ± 0.00
TCE-PHX	9539 0.10 ± 0.00	8707 91.28 ± 0.29	8485 97.45 ± 0.17	8480 99.94 ± 0.03	8227 97.02 ± 0.18	7 0.09 ± 0.03	5 71.43 ± 17.07	4 80.00 ± 17.89	4 100.00 ± 0.00
ee	21607 0.23 ± 0.00	19463 90.08 ± 0.20	18172 93.37 ± 0.18	18066 99.42 ± 0.06	17494 96.83 ± 0.13	15 0.09 ± 0.02	11 73.33 ± 11.42	6 54.55 ± 15.01	6 100.00 ± 0.00
TCE-CMUP	372 0.00 ± 0.00	109 29.30 ± 2.36	84 77.06 ± 4.03	81 96.43 ± 2.02	70 86.42 ± 3.81	3 4.29 ± 2.42	3 100.00 ± 0.00	2 66.67 ± 27.22	2 100.00 ± 0.00
TCE-CMX	219 0.00 ± 0.00	52 23.74 ± 2.88	41 78.85 ± 5.66	41 100.00 ± 0.00	37 90.24 ± 4.63	4 10.81 ± 5.10	4 100.00 ± 0.00	3 75.00 ± 21.65	3 100.00 ± 0.00
TCE-CMU	52 0.00 ± 0.00	14 26.92 ± 6.15	9 64.29 ± 12.81	9 100.00 ± 0.00	8 88.89 ± 10.48	0 0.00 ± 0.00	0 0.00 ± 0.00	0 0.00 ± 0.00	0 0.00 ± 0.00
TCE-CMP	105 0.00 ± 0.00	25 23.81 ± 4.16	14 56.00 ± 9.93	14 100.00 ± 0.00	12 85.71 ± 9.35	1 8.33 ± 7.98	1 100.00 ± 0.00	0 0.00 ± 0.00	0 0.00 ± 0.00
TCE-CMIO	146 0.00 ± 0.00	37 25.34 ± 3.60	6 16.22 ± 6.06	6 100.00 ± 0.00	6 100.00 ± 0.00	1 16.67 ± 15.21	1 100.00 ± 0.00	1 100.00 ± 0.00	0 0.00 ± 0.00
PHX-CMUP	120 0.00 ± 0.00	80 66.67 ± 4.30	36 45.00 ± 5.56	36 100.00 ± 0.00	33 91.67 ± 4.61	3 9.09 ± 5.00	0 0.00 ± 0.00	0 0.00 ± 0.00	0 0.00 ± 0.00
PHX-CMX	64 0.00 ± 0.00	50 78.12 ± 5.17	24 48.00 ± 7.07	24 100.00 ± 0.00	24 100.00 ± 0.00	0 0.00 ± 0.00	0 0.00 ± 0.00	0 0.00 ± 0.00	0 0.00 ± 0.00
PHX-CMU	22 0.00 ± 0.00	16 72.73 ± 9.50	5 31.25 ± 11.59	5 100.00 ± 0.00	5 100.00 ± 0.00	0 0.00 ± 0.00	0 0.00 ± 0.00	0 0.00 ± 0.00	0 0.00 ± 0.00
PHX-CMP	46 0.00 ± 0.00	38 82.61 ± 5.59	9 23.68 ± 6.90	9 100.00 ± 0.00	7 77.78 ± 13.86	2 28.57 ± 17.07	2 100.00 ± 0.00	1 50.00 ± 35.36	1 100.00 ± 0.00
PHX-CMIO	77 0.00 ± 0.00	55 71.43 ± 5.15	4 7.27 ± 3.50	4 100.00 ± 0.00	4 100.00 ± 0.00	1 25.00 ± 21.65	0 0.00 ± 0.00	0 0.00 ± 0.00	0 0.00 ± 0.00
$e\mu$	1223 0.01 ± 0.00	476 38.92 ± 1.39	232 48.74 ± 2.29	229 98.71 ± 0.74	206 89.96 ± 1.99	15 7.28 ± 1.81	11 73.33 ± 11.42	7 63.64 ± 14.50	6 85.71 ± 13.23
CMUP-CMUP	2668 0.03 ± 0.00	2258 84.63 ± 0.70	2106 93.27 ± 0.53	2086 99.05 ± 0.21	2010 96.36 ± 0.41	3 0.15 ± 0.09	3 100.00 ± 0.00	3 100.00 ± 0.00	3 100.00 ± 0.00
CMUP-CMX	2531 0.03 ± 0.00	2438 96.33 ± 0.37	2273 93.23 ± 0.51	2260 99.43 ± 0.16	2175 96.24 ± 0.40	2 0.09 ± 0.06	2 100.00 ± 0.00	2 100.00 ± 0.00	1 50.00 ± 35.36
CMUP-CMU	931 0.01 ± 0.00	884 94.95 ± 0.72	845 95.59 ± 0.69	841 99.53 ± 0.24	811 96.43 ± 0.64	0 0.00 ± 0.00	0 0.00 ± 0.00	0 0.00 ± 0.00	0 0.00 ± 0.00
CMUP-CMP	1285 0.01 ± 0.00	1152 89.65 ± 0.85	1069 92.80 ± 0.76	1059 99.06 ± 0.29	1017 96.03 ± 0.60	2 0.20 ± 0.14	2 100.00 ± 0.00	2 100.00 ± 0.00	1 50.00 ± 35.36
CMUP-CMIO	515 0.01 ± 0.00	404 78.45 ± 1.81	374 92.57 ± 1.30	371 99.20 ± 0.46	357 96.23 ± 0.99	0 0.00 ± 0.00	0 0.00 ± 0.00	0 0.00 ± 0.00	0 0.00 ± 0.00
CMX-CMX	1116 0.01 ± 0.00	858 76.88 ± 1.26	796 92.77 ± 0.88	794 99.75 ± 0.18	773 97.36 ± 0.57	0 0.00 ± 0.00	0 0.00 ± 0.00	0 0.00 ± 0.00	0 0.00 ± 0.00
CMX-CMU	506 0.01 ± 0.00	486 96.05 ± 0.87	454 93.42 ± 1.12	451 99.34 ± 0.38	440 97.56 ± 0.73	0 0.00 ± 0.00	0 0.00 ± 0.00	0 0.00 ± 0.00	0 0.00 ± 0.00
CMX-CMP	555 0.01 ± 0.00	539 97.12 ± 0.71	499 92.58 ± 1.13	496 99.40 ± 0.35	477 96.17 ± 0.86	0 0.00 ± 0.00	0 0.00 ± 0.00	0 0.00 ± 0.00	0 0.00 ± 0.00
CMX-CMIO	176 0.00 ± 0.00	161 91.48 ± 2.10	144 89.44 ± 2.42	144 100.00 ± 0.00	137 95.14 ± 1.79	0 0.00 ± 0.00	0 0.00 ± 0.00	0 0.00 ± 0.00	0 0.00 ± 0.00
$\mu\mu$	10283 0.11 ± 0.00	9180 89.27 ± 0.31	8560 93.25 ± 0.26	8502 99.32 ± 0.09	8197 96.41 ± 0.20	7 0.09 ± 0.03	7 100.00 ± 0.00	7 100.00 ± 0.00	5 71.43 ± 17.07
total	33113 0.35 ± 0.00	29119 87.94 ± 0.18	26964 92.60 ± 0.15	26797 99.38 ± 0.05	25897 96.64 ± 0.11	37 0.14 ± 0.02	29 78.38 ± 6.77	20 68.97 ± 8.59	17 85.00 ± 7.98

Table 40: data acceptance table, assuming $M_H^{\rm SM} = 180$ GeV

Table 41: HWW dilepton MC acceptance table, assuming $M_H^{\mathrm{SM}} = 160$ GeV

Categ	Lep ID	Lep1 Isol	Lep2 Isol	$M_{\ell\ell} > 16$	jet veto	$\not\!\!E_t$	opp sign	$M_{\ell\ell} < M_u$	$H_T < M_H$
TCE-TCE	24161 2.16 ± 0.01	20561 85.10 ± 0.23	17915 87.13 ± 0.23	17087 95.38 ± 0.16	14876 87.06 ± 0.26	11941 80.27 ± 0.33	11938 99.97 ± 0.01	11640 97.50 ± 0.14	11030 94.76 ± 0.21
TCE-PHX	10197 0.91 ± 0.01	9044 88.69 ± 0.31	8784 97.13 ± 0.18	8645 98.42 ± 0.13	7654 88.54 ± 0.34	5999 78.38 ± 0.47	5538 92.32 ± 0.34	5274 95.23 ± 0.29	5193 98.46 ± 0.17
ee	37964 3.39 ± 0.02	32958 86.81 ± 0.17	29895 90.71 ± 0.16	28747 96.16 ± 0.11	25197 87.65 ± 0.19	19817 78.65 ± 0.26	18989 95.82 ± 0.14	18387 96.83 ± 0.13	17640 95.94 ± 0.15
TCE-CMUP	30764 2.75 ± 0.02	25318 82.30 ± 0.22	23851 94.21 ± 0.15	22637 94.91 ± 0.14	19652 86.81 ± 0.22	15633 79.55 ± 0.29	15632 99.99 ± 0.01	15246 97.53 ± 0.12	14581 95.64 ± 0.17
TCE-CMX	12516 1.12 ± 0.01	10426 83.30 ± 0.33	9819 94.18 ± 0.23	9423 95.97 ± 0.20	8233 87.37 ± 0.34	6527 79.28 ± 0.45	6525 99.97 ± 0.02	6345 97.24 ± 0.20	6125 96.53 ± 0.23
TCE-CMU	5699 0.51 ± 0.01	4731 83.01 ± 0.50	4429 93.62 ± 0.36	4258 96.14 ± 0.29	3710 87.13 ± 0.51	3003 80.94 ± 0.64	3003 100.00 ± 0.00	2919 97.20 ± 0.30	2790 95.58 ± 0.38
TCE-CMP	7897 0.71 ± 0.01	6602 83.60 ± 0.42	6195 93.84 ± 0.30	5940 95.88 ± 0.25	5191 87.39 ± 0.43	4329 83.39 ± 0.52	4329 100.00 ± 0.00	4227 97.64 ± 0.23	4032 95.39 ± 0.32
TCE-CMIO	842 0.08 ± 0.00	694 82.42 ± 1.31	641 92.36 ± 1.01	605 94.38 ± 0.91	539 89.09 ± 1.27	440 81.63 ± 1.67	440 100.00 ± 0.00	426 96.82 ± 0.84	411 96.48 ± 0.89
PHX-CMUP	4940 0.44 ± 0.01	4788 96.92 ± 0.25	4509 94.17 ± 0.34	4506 99.93 ± 0.04	4025 89.33 ± 0.46	3208 79.70 ± 0.63	2980 92.89 ± 0.45	2814 94.43 ± 0.42	2803 99.61 ± 0.12
PHX-CMX	3682 0.33 ± 0.01	3577 97.15 ± 0.27	3311 92.56 ± 0.44	3207 96.86 ± 0.30	2814 87.75 ± 0.58	2189 77.79 ± 0.78	1975 90.22 ± 0.63	1912 96.81 ± 0.40	1870 97.80 ± 0.34
PHX-CMU	1092 0.10 ± 0.00	1068 97.80 ± 0.44	1013 94.85 ± 0.68	1011 99.80 ± 0.14	876 86.65 ± 1.07	718 81.96 ± 1.30	660 91.92 ± 1.02	621 94.09 ± 0.92	614 98.87 ± 0.42
PHX-CMP	1113 0.10 ± 0.00	1086 97.57 ± 0.46	1015 93.46 ± 0.75	1014 99.90 ± 0.10	901 88.86 ± 0.99	734 81.47 ± 1.29	678 92.37 ± 0.98	632 93.22 ± 0.97	632 100.00 ± 0.00
PHX-CMIO	131 0.01 ± 0.00	130 99.24 ± 0.76	118 90.77 ± 2.54	118 100.00 ± 0.00	105 88.98 ± 2.88	93 88.57 ± 3.10	86 92.47 ± 2.74	82 95.35 ± 2.27	82 100.00 ± 0.00
$e\mu$	68676 6.14 ± 0.02	58420 85.07 ± 0.14	54901 93.98 ± 0.10	52719 96.03 ± 0.08	46046 87.34 ± 0.14	36874 80.08 ± 0.19	36308 98.47 ± 0.06	35224 97.01 ± 0.09	33940 96.35 ± 0.10
CMUP-CMUP	10143 0.91 ± 0.01	8473 83.54 ± 0.37	7831 92.42 ± 0.29	7362 94.01 ± 0.27	6332 86.01 ± 0.40	4977 78.60 ± 0.52	4977 100.00 ± 0.00	4866 97.77 ± 0.21	4675 96.07 ± 0.28
CMUP-CMX	7505 0.67 ± 0.01	7068 94.18 ± 0.27	6536 92.47 ± 0.31	6329 96.83 ± 0.22	5533 87.42 ± 0.42	4432 80.10 ± 0.54	4432 100.00 ± 0.00	4317 97.41 ± 0.24	4235 98.10 ± 0.21
CMUP-CMU	3594 0.32 ± 0.01	3205 89.18 ± 0.52	2975 92.82 ± 0.46	2873 96.57 ± 0.33	2469 85.94 ± 0.65	1971 79.83 ± 0.81	1971 100.00 ± 0.00	1927 97.77 ± 0.33	1877 97.41 ± 0.36
CMUP-CMP	5592 0.50 ± 0.01	4676 83.62 ± 0.49	4345 92.92 ± 0.38	4124 94.91 ± 0.33	3581 86.83 ± 0.53	2888 80.65 ± 0.66	2888 100.00 ± 0.00	2832 98.06 ± 0.26	2735 96.57 ± 0.34
CMUP-CMIO	586 0.05 ± 0.00	478 81.57 ± 1.60	442 92.47 ± 1.21	408 92.31 ± 1.27	359 87.99 ± 1.61	291 81.06 ± 2.07	291 100.00 ± 0.00	281 96.56 ± 1.07	270 96.09 ± 1.16
CMX-CMX	1795 0.16 ± 0.00	1341 74.71 ± 1.03	1215 90.60 ± 0.80	1141 93.91 ± 0.69	998 87.47 ± 0.98	732 73.35 ± 1.40	732 100.00 ± 0.00	713 97.40 ± 0.59	689 96.63 ± 0.68
CMX-CMU	1103 0.10 ± 0.00	945 85.68 ± 1.05	868 91.85 ± 0.89	816 94.01 ± 0.81	730 89.46 ± 1.07	591 80.96 ± 1.45	591 100.00 ± 0.00	571 96.62 ± 0.74	552 96.67 ± 0.75
CMX-CMP	1583 0.14 ± 0.00	1514 95.64 ± 0.51	1416 93.53 ± 0.63	1392 98.31 ± 0.34	1186 85.20 ± 0.95	967 81.53 ± 1.13	967 100.00 ± 0.00	947 97.93 ± 0.46	929 98.10 ± 0.44
CMX-CMIO	158 0.01 ± 0.00	146 92.41 ± 2.11	135 92.47 ± 2.18	129 95.56 ± 1.77	116 89.92 ± 2.65	93 80.17 ± 3.70	93 100.00 ± 0.00	89 95.70 ± 2.10	89 100.00 ± 0.00
$\mu\mu$	32059 2.87 ± 0.02	27846 86.86 ± 0.19	25763 92.52 ± 0.16	24574 95.38 ± 0.13	21304 86.69 ± 0.22	16942 79.52 ± 0.28	16942 100.00 ± 0.00	16543 97.64 ± 0.12	16051 97.03 ± 0.13
total	138699 12.40 ± 0.03	119224 85.96 ± 0.09	110559 92.73 ± 0.08	106040 95.91 ± 0.06	92547 87.28 ± 0.10	73633 79.56 ± 0.13	72239 98.11 ± 0.05	70154 97.11 ± 0.06	67631 96.40 ± 0.07

Table 42: WW MC acceptance table, assuming $M_H^{\mathrm{SM}} = 160$ GeV

Categ	Lep ID	Lep1 Isol	Lep2 Isol	$M_{\ell\ell} > 16$	jet veto	$\not\!\!E_t$	opp sign	$M_{\ell\ell} < M_u$	$H_T < M_H$
TCE-TCE	826 0.20 ± 0.01	756 91.53 ± 0.97	652 86.24 ± 1.25	638 97.85 ± 0.57	596 93.42 ± 0.98	296 49.66 ± 2.05	296 100.00 ± 0.00	180 60.81 ± 2.84	161 89.44 ± 2.29
TCE-PHX	635 0.15 ± 0.01	570 89.76 ± 1.20	556 97.54 ± 0.65	553 99.46 ± 0.31	516 93.31 ± 1.06	268 51.94 ± 2.20	237 88.43 ± 1.95	119 50.21 ± 3.25	111 93.28 ± 2.30
ee	1597 0.38 ± 0.01	1460 91.42 ± 0.70	1339 91.71 ± 0.72	1318 98.43 ± 0.34	1231 93.40 ± 0.68	621 50.45 ± 1.43	578 93.08 ± 1.02	323 55.88 ± 2.07	293 90.71 ± 1.62
TCE-CMUP	883 0.21 ± 0.01	767 86.86 ± 1.14	733 95.57 ± 0.74	713 97.27 ± 0.60	677 94.95 ± 0.82	324 47.86 ± 1.92	324 100.00 ± 0.00	207 63.89 ± 2.67	184 88.89 ± 2.18
TCE-CMX	460 0.11 ± 0.01	409 88.91 ± 1.46	382 93.40 ± 1.23	374 97.91 ± 0.73	345 92.25 ± 1.38	171 49.57 ± 2.69	171 100.00 ± 0.00	113 66.08 ± 3.62	104 92.04 ± 2.55
TCE-CMU	170 0.04 ± 0.00	157 92.35 ± 2.04	150 95.54 ± 1.65	145 96.67 ± 1.47	136 93.79 ± 2.00	70 51.47 ± 4.29	70 100.00 ± 0.00	44 62.86 ± 5.78	41 93.18 ± 3.80
TCE-CMP	228 0.05 ± 0.00	199 87.28 ± 2.21	183 91.96 ± 1.93	176 96.17 ± 1.42	167 94.89 ± 1.66	80 47.90 ± 3.87	80 100.00 ± 0.00	47 58.75 ± 5.50	39 82.98 ± 5.48
TCE-CMIO	14 0.00 ± 0.00	11 78.57 ± 10.97	9 81.82 ± 11.63	9 100.00 ± 0.00	7 77.78 ± 13.86	2 28.57 ± 17.07	2 100.00 ± 0.00	2 100.00 ± 0.00	2 100.00 ± 0.00
PHX-CMUP	332 0.08 ± 0.00	326 98.19 ± 0.73	299 91.72 ± 1.53	299 100.00 ± 0.00	282 94.31 ± 1.34	148 52.48 ± 2.97	127 85.81 ± 2.87	65 51.18 ± 4.44	62 95.38 ± 2.60
PHX-CMX	178 0.04 ± 0.00	166 93.26 ± 1.88	149 89.76 ± 2.35	148 99.33 ± 0.67	141 95.27 ± 1.74	56 39.72 ± 4.12	50 89.29 ± 4.13	25 50.00 ± 7.07	25 100.00 ± 0.00
PHX-CMU	67 0.02 ± 0.00	66 98.51 ± 1.48	62 93.94 ± 2.94	62 100.00 ± 0.00	59 95.16 ± 2.73	24 40.68 ± 6.40	19 79.17 ± 8.29	11 57.89 ± 11.33	11 100.00 ± 0.00
PHX-CMP	87 0.02 ± 0.00	82 94.25 ± 2.50	78 95.12 ± 2.38	78 100.00 ± 0.00	77 98.72 ± 1.27	40 51.95 ± 5.69	38 95.00 ± 3.45	11 28.95 ± 7.36	9 81.82 ± 11.63
PHX-CMIO	14 0.00 ± 0.00	13 92.86 ± 6.88	6 46.15 ± 13.83	6 100.00 ± 0.00	6 100.00 ± 0.00	4 66.67 ± 19.25	3 75.00 ± 21.65	1 33.33 ± 27.22	1 100.00 ± 0.00
$e\mu$	2433 0.58 ± 0.01	2196 90.26 ± 0.60	2051 93.40 ± 0.53	2010 98.00 ± 0.31	1897 94.38 ± 0.51	919 48.44 ± 1.15	884 96.19 ± 0.63	526 59.50 ± 1.65	478 90.87 ± 1.26
CMUP-CMUP	273 0.07 ± 0.00	254 93.04 ± 1.54	241 94.88 ± 1.38	232 96.27 ± 1.22	220 94.83 ± 1.45	108 49.09 ± 3.37	108 100.00 ± 0.00	70 64.81 ± 4.60	64 91.43 ± 3.35
CMUP-CMX	290 0.07 ± 0.00	283 97.59 ± 0.90	263 92.93 ± 1.52	258 98.10 ± 0.84	240 93.02 ± 1.59	124 51.67 ± 3.23	124 100.00 ± 0.00	76 61.29 ± 4.37	72 94.74 ± 2.56
CMUP-CMU	87 0.02 ± 0.00	85 97.70 ± 1.61	79 92.94 ± 2.78	77 97.47 ± 1.77	76 98.70 ± 1.29	40 52.63 ± 5.73	40 100.00 ± 0.00	27 67.50 ± 7.41	22 81.48 ± 7.48
CMUP-CMP	161 0.04 ± 0.00	155 96.27 ± 1.49	148 95.48 ± 1.67	144 97.30 ± 1.33	135 93.75 ± 2.02	67 49.63 ± 4.30	67 100.00 ± 0.00	50 74.63 ± 5.32	45 90.00 ± 4.24
CMUP-CMIO	19 0.00 ± 0.00	16 84.21 ± 8.37	13 81.25 ± 9.76	13 100.00 ± 0.00	13 100.00 ± 0.00	6 46.15 ± 13.83	6 100.00 ± 0.00	4 66.67 ± 19.25	3 75.00 ± 21.65
CMX-CMX	66 0.02 ± 0.00	60 90.91 ± 3.54	54 90.00 ± 3.87	54 100.00 ± 0.00	54 100.00 ± 0.00	23 42.59 ± 6.73	23 100.00 ± 0.00	10 43.48 ± 10.34	9 90.00 ± 9.49
CMX-CMU	29 0.01 ± 0.00	27 93.10 ± 4.71	25 92.59 ± 5.04	25 100.00 ± 0.00	25 100.00 ± 0.00	9 36.00 ± 9.60	9 100.00 ± 0.00	6 66.67 ± 15.71	6 100.00 ± 0.00
CMX-CMP	59 0.01 ± 0.00	57 96.61 ± 2.36	55 96.49 ± 2.44	55 100.00 ± 0.00	52 94.55 ± 3.06	18 34.62 ± 6.60	18 100.00 ± 0.00	9 50.00 ± 11.79	8 88.89 ± 10.48
CMX-CMIO	7 0.00 ± 0.00	7 100.00 ± 0.00	6 85.71 ± 13.23	5 83.33 ± 15.21	5 100.00 ± 0.00	0 0.00 ± 0.00	0 0.00 ± 0.00	0 0.00 ± 0.00	0 0.00 ± 0.00
$\mu\mu$	991 0.24 ± 0.01	944 95.26 ± 0.68	884 93.64 ± 0.79	863 97.62 ± 0.51	820 95.02 ± 0.74	395 48.17 ± 1.74	395 100.00 ± 0.00	252 63.80 ± 2.42	229 90.87 ± 1.81
total	5021 1.20 ± 0.02	4600 91.62 ± 0.39	4274 92.91 ± 0.38	4191 98.06 ± 0.21	3948 94.20 ± 0.36	1935 49.01 ± 0.80	1857 95.97 ± 0.45	1101 59.29 ± 1.14	1000 90.83 ± 0.87

Table 43: WZ MC acceptance table, assuming $M_H^{\mathrm{SM}} = 160$ GeV

Categ	Lep ID	Lep1 Isol	Lep2 Isol	$M_{\ell\ell} > 16$	jet veto	$\not\!\!E_t$	opp sign	$M_{\ell\ell} < M_u$	$H_T < M_H$
TCE-TCE	1519 0.37 ± 0.01	1410 92.82 ± 0.66	1188 84.26 ± 0.97	1186 99.83 ± 0.12	547 46.12 ± 1.45	174 31.81 ± 1.99	152 87.36 ± 2.52	19 12.50 ± 2.68	18 94.74 ± 5.12
TCE-PHX	1609 0.39 ± 0.01	1444 89.75 ± 0.76	1404 97.23 ± 0.43	1403 99.93 ± 0.07	618 44.05 ± 1.33	173 27.99 ± 1.81	140 80.92 ± 2.99	20 14.29 ± 2.96	17 85.00 ± 7.98
ee	3518 0.86 ± 0.01	3238 92.04 ± 0.46	2967 91.63 ± 0.49	2962 99.83 ± 0.08	1351 45.61 ± 0.92	380 28.13 ± 1.22	318 83.68 ± 1.90	40 12.58 ± 1.86	36 90.00 ± 4.74
TCE-CMUP	296 0.07 ± 0.00	255 86.15 ± 2.01	234 91.76 ± 1.72	223 95.30 ± 1.38	170 76.23 ± 2.85	98 57.65 ± 3.79	46 46.94 ± 5.04	27 58.70 ± 7.26	24 88.89 ± 6.05
TCE-CMX	160 0.04 ± 0.00	137 85.62 ± 2.77	124 90.51 ± 2.50	121 97.58 ± 1.38	87 71.90 ± 4.09	53 60.92 ± 5.23	28 52.83 ± 6.86	17 60.71 ± 9.23	15 88.24 ± 7.81
TCE-CMU	52 0.01 ± 0.00	46 88.46 ± 4.43	44 95.65 ± 3.01	42 95.45 ± 3.14	26 61.90 ± 7.49	18 69.23 ± 9.05	10 55.56 ± 11.71	5 50.00 ± 15.81	5 100.00 ± 0.00
TCE-CMP	66 0.02 ± 0.00	59 89.39 ± 3.79	51 86.44 ± 4.46	50 98.04 ± 1.94	34 68.00 ± 6.60	14 41.18 ± 8.44	8 57.14 ± 13.23	3 37.50 ± 17.12	2 66.67 ± 27.22
TCE-CMIO	10 0.00 ± 0.00	10 100.00 ± 0.00	8 80.00 ± 12.65	7 87.50 ± 11.69	4 57.14 ± 18.70	3 75.00 ± 21.65	0 0.00 ± 0.00	0 0.00 ± 0.00	0 0.00 ± 0.00
PHX-CMUP	139 0.03 ± 0.00	135 97.12 ± 1.42	123 91.11 ± 2.45	123 100.00 ± 0.00	96 78.05 ± 3.73	55 57.29 ± 5.05	22 40.00 ± 6.61	8 36.36 ± 10.26	8 100.00 ± 0.00
PHX-CMX	77 0.02 ± 0.00	77 100.00 ± 0.00	69 89.61 ± 3.48	69 100.00 ± 0.00	49 71.01 ± 5.46	21 42.86 ± 7.07	13 61.90 ± 10.60	3 23.08 ± 11.69	3 100.00 ± 0.00
PHX-CMU	28 0.01 ± 0.00	28 100.00 ± 0.00	21 75.00 ± 8.18	21 100.00 ± 0.00	16 76.19 ± 9.29	9 56.25 ± 12.40	3 33.33 ± 15.71	1 33.33 ± 27.22	1 100.00 ± 0.00
PHX-CMP	36 0.01 ± 0.00	35 97.22 ± 2.74	31 88.57 ± 5.38	31 100.00 ± 0.00	21 67.74 ± 8.40	12 57.14 ± 10.80	6 50.00 ± 14.43	2 33.33 ± 19.25	2 100.00 ± 0.00
PHX-CMIO	2 0.00 ± 0.00	2 100.00 ± 0.00	2 100.00 ± 0.00	2 100.00 ± 0.00	1 50.00 ± 35.36	0 0.00 ± 0.00	0 0.00 ± 0.00	0 0.00 ± 0.00	0 0.00 ± 0.00
$e\mu$	866 0.21 ± 0.01	784 90.53 ± 0.99	707 90.18 ± 1.06	689 97.45 ± 0.59	504 73.15 ± 1.69	283 56.15 ± 2.21	136 48.06 ± 2.97	66 48.53 ± 4.29	60 90.91 ± 3.54
CMUP-CMUP	518 0.13 ± 0.01	494 95.37 ± 0.92	444 89.88 ± 1.36	443 99.77 ± 0.22	239 53.95 ± 2.37	85 35.56 ± 3.10	71 83.53 ± 4.02	14 19.72 ± 4.72	11 78.57 ± 10.97
CMUP-CMX	511 0.13 ± 0.01	497 97.26 ± 0.72	436 87.73 ± 1.47	435 99.77 ± 0.23	212 48.74 ± 2.40	70 33.02 ± 3.23	55 78.57 ± 4.90	17 30.91 ± 6.23	11 64.71 ± 11.59
CMUP-CMU	223 0.05 ± 0.00	217 97.31 ± 1.08	193 88.94 ± 2.13	192 99.48 ± 0.52	111 57.81 ± 3.56	41 36.94 ± 4.58	36 87.80 ± 5.11	5 13.89 ± 5.76	4 80.00 ± 17.89
CMUP-CMP	306 0.08 ± 0.00	298 97.39 ± 0.91	261 87.58 ± 1.91	258 98.85 ± 0.66	135 52.33 ± 3.11	40 29.63 ± 3.93	34 85.00 ± 5.65	5 14.71 ± 6.07	5 100.00 ± 0.00
CMUP-CMIO	24 0.01 ± 0.00	23 95.83 ± 4.08	19 82.61 ± 7.90	19 100.00 ± 0.00	10 52.63 ± 11.45	1 10.00 ± 9.49	0 0.00 ± 0.00	0 0.00 ± 0.00	0 0.00 ± 0.00
CMX-CMX	125 0.03 ± 0.00	125 100.00 ± 0.00	110 88.00 ± 2.91	110 100.00 ± 0.00	52 47.27 ± 4.76	24 46.15 ± 6.91	19 79.17 ± 8.29	5 26.32 ± 10.10	5 100.00 ± 0.00
CMX-CMU	85 0.02 ± 0.00	84 98.82 ± 1.17	76 90.48 ± 3.20	76 100.00 ± 0.00	44 57.89 ± 5.66	13 29.55 ± 6.88	11 84.62 ± 10.01	4 36.36 ± 14.50	3 75.00 ± 21.65
CMX-CMP	115 0.03 ± 0.00	113 98.26 ± 1.22	104 92.04 ± 2.55	102 98.08 ± 1.35	50 49.02 ± 4.95	17 34.00 ± 6.70	13 76.47 ± 10.29	4 30.77 ± 12.80	4 100.00 ± 0.00
CMX-CMIO	16 0.00 ± 0.00	15 93.75 ± 6.05	13 86.67 ± 8.78	13 100.00 ± 0.00	4 30.77 ± 12.80	3 75.00 ± 21.65	3 100.00 ± 0.00	0 0.00 ± 0.00	0 0.00 ± 0.00
$\mu\mu$	1923 0.47 ± 0.01	1866 97.04 ± 0.39	1656 88.75 ± 0.73	1648 99.52 ± 0.17	857 52.00 ± 1.23	294 34.31 ± 1.62	242 82.31 ± 2.23	54 22.31 ± 2.68	43 79.63 ± 5.48
total	6307 1.55 ± 0.02	5888 93.36 ± 0.31	5330 90.52 ± 0.38	5299 99.42 ± 0.10	2712 51.18 ± 0.69	957 35.29 ± 0.92	696 72.73 ± 1.44	160 22.99 ± 1.59	139 86.88 ± 2.67

Categ	Lep ID	Lep1 Isol	Lep2 Isol	$M_{\ell\ell} > 16$	jet veto	$\not\!\!E_t$	opp sign	$M_{\ell\ell} < M_u$	$H_T < M_H$
TCE-TCE	3463 0.30 ± 0.01	2988 86.28 ± 0.58	2075 69.44 ± 0.84	2053 98.94 ± 0.22	195 9.50 ± 0.65	137 70.26 ± 3.27	137 100.00 ± 0.00	50 36.50 ± 4.11	35 70.00 ± 6.48
TCE-PHX	1529 0.13 ± 0.00	1199 78.42 ± 1.05	1134 94.58 ± 0.65	1131 99.74 ± 0.15	94 8.31 ± 0.82	63 67.02 ± 4.85	58 92.06 ± 3.41	21 36.21 ± 6.31	15 71.43 ± 9.86
ee	5173 0.45 ± 0.01	4361 84.30 ± 0.51	3377 77.44 ± 0.63	3349 99.17 ± 0.16	304 9.08 ± 0.50	211 69.41 ± 2.64	205 97.16 ± 1.14	72 35.12 ± 3.33	51 70.83 ± 5.36
TCE-CMUP	4377 0.38 ± 0.01	3335 76.19 ± 0.64	2607 78.17 ± 0.72	2575 98.77 ± 0.22	231 8.97 ± 0.56	159 68.83 ± 3.05	159 100.00 ± 0.00	62 38.99 ± 3.87	41 66.13 ± 6.01
TCE-CMX	1864 0.16 ± 0.00	1440 77.25 ± 0.97	1081 75.07 ± 1.14	1066 98.61 ± 0.36	101 9.47 ± 0.90	61 60.40 ± 4.87	61 100.00 ± 0.00	23 37.70 ± 6.21	15 65.22 ± 9.93
TCE-CMU	789 0.07 ± 0.00	635 80.48 ± 1.41	502 79.06 ± 1.61	497 99.00 ± 0.44	47 9.46 ± 1.31	32 68.09 ± 6.80	32 100.00 ± 0.00	11 34.38 ± 8.40	4 36.36 ± 14.50
TCE-CMP	1096 0.10 ± 0.00	890 81.20 ± 1.18	672 75.51 ± 1.44	669 99.55 ± 0.26	55 8.22 ± 1.06	41 74.55 ± 5.87	41 100.00 ± 0.00	12 29.27 ± 7.11	10 83.33 ± 10.76
TCE-CMIO	135 0.01 ± 0.00	105 77.78 ± 3.58	63 60.00 ± 4.78	62 98.41 ± 1.57	8 12.90 ± 4.26	4 50.00 ± 17.68	4 100.00 ± 0.00	2 50.00 ± 25.00	1 50.00 ± 35.36
PHX-CMUP	1039 0.09 ± 0.00	983 94.61 ± 0.70	735 74.77 ± 1.39	735 100.00 ± 0.00	49 6.67 ± 0.92	30 61.22 ± 6.96	25 83.33 ± 6.80	6 24.00 ± 8.54	6 100.00 ± 0.00
PHX-CMX	433 0.04 ± 0.00	414 95.61 ± 0.98	319 77.05 ± 2.07	319 100.00 ± 0.00	31 9.72 ± 1.66	26 83.87 ± 6.61	24 92.31 ± 5.23	7 29.17 ± 9.28	3 42.86 ± 18.70
PHX-CMU	197 0.02 ± 0.00	186 94.42 ± 1.64	142 76.34 ± 3.12	142 100.00 ± 0.00	14 9.86 ± 2.50	10 71.43 ± 12.07	9 90.00 ± 9.49	2 22.22 ± 13.86	2 100.00 ± 0.00
PHX-CMP	281 0.02 ± 0.00	274 97.51 ± 0.93	203 74.09 ± 2.65	203 100.00 ± 0.00	19 9.36 ± 2.04	10 52.63 ± 11.45	9 90.00 ± 9.49	1 11.11 ± 10.48	1 100.00 ± 0.00
PHX-CMIO	37 0.00 ± 0.00	34 91.89 ± 4.49	20 58.82 ± 8.44	20 100.00 ± 0.00	1 5.00 ± 4.87	1 100.00 ± 0.00	0 0.00 ± 0.00	0 0.00 ± 0.00	0 0.00 ± 0.00
$e\mu$	10248 0.90 ± 0.01	8296 80.95 ± 0.39	6344 76.47 ± 0.47	6288 99.12 ± 0.12	556 8.84 ± 0.36	374 67.27 ± 1.99	364 97.33 ± 0.83	126 34.62 ± 2.49	83 65.87 ± 4.22
CMUP-CMUP	1419 0.12 ± 0.00	1249 88.02 ± 0.86	879 70.38 ± 1.29	863 98.18 ± 0.45	101 11.70 ± 1.09	65 64.36 ± 4.77	65 100.00 ± 0.00	27 41.54 ± 6.11	18 66.67 ± 9.07
CMUP-CMX	1188 0.10 ± 0.00	1080 90.91 ± 0.83	721 66.76 ± 1.43	713 98.89 ± 0.39	67 9.40 ± 1.09	49 73.13 ± 5.42	49 100.00 ± 0.00	19 38.78 ± 6.96	13 68.42 ± 10.66
CMUP-CMU	523 0.05 ± 0.00	475 90.82 ± 1.26	350 73.68 ± 2.02	343 98.00 ± 0.75	37 10.79 ± 1.68	32 86.49 ± 5.62	32 100.00 ± 0.00	11 34.38 ± 8.40	6 54.55 ± 15.01
CMUP-CMP	721 0.06 ± 0.00	608 84.33 ± 1.35	420 69.08 ± 1.87	409 97.38 ± 0.78	29 7.09 ± 1.27	20 68.97 ± 8.59	20 100.00 ± 0.00	4 20.00 ± 8.94	2 50.00 ± 25.00
CMUP-CMIO	93 0.01 ± 0.00	82 88.17 ± 3.35	56 68.29 ± 5.14	56 100.00 ± 0.00	7 12.50 ± 4.42	5 71.43 ± 17.07	5 100.00 ± 0.00	3 60.00 ± 21.91	2 66.67 ± 27.22
CMX-CMX	239 0.02 ± 0.00	197 82.43 ± 2.46	124 62.94 ± 3.44	121 97.58 ± 1.38	8 6.61 ± 2.26	3 37.50 ± 17.12	3 100.00 ± 0.00	1 33.33 ± 27.22	1 100.00 ± 0.00
CMX-CMU	174 0.02 ± 0.00	154 88.51 ± 2.42	108 70.13 ± 3.69	107 99.07 ± 0.92	14 13.08 ± 3.26	9 64.29 ± 12.81	9 100.00 ± 0.00	4 44.44 ± 16.56	3 75.00 ± 21.65
CMX-CMP	239 0.02 ± 0.00	224 93.72 ± 1.57	171 76.34 ± 2.84	170 99.42 ± 0.58	8 4.71 ± 1.62	3 37.50 ± 17.12	3 100.00 ± 0.00	1 33.33 ± 27.22	1 100.00 ± 0.00
CMX-CMIO	21 0.00 ± 0.00	20 95.24 ± 4.65	6 30.00 ± 10.25	6 100.00 ± 0.00	1 16.67 ± 15.21	0 0.00 ± 0.00	0 0.00 ± 0.00	0 0.00 ± 0.00	0 0.00 ± 0.00
$\mu\mu$	4617 0.40 ± 0.01	4089 88.56 ± 0.47	2835 69.33 ± 0.72	2788 98.34 ± 0.24	272 9.76 ± 0.56	186 68.38 ± 2.82	186 100.00 ± 0.00	70 37.63 ± 3.55	46 65.71 ± 5.67
total	20038 1.75 ± 0.01	16746 83.57 ± 0.26	12556 74.98 ± 0.33	12425 98.96 ± 0.09	1132 9.11 ± 0.26	771 68.11 ± 1.39	755 97.92 ± 0.51	268 35.50 ± 1.74	180 67.16 ± 2.87

Table 44: $t\bar{t}$ MC acceptance table, assuming $M_H^{\rm SM} = 160$ GeV

Categ	Lep ID	Lep1 Isol	Lep2 Isol	$M_{\ell\ell} > 16$	jet veto	$\not\!\!E_t$	opp sign	$M_{\ell\ell} < M_u$	$H_T < M_H$
TCE-TCE	108087 3.42 ± 0.01	103225 95.50 ± 0.06	92356 89.47 ± 0.10	92099 99.72 ± 0.02	89166 96.82 ± 0.06	35 0.04 ± 0.01	35 100.00 ± 0.00	19 54.29 ± 8.42	19 100.00 ± 0.00
TCE-PHX	143446 4.53 ± 0.01	131365 91.58 ± 0.07	129564 98.63 ± 0.03	129512 99.96 ± 0.01	125820 97.15 ± 0.05	17 0.01 ± 0.00	16 94.12 ± 5.71	4 25.00 ± 10.83	4 100.00 ± 0.00
ee	272262 8.60 ± 0.02	255175 93.72 ± 0.05	242112 94.88 ± 0.04	241775 99.86 ± 0.01	234599 97.03 ± 0.03	54 0.02 ± 0.00	53 98.15 ± 1.83	25 47.17 ± 6.86	25 100.00 ± 0.00
TCE-CMUP	1115 0.04 ± 0.00	965 86.55 ± 1.02	882 91.40 ± 0.90	877 99.43 ± 0.25	851 97.04 ± 0.57	12 1.41 ± 0.40	9 75.00 ± 12.50	6 66.67 ± 15.71	6 100.00 ± 0.00
TCE-CMX	550 0.02 ± 0.00	478 86.91 ± 1.44	449 93.93 ± 1.09	449 100.00 ± 0.00	434 96.66 ± 0.85	8 1.84 ± 0.65	8 100.00 ± 0.00	6 75.00 ± 15.31	5 83.33 ± 15.21
TCE-CMU	131 0.00 ± 0.00	121 92.37 ± 2.32	107 88.43 ± 2.91	107 100.00 ± 0.00	103 96.26 ± 1.83	1 0.97 ± 0.97	1 100.00 ± 0.00	0 0.00 ± 0.00	0 0.00 ± 0.00
TCE-CMP	204 0.01 ± 0.00	187 91.67 ± 1.94	171 91.44 ± 2.05	171 100.00 ± 0.00	165 96.49 ± 1.41	3 1.82 ± 1.04	3 100.00 ± 0.00	0 0.00 ± 0.00	0 0.00 ± 0.00
TCE-CMIO	33 0.00 ± 0.00	30 90.91 ± 5.00	24 80.00 ± 7.30	24 100.00 ± 0.00	24 100.00 ± 0.00	0 0.00 ± 0.00	0 0.00 ± 0.00	0 0.00 ± 0.00	0 0.00 ± 0.00
PHX-CMUP	394 0.01 ± 0.00	379 96.19 ± 0.96	353 93.14 ± 1.30	353 100.00 ± 0.00	327 92.63 ± 1.39	2 0.61 ± 0.43	2 100.00 ± 0.00	2 100.00 ± 0.00	2 100.00 ± 0.00
PHX-CMX	281 0.01 ± 0.00	277 98.58 ± 0.71	258 93.14 ± 1.52	255 98.84 ± 0.67	241 94.51 ± 1.43	3 1.24 ± 0.71	1 33.33 ± 27.22	1 100.00 ± 0.00	1 100.00 ± 0.00
PHX-CMU	69 0.00 ± 0.00	67 97.10 ± 2.02	59 88.06 ± 3.96	59 100.00 ± 0.00	56 94.92 ± 2.86	2 3.57 ± 2.48	1 50.00 ± 35.36	0 0.00 ± 0.00	0 0.00 ± 0.00
PHX-CMP	99 0.00 ± 0.00	96 96.97 ± 1.72	91 94.79 ± 2.27	91 100.00 ± 0.00	89 97.80 ± 1.54	1 1.12 ± 1.12	1 100.00 ± 0.00	0 0.00 ± 0.00	0 0.00 ± 0.00
PHX-CMIO	7 0.00 ± 0.00	7 100.00 ± 0.00	6 85.71 ± 13.23	6 100.00 ± 0.00	6 100.00 ± 0.00	0 0.00 ± 0.00	0 0.00 ± 0.00	0 0.00 ± 0.00	0 0.00 ± 0.00
$e\mu$	2883 0.09 ± 0.00	2607 90.43 ± 0.55	2400 92.06 ± 0.53	2392 99.67 ± 0.12	2296 95.99 ± 0.40	32 1.39 ± 0.24	26 81.25 ± 6.90	15 57.69 ± 9.69	14 93.33 ± 6.44
CMUP-CMUP	34906 1.10 ± 0.01	34422 98.61 ± 0.06	32566 94.61 ± 0.12	32460 99.67 ± 0.03	31392 96.71 ± 0.10	6 0.02 ± 0.01	6 100.00 ± 0.00	1 16.67 ± 15.21	1 100.00 ± 0.00
CMUP-CMX	36203 1.14 ± 0.01	35770 98.80 ± 0.06	33745 94.34 ± 0.12	33663 99.76 ± 0.03	32543 96.67 ± 0.10	9 0.03 ± 0.01	9 100.00 ± 0.00	2 22.22 ± 13.86	2 100.00 ± 0.00
CMUP-CMU	14515 0.46 ± 0.00	14341 98.80 ± 0.09	13586 94.74 ± 0.19	13558 99.79 ± 0.04	13064 96.36 ± 0.16	3 0.02 ± 0.01	3 100.00 ± 0.00	1 33.33 ± 27.22	1 100.00 ± 0.00
CMUP-CMP	19027 0.60 ± 0.00	18793 98.77 ± 0.08	17806 94.75 ± 0.16	17766 99.78 ± 0.04	17206 96.85 ± 0.13	3 0.02 ± 0.01	3 100.00 ± 0.00	1 33.33 ± 27.22	1 100.00 ± 0.00
CMUP-CMIO	1752 0.06 ± 0.00	1729 98.69 ± 0.27	1630 94.27 ± 0.56	1628 99.88 ± 0.09	1556 95.58 ± 0.51	0 0.00 ± 0.00	0 0.00 ± 0.00	0 0.00 ± 0.00	0 0.00 ± 0.00
CMX-CMX	11158 0.35 ± 0.00	10958 98.21 ± 0.13	10339 94.35 ± 0.22	10314 99.76 ± 0.05	10035 97.29 ± 0.16	1 0.01 ± 0.01	1 100.00 ± 0.00	0 0.00 ± 0.00	0 0.00 ± 0.00
CMX-CMU	7062 0.22 ± 0.00	6968 98.67 ± 0.14	6609 94.85 ± 0.26	6599 99.85 ± 0.05	6427 97.39 ± 0.20	1 0.02 ± 0.02	1 100.00 ± 0.00	1 100.00 ± 0.00	1 100.00 ± 0.00
CMX-CMP	8045 0.25 ± 0.00	7962 98.97 ± 0.11	7529 94.56 ± 0.25	7520 99.88 ± 0.04	7303 97.11 ± 0.19	1 0.01 ± 0.01	1 100.00 ± 0.00	0 0.00 ± 0.00	0 0.00 ± 0.00
CMX-CMIO	737 0.02 ± 0.00	726 98.51 ± 0.45	689 94.90 ± 0.82	687 99.71 ± 0.20	660 96.07 ± 0.74	0 0.00 ± 0.00	0 0.00 ± 0.00	0 0.00 ± 0.00	0 0.00 ± 0.00
$\mu\mu$	133405 4.22 ± 0.01	131669 98.70 ± 0.03	124499 94.55 ± 0.06	124195 99.76 ± 0.01	120186 96.77 ± 0.05	24 0.02 ± 0.00	24 100.00 ± 0.00	6 25.00 ± 8.84	6 100.00 ± 0.00
total	408550 12.91 ± 0.02	389451 95.33 ± 0.03	369011 94.75 ± 0.04	368362 99.82 ± 0.01	357081 96.94 ± 0.03	110 0.03 ± 0.00	103 93.64 ± 2.33	46 44.66 ± 4.90	45 97.83 ± 2.15

Table 45: Drell-Yan MC acceptance table, assuming $M_H^{\rm SM} = 160$ GeV

Categ	Lep ID	Lep1 Isol	Lep2 Isol	$M_{\ell\ell} > 16$	jet veto	$\not\!\!E_t$	opp sign	$M_{\ell\ell} < M_u$	$H_T < M_H$
TCE-TCE	1852 0.47 ± 0.01	1660 89.63 ± 0.71	1386 83.49 ± 0.91	1357 97.91 ± 0.38	714 52.62 ± 1.36	165 23.11 ± 1.58	165 100.00 ± 0.00	9 5.45 ± 1.77	6 66.67 ± 15.71
TCE-PHX	1542 0.39 ± 0.01	1351 87.61 ± 0.84	1309 96.89 ± 0.47	1308 99.92 ± 0.08	728 55.66 ± 1.37	131 17.99 ± 1.42	118 90.08 ± 2.61	6 5.08 ± 2.02	5 83.33 ± 15.21
ee	3778 0.95 ± 0.02	3382 89.52 ± 0.50	3051 90.21 ± 0.51	3014 98.79 ± 0.20	1662 55.14 ± 0.91	315 18.95 ± 0.96	297 94.29 ± 1.31	17 5.72 ± 1.35	13 76.47 ± 10.29
TCE-CMUP	116 0.03 ± 0.00	96 82.76 ± 3.51	85 88.54 ± 3.25	85 100.00 ± 0.00	45 52.94 ± 5.41	7 15.56 ± 5.40	5 71.43 ± 17.07	3 60.00 ± 21.91	3 100.00 ± 0.00
TCE-CMX	60 0.02 ± 0.00	47 78.33 ± 5.32	34 72.34 ± 6.52	34 100.00 ± 0.00	22 64.71 ± 8.20	5 22.73 ± 8.93	1 20.00 ± 17.89	1 100.00 ± 0.00	1 100.00 ± 0.00
TCE-CMU	22 0.01 ± 0.00	15 68.18 ± 9.93	14 93.33 ± 6.44	14 100.00 ± 0.00	8 57.14 ± 13.23	2 25.00 ± 15.31	0 0.00 ± 0.00	0 0.00 ± 0.00	0 0.00 ± 0.00
TCE-CMP	19 0.00 ± 0.00	12 63.16 ± 11.07	11 91.67 ± 7.98	10 90.91 ± 8.67	7 70.00 ± 14.49	2 28.57 ± 17.07	2 100.00 ± 0.00	2 100.00 ± 0.00	2 100.00 ± 0.00
TCE-CMIO	3 0.00 ± 0.00	2 66.67 ± 27.22	1 50.00 ± 35.36	1 100.00 ± 0.00	1 100.00 ± 0.00	0 0.00 ± 0.00	0 0.00 ± 0.00	0 0.00 ± 0.00	0 0.00 ± 0.00
PHX-CMUP	40 0.01 ± 0.00	37 92.50 ± 4.16	31 83.78 ± 6.06	31 100.00 ± 0.00	15 48.39 ± 8.98	5 33.33 ± 12.17	1 20.00 ± 17.89	1 100.00 ± 0.00	1 100.00 ± 0.00
PHX-CMX	22 0.01 ± 0.00	22 100.00 ± 0.00	19 86.36 ± 7.32	19 100.00 ± 0.00	10 52.63 ± 11.45	6 60.00 ± 15.49	4 66.67 ± 19.25	2 50.00 ± 25.00	2 100.00 ± 0.00
PHX-CMU	6 0.00 ± 0.00	6 100.00 ± 0.00	5 83.33 ± 15.21	5 100.00 ± 0.00	5 100.00 ± 0.00	2 40.00 ± 21.91	0 0.00 ± 0.00	0 0.00 ± 0.00	0 0.00 ± 0.00
PHX-CMP	11 0.00 ± 0.00	10 90.91 ± 8.67	7 70.00 ± 14.49	7 100.00 ± 0.00	5 71.43 ± 17.07	0 0.00 ± 0.00	0 0.00 ± 0.00	0 0.00 ± 0.00	0 0.00 ± 0.00
PHX-CMIO	3 0.00 ± 0.00	3 100.00 ± 0.00	1 33.33 ± 27.22	1 100.00 ± 0.00	1 100.00 ± 0.00	0 0.00 ± 0.00	0 0.00 ± 0.00	0 0.00 ± 0.00	0 0.00 ± 0.00
$e\mu$	302 0.08 ± 0.00	250 82.78 ± 2.17	208 83.20 ± 2.36	207 99.52 ± 0.48	119 57.49 ± 3.44	29 24.37 ± 3.94	13 44.83 ± 9.23	9 69.23 ± 12.80	9 100.00 ± 0.00
CMUP-CMUP	704 0.18 ± 0.01	602 85.51 ± 1.33	528 87.71 ± 1.34	506 95.83 ± 0.87	256 50.59 ± 2.22	59 23.05 ± 2.63	57 96.61 ± 2.36	5 8.77 ± 3.75	4 80.00 ± 17.89
CMUP-CMX	544 0.14 ± 0.01	522 95.96 ± 0.84	463 88.70 ± 1.39	456 98.49 ± 0.57	251 55.04 ± 2.33	66 26.29 ± 2.78	64 96.97 ± 2.11	5 7.81 ± 3.35	4 80.00 ± 17.89
CMUP-CMU	257 0.06 ± 0.00	241 93.77 ± 1.51	213 88.38 ± 2.06	211 99.06 ± 0.66	113 53.55 ± 3.43	30 26.55 ± 4.15	28 93.33 ± 4.55	2 7.14 ± 4.87	2 100.00 ± 0.00
CMUP-CMP	384 0.10 ± 0.00	348 90.62 ± 1.49	310 89.08 ± 1.67	304 98.06 ± 0.78	158 51.97 ± 2.87	41 25.95 ± 3.49	40 97.56 ± 2.41	2 5.00 ± 3.45	2 100.00 ± 0.00
CMUP-CMIO	32 0.01 ± 0.00	26 81.25 ± 6.90	24 92.31 ± 5.23	24 100.00 ± 0.00	10 41.67 ± 10.06	2 20.00 ± 12.65	2 100.00 ± 0.00	0 0.00 ± 0.00	0 0.00 ± 0.00
CMX-CMX	182 0.05 ± 0.00	141 77.47 ± 3.10	121 85.82 ± 2.94	119 98.35 ± 1.16	69 57.98 ± 4.52	13 18.84 ± 4.71	12 92.31 ± 7.39	1 8.33 ± 7.98	1 100.00 ± 0.00
CMX-CMU	99 0.02 ± 0.00	93 93.94 ± 2.40	87 93.55 ± 2.55	85 97.70 ± 1.61	47 55.29 ± 5.39	12 25.53 ± 6.36	10 83.33 ± 10.76	2 20.00 ± 12.65	1 50.00 ± 35.36
CMX-CMP	121 0.03 ± 0.00	117 96.69 ± 1.63	107 91.45 ± 2.58	106 99.07 ± 0.93	59 55.66 ± 4.83	15 25.42 ± 5.67	15 100.00 ± 0.00	2 13.33 ± 8.78	1 50.00 ± 35.36
CMX-CMIO	9 0.00 ± 0.00	9 100.00 ± 0.00	8 88.89 ± 10.48	8 100.00 ± 0.00	4 50.00 ± 17.68	0 0.00 ± 0.00	0 0.00 ± 0.00	0 0.00 ± 0.00	0 0.00 ± 0.00
$\mu\mu$	2332 0.59 ± 0.01	2099 90.01 ± 0.62	1861 88.66 ± 0.69	1819 97.74 ± 0.34	967 53.16 ± 1.17	238 24.61 ± 1.39	228 95.80 ± 1.30	19 8.33 ± 1.83	15 78.95 ± 9.35
total	6412 1.61 ± 0.02	5731 89.38 ± 0.38	5120 89.34 ± 0.41	5040 98.44 ± 0.17	2748 54.52 ± 0.70	582 21.18 ± 0.78	538 92.44 ± 1.10	45 8.36 ± 1.19	37 82.22 ± 5.70

Table 46: ZZ MC acceptance table, assuming $M_H^{\rm SM} = 160$ GeV

Table 47: $W\gamma$ MC acceptance table, assuming $M_H^{\rm SM} = 160$ GeV

Categ	Lep ID	Lep1 Isol	Lep2 Isol	$M_{\ell\ell} > 16$	jet veto	$\not\!\!E_t$	opp sign	$M_{\ell\ell} < M_u$	$H_T < M_H$
TCE-TCE	102 0.03 ± 0.00	64 62.75 ± 4.79	49 76.56 ± 5.30	32 65.31 ± 6.80	32 100.00 ± 0.00	9 28.12 ± 7.95	4 44.44 ± 16.56	4 100.00 ± 0.00	4 100.00 ± 0.00
TCE-PHX	122 0.03 ± 0.00	102 83.61 ± 3.35	100 98.04 ± 1.37	88 88.00 ± 3.25	86 97.73 ± 1.59	21 24.42 ± 4.63	10 47.62 ± 10.90	8 80.00 ± 12.65	8 100.00 ± 0.00
ee	322 0.09 ± 0.00	237 73.60 ± 2.46	215 90.72 ± 1.88	169 78.60 ± 2.80	166 98.22 ± 1.02	39 23.49 ± 3.29	19 48.72 ± 8.00	14 73.68 ± 10.10	14 100.00 ± 0.00
TCE-CMUP	73 0.02 ± 0.00	28 38.36 ± 5.69	27 96.43 ± 3.51	15 55.56 ± 9.56	15 100.00 ± 0.00	3 20.00 ± 10.33	2 66.67 ± 27.22	2 100.00 ± 0.00	2 100.00 ± 0.00
TCE-CMX	43 0.01 ± 0.00	11 25.58 ± 6.65	11 100.00 ± 0.00	10 90.91 ± 8.67	10 100.00 ± 0.00	0 0.00 ± 0.00	0 0.00 ± 0.00	0 0.00 ± 0.00	0 0.00 ± 0.00
TCE-CMU	8 0.00 ± 0.00	6 75.00 ± 15.31	6 100.00 ± 0.00	5 83.33 ± 15.21	5 100.00 ± 0.00	1 20.00 ± 17.89	1 100.00 ± 0.00	0 0.00 ± 0.00	0 0.00 ± 0.00
TCE-CMP	4 0.00 ± 0.00	2 50.00 ± 25.00	2 100.00 ± 0.00	0 0.00 ± 0.00	0 0.00 ± 0.00	0 0.00 ± 0.00	0 0.00 ± 0.00	0 0.00 ± 0.00	0 0.00 ± 0.00
TCE-CMIO	3 0.00 ± 0.00	2 66.67 ± 27.22	1 50.00 ± 35.36	1 100.00 ± 0.00	1 100.00 ± 0.00	0 0.00 ± 0.00	0 0.00 ± 0.00	0 0.00 ± 0.00	0 0.00 ± 0.00
PHX-CMUP	47 0.01 ± 0.00	43 91.49 ± 4.07	43 100.00 ± 0.00	43 100.00 ± 0.00	41 95.35 ± 3.21	10 24.39 ± 6.71	6 60.00 ± 15.49	3 50.00 ± 20.41	2 66.67 ± 27.22
PHX-CMX	38 0.01 ± 0.00	37 97.37 ± 2.60	32 86.49 ± 5.62	28 87.50 ± 5.85	27 96.43 ± 3.51	7 25.93 ± 8.43	1 14.29 ± 13.23	1 100.00 ± 0.00	1 100.00 ± 0.00
PHX-CMU	9 0.00 ± 0.00	9 100.00 ± 0.00	9 100.00 ± 0.00	9 100.00 ± 0.00	9 100.00 ± 0.00	0 0.00 ± 0.00	0 0.00 ± 0.00	0 0.00 ± 0.00	0 0.00 ± 0.00
PHX-CMP	11 0.00 ± 0.00	11 100.00 ± 0.00	11 100.00 ± 0.00	11 100.00 ± 0.00	10 90.91 ± 8.67	3 30.00 ± 14.49	2 66.67 ± 27.22	1 50.00 ± 35.36	1 100.00 ± 0.00
PHX-CMIO	0 0.00 ± 0.00	0 0.00 ± 0.00	0 0.00 ± 0.00	0 0.00 ± 0.00	0 0.00 ± 0.00	0 0.00 ± 0.00	0 0.00 ± 0.00	0 0.00 ± 0.00	0 0.00 ± 0.00
$e\mu$	236 0.06 ± 0.00	149 63.14 ± 3.14	142 95.30 ± 1.73	122 85.92 ± 2.92	118 96.72 ± 1.61	24 20.34 ± 3.71	12 50.00 ± 10.21	7 58.33 ± 14.23	6 85.71 ± 13.23
CMUP-CMUP	0 0.00 ± 0.00	0 0.00 ± 0.00	0 0.00 ± 0.00	0 0.00 ± 0.00	0 0.00 ± 0.00	0 0.00 ± 0.00	0 0.00 ± 0.00	0 0.00 ± 0.00	0 0.00 ± 0.00
CMUP-CMX	0 0.00 ± 0.00	0 0.00 ± 0.00	0 0.00 ± 0.00	0 0.00 ± 0.00	0 0.00 ± 0.00	0 0.00 ± 0.00	0 0.00 ± 0.00	0 0.00 ± 0.00	0 0.00 ± 0.00
CMUP-CMU	0 0.00 ± 0.00	0 0.00 ± 0.00	0 0.00 ± 0.00	0 0.00 ± 0.00	0 0.00 ± 0.00	0 0.00 ± 0.00	0 0.00 ± 0.00	0 0.00 ± 0.00	0 0.00 ± 0.00
CMUP-CMP	0 0.00 ± 0.00	0 0.00 ± 0.00	0 0.00 ± 0.00	0 0.00 ± 0.00	0 0.00 ± 0.00	0 0.00 ± 0.00	0 0.00 ± 0.00	0 0.00 ± 0.00	0 0.00 ± 0.00
CMUP-CMIO	1 0.00 ± 0.00	0 0.00 ± 0.00	0 0.00 ± 0.00	0 0.00 ± 0.00	0 0.00 ± 0.00	0 0.00 ± 0.00	0 0.00 ± 0.00	0 0.00 ± 0.00	0 0.00 ± 0.00
CMX-CMX	0 0.00 ± 0.00	0 0.00 ± 0.00	0 0.00 ± 0.00	0 0.00 ± 0.00	0 0.00 ± 0.00	0 0.00 ± 0.00	0 0.00 ± 0.00	0 0.00 ± 0.00	0 0.00 ± 0.00
CMX-CMU	0 0.00 ± 0.00	0 0.00 ± 0.00	0 0.00 ± 0.00	0 0.00 ± 0.00	0 0.00 ± 0.00	0 0.00 ± 0.00	0 0.00 ± 0.00	0 0.00 ± 0.00	0 0.00 ± 0.00
CMX-CMP	0 0.00 ± 0.00	0 0.00 ± 0.00	0 0.00 ± 0.00	0 0.00 ± 0.00	0 0.00 ± 0.00	0 0.00 ± 0.00	0 0.00 ± 0.00	0 0.00 ± 0.00	0 0.00 ± 0.00
CMX-CMIO	0 0.00 ± 0.00	0 0.00 ± 0.00	0 0.00 ± 0.00	0 0.00 ± 0.00	0 0.00 ± 0.00	0 0.00 ± 0.00	0 0.00 ± 0.00	0 0.00 ± 0.00	0 0.00 ± 0.00
$\mu\mu$	1 0.00 ± 0.00	0 0.00 ± 0.00	0 0.00 ± 0.00	0 0.00 ± 0.00	0 0.00 ± 0.00	0 0.00 ± 0.00	0 0.00 ± 0.00	0 0.00 ± 0.00	0 0.00 ± 0.00
total	559 0.15 ± 0.01	386 69.05 ± 1.96	357 92.49 ± 1.34	291 81.51 ± 2.05	284 97.59 ± 0.90	63 22.18 ± 2.47	31 49.21 ± 6.30	21 67.74 ± 8.40	20 95.24 ± 4.65